

GEOSPHERE; v. 12, no. 1

doi:10.1130/GES01182.1

12 figures; 1 supplemental file

CORRESPONDENCE: [cjbusby@ucdavis.edu](mailto:cjbusby@ucdavis.edu)

CITATION: Busby, C.J., Andrews, G.D.M., Koerner, A.K., Brown, S.R., Melosh, B.L., and Hagan, J.C., 2016, Progressive derangement of ancient (Mesozoic) east-west Nevadaplano paleochannels into modern (Miocene–Holocene) north-northwest trends in the Walker Lane Belt, central Sierra Nevada: *Geosphere*, v. 12, no. 1, p. 135–175, doi:10.1130/GES01182.1.

Received 19 February 2015

Revision received 29 July 2015

Accepted 19 October 2015

Published online 13 January 2016

# Progressive derangement of ancient (Mesozoic) east-west Nevadaplano paleochannels into modern (Miocene–Holocene) north-northwest trends in the Walker Lane Belt, central Sierra Nevada

**C.J. Busby<sup>1</sup>, G.D.M. Andrews<sup>2</sup>, A.K. Koerner<sup>3</sup>, S.R. Brown<sup>2</sup>, B.L. Melosh<sup>4</sup>, and J.C. Hagan<sup>5</sup>**

<sup>1</sup>Department of Earth and Space Sciences, University of California Davis, One Shields Avenue, Davis, California 95616, USA

<sup>2</sup>Department of Geosciences, California State University Bakersfield, 9001 Stockdale Highway, Bakersfield, California 93311, USA

<sup>3</sup>Chevron Corporation, 9525 Camino Media, Bakersfield, California 93311, USA

<sup>4</sup>Department of Earth and Planetary Sciences, McGill University, 3450 University Street, Montreal, Quebec H2A 3A7, Canada

<sup>5</sup>Exxon Mobil Upstream Research Company, 3120 Buffalo Speedway, Houston, Texas 77098, USA

## ABSTRACT

Eocene to Pliocene paleochannels of the Sierra Nevada (California, USA) were first exploited for gold placer deposits during the California gold rush (1848), and then mapped in surveys more than century ago. The surveys showed that the paleochannels flowed westward, like the modern rivers of the range; it then was assumed that the heads of the paleochannels were at the modern range crest. A first paradigm shift occurred ~50 yr ago, when it was recognized that at least some of the paleochannel fill was sourced from the region of the current state of Nevada, and it was proposed that the Sierra Nevada range was younger than the paleochannels (younger than 6 Ma). More recent work has demonstrated that Sierran paleochannels are ancient features that formed on the shoulder of a broad high uplift (the Nevadaplano) formed during Cretaceous crustal shortening; the headwaters were in central Nevada prior to disruption of the plateau by Basin and Range extension. A second paradigm shift occurred in the past decade: the Sierra Nevada range front is formed of north-northwest transtensional structures of the younger than 12 Ma Walker Lane belt, not north-south to north-northeast–south-southwest extensional structures of the Basin and Range. In this paper we use detailed geologic mapping to reconstruct the paleogeographic evolution of three Oligocene to Pliocene east-west paleochannels in the central Sierra Nevada, and their progressive south to north derangement by Walker Lane structures: the Stanislaus in the south, the Cataract in the middle, and the Mokelumne in the north.

Previous work has shown that east-west Nevadaplano paleochannels in the central Sierra have four stratigraphic sequences floored by erosional unconformities; we describe distinguishing characteristics between the ancient Nevadaplano paleochannels and the north-northwest-deranged paleochannels of the Walker Lane grabens. In the east-west paleochannels unconformity 1 is the deepest, eroded into mesozonal Cretaceous plutons; it is

overlain by the Oligocene to early Miocene Valley Springs Formation (sequence 1), consisting of ignimbrites erupted ~250 km to the east in Nevada. Sequence 1 is the most useful for tracing the courses of the paleochannels because it was deposited before faulting began; however, it is incompletely preserved, due to erosion along unconformity 2 (with as much as 500 m of relief) as well as later erosional events. Sequence 2 consists of ca. 16–12 Ma andesitic volcaniclastic rocks referred to as the Relief Peak Formation; it occurs in all three paleochannels (Stanislaus, Cataract, and Mokelumne) as stratified fluvial and debris flow deposits, with abundant cut and fill structures. However, we show for the first time that Relief Peak Formation also forms the basal fill of a Walker Lane transtensional basin system that began to form by ca. 12 Ma, in a full graben along what is now the Sierra Crest, and in transfer zone basins and half-grabens on what is now the eastern range front. The Relief Peak Formation in the Walker Lane transtensional basins consists of massive (nonstratified) andesitic debris flow deposits and debris avalanche deposits, with slabs as much as 2 km long, including slabs of the Valley Springs Formation. Sequence 3 in the Nevadaplano paleochannels consists of distinctive, voluminous high-K lavas and ignimbrites of the Stanislaus Group. The lavas were erupted from fissures in the transtensional Sierra Crest graben-vent system, which beheaded the Stanislaus paleochannel prior to development of unconformity 3 and eruption of the voluminous basal lavas, referred to as the Table Mountain Latite (TML). In the Cataract paleochannel, TML lavas are inset as much as 100 m into the Relief Peak Formation along unconformity 3, indicating fluvial reincision within the paleochannel; TML lavas were ponded in the graben-vent system to thicknesses 6 times greater than the paleochannel fill, with no reincision surfaces. Sequence 3 ignimbrites of the Stanislaus Group (Eureka Valley Tuff) were erupted from the Little Walker caldera, and mark the course of all three paleochannels, with channel reincision surfaces between them (but not in the grabens). Sequence 3 lavas in the paleochannels differ from those in the grabens by having interstratified fluvial deposits, stretched vesicles parallel to the



For permission to copy, contact Copyright  
Permissions, GSA, or editing@geosociety.org.

© 2016 Geological Society of America

paleochannels, tree molds, peperitic bases, and kuppaberg (cobble jointed) tops, which form when water penetrates into a cooling lava along vertical joints, allowing secondary joints to form perpendicular to them. The Cataract paleochannel was deranged from its ancient (Mesozoic) east-west Nevadaplano trend into the north-northwest Walker Lane tectonic trend prior to development of unconformity 4 and deposition of sequence 4 (Disaster Peak Formation). The north-northwest–deranged Cataract paleochannel is along the Sierra Crest between the Stanislaus and Mokelumne paleochannels, with fluvial deposits indicating northward flow; this paleochannel is perpendicular to the ancient east-west Nevadaplano paleochannels, and parallel to modern Walker Lane drainages, indicating tectonic reorganization of the landscape ca. 9–5 Ma. This derangement was followed by progressive beheading of the Mokelumne paleochannel, development of the Ebbetts Pass pull-apart basin (ca. 6 Ma) and the Ebbetts Pass stratovolcano within it (ca. 5–4 Ma), which fed lava into the relict Mokelumne paleochannel.

The derangement of central Sierran paleochannels proceeded as follows, from south to north: (1) the Stanislaus paleochannel was beheaded by ca. 11 Ma; (2) the Cataract paleochannel became deranged from an east-west Nevadaplano trend into a north-northwest Walker Lane trend by ca. 9 Ma, now exposed along the Sierran crest; and (3) the Mokelumne paleochannel was beheaded by ca. 6–5 Ma, and the Carson Pass–Kirkwood paleochannel several kilometers to the north was deranged from east-west into the north-northwest Hope Valley graben ca. 6 Ma. The next paleochannel to the north is in the southern part of the northern Sierra at Lake Tahoe, and based on published descriptions was beheaded ca. 3 Ma. The timing of paleochannel beheading corresponds to the northward migration of the Mendocino Triple Junction and northward propagation of the Walker Lane transtensional strain regime.

This paper illustrates in detail the interplay between tectonics and drainage development, exportable to a very broad variety of settings.

## ■ INTRODUCTION

The Sierra Nevada (California, USA) forms an asymmetrical block-faulted mountain range with a steep fault-bound range front on the east and a gently sloping western slope (Fig. 1). The crest of the range is on the east, and modern rivers flow from east to west. Lindgren (1911) recognized that Cenozoic (mainly Eocene to Miocene) volcaniclastic and volcanic rocks in the Sierra Nevada (including gold placer deposits) were deposited into and preserved within paleochannels cut into the deeply eroded Mesozoic Sierra Nevada batholith. It was then assumed that these paleochannels, which parallel the modern ones (Fig. 1), had their heads within the Sierra Nevada, at what is now the modern range crest (Ransome, 1898; Lindgren, 1911).

By the mid-twentieth century, a paradigm shift occurred. It was realized that the fault-bound eastern range crest (Fig. 1, inset) is a relatively young feature, then inferred to be <6 m.y. old; it was also recognized that at least some of the detritus in the paleochannels was derived from the region of the current state

of Nevada (USA) to the east of the modern range front, indicating that the paleochannels existed before faulting at the range front began (Slemmons, 1953; Curtis, 1954; Bateman and Wahraftig, 1966; cf. Wakabayashi, 2013). The Sierra Nevada paleochannels are now widely agreed to represent the lower reaches of channels that originated far to the east, in central Nevada (cf. Henry, 2008; Henry et al., 2012). These paleochannels are inferred to have been carved into an areally extensive, high plateau created by Cretaceous low-angle subduction, termed the Nevadaplano, and the Sierra Nevada is inferred to have formed the western shoulder of this broad uplift, prior to disruption of the plateau by Basin and Range extension (Wolfe et al., 1997; De Celles, 2004).

A second paradigm shift has occurred in the past decade, regarding the nature of the eastern range front of the Sierra Nevada. It has long been interpreted to form the western edge of the Basin and Range extensional province (Bateman and Wahraftig, 1966; Slemmons, 1953, 1966) with its approximately north-south grabens and horst blocks formed by east-west extension (see Fig. 2A). However, over the past two decades, a growing body of geophysical, geodetic, and geological studies demonstrate that the Sierra Nevada range front forms the western boundary of the Walker Lane belt, a north-northwest zone of dextral strike-slip and oblique normal faults at the western edge of the Basin and Range, which parallels the San Andreas fault to the west (Fig. 2A). The Walker Lane belt is now known to form a transtensional plate boundary on the trailing edge of the Sierra Nevada microplate, which is between the Pacific plate west of the San Andreas fault, and the North American plate, east of the Walker Lane belt (Argus and Gordon, 1991; Dixon et al., 2000; see overviews by Faulds and Henry, 2008; Jayko and Bursik, 2012; Busby, 2013). Unruh et al. (2003) demonstrated the importance of right transtensional strain along the Sierra Nevada frontal fault system, even for those reaches that do not have obvious dextral faults.

Like the San Andreas fault, the Walker Lane belt has grown northward with time, in concert with northward migration of the Mendocino Triple Junction (Fig. 2A; Faulds and Henry, 2008; see references in Busby, 2013). Along the central Sierra Nevada range front (Hagan et al., 2009; Busby et al., 2013a, 2013b), and in the Walker Lane belt in general (see fig. 1 of Busby, 2013), modern rivers mainly run parallel to the dominantly north-northwest-trending structural grain, at a high angle to Basin and Range structures (which strike north-south to north-northeast–south-southwest), and approximately perpendicular to the west-flowing rivers west of the Sierra Nevada range crest (Fig. 1).

Until recently, it was assumed that Paleogene–Neogene strata in the central Sierra Nevada were all preserved in paleochannels, including all of the volcaniclastic–volcanic rocks; the grabens were inferred to be postvolcanic (Slemmons, 1953, 1966), and the initiation of faulting was inferred to be younger than the paleochannel fill (ca. 6–3.5 Ma; cf. Surpless et al., 2002). However, we have shown that transtensional deformation began by ca. 12 Ma, while the paleochannels were still active, and active faults controlled the sites of eruption and deposition of volcanic and volcaniclastic rocks in grabens on the range front and in the crestal area of the range (Fig. 2B; Busby et al., 2008a, 2013a, 2103b; Busby, 2013).

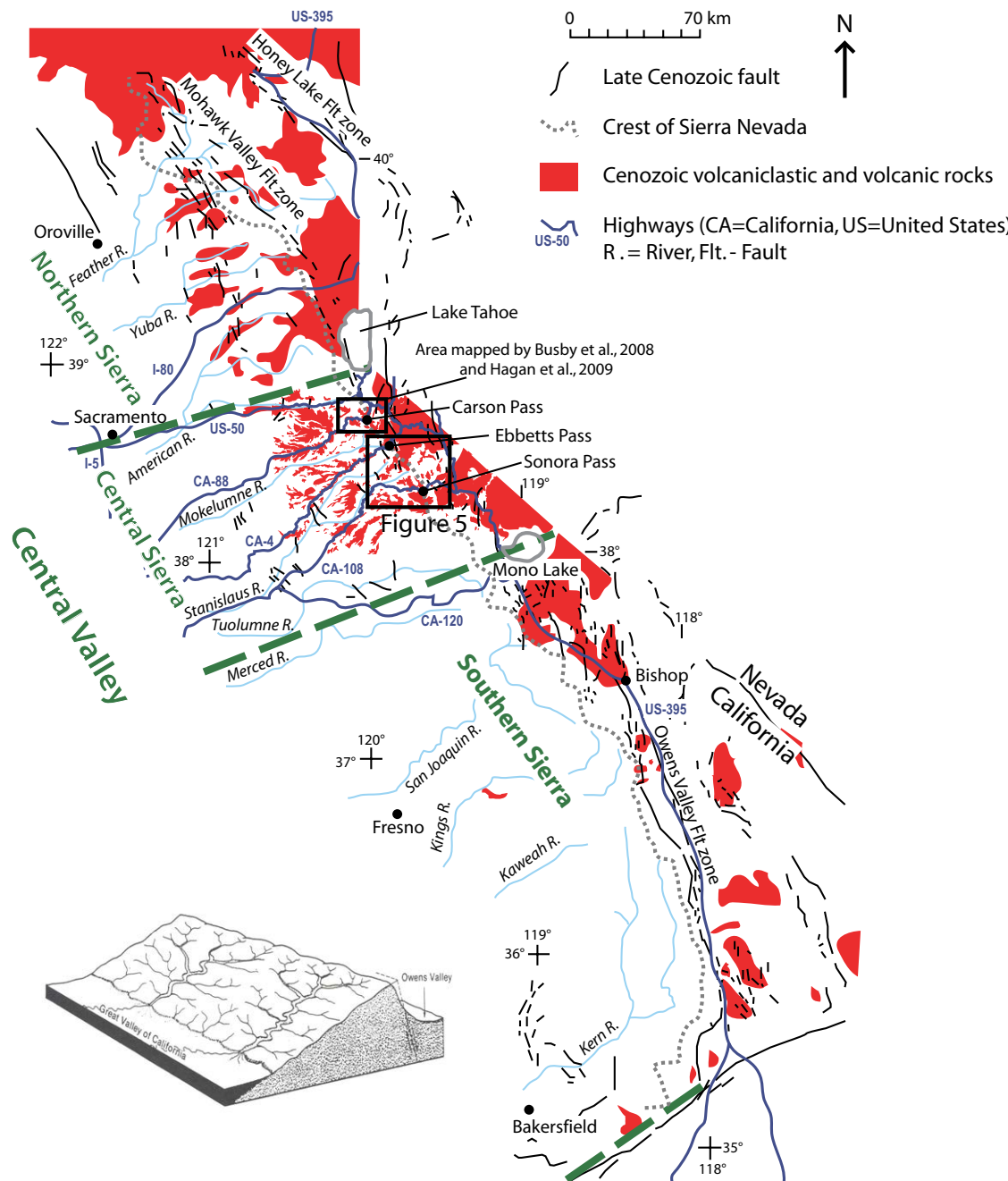
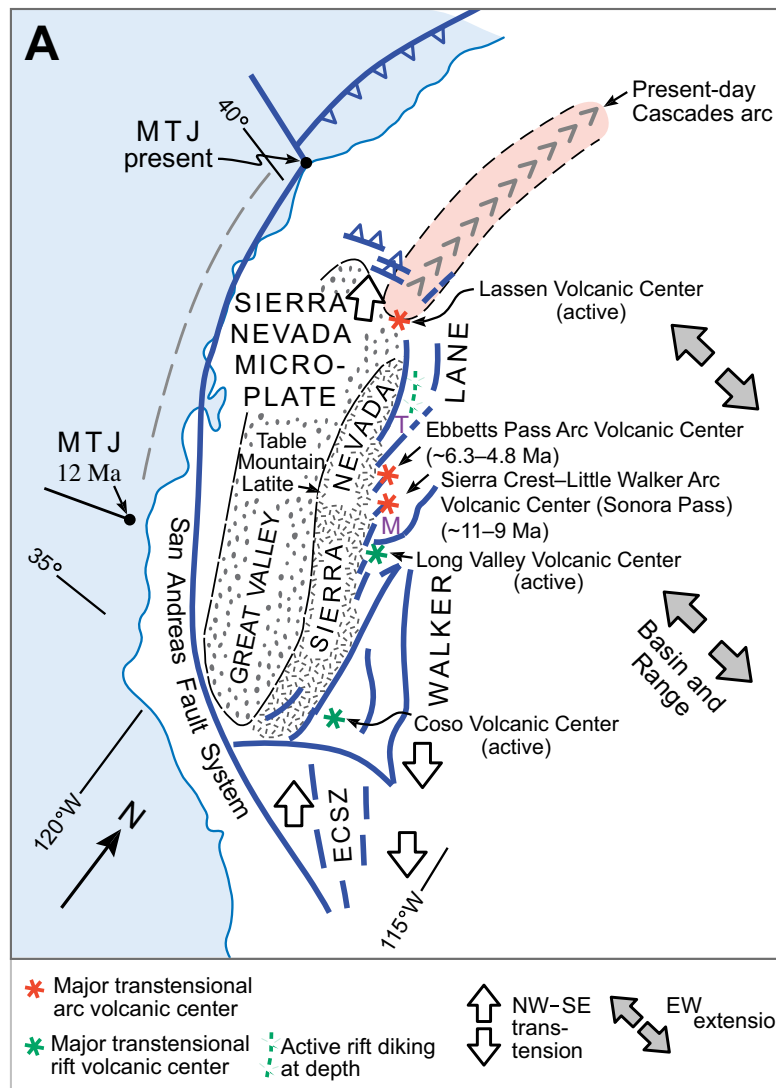


Figure 1. Cenozoic volcaniclastic and volcanic rocks (shown in red), faults, and geographic features of the Sierra Nevada and adjacent easternmost California (revised from Busby et al., 2008a). Cenozoic volcaniclastic and volcanic rocks are largely preserved in paleochannels in the northern and central Sierra. The crest of this highly asymmetric range (shown by dot pattern) is very close to the Sierra Nevada frontal fault system. Green dashed lines indicate our usage of subdivisions between northern, central, and southern Sierra Nevada, labeled in green letters (for full discussion see Busby et al., 2008a, 2008b). The area of the detailed map of the range crest and range front (presented in Fig. 5) is outlined here. Areas mapped in detail in Busby et al. (2008b) and Hagan et al. (2009) are shown. Inset: Simplified diagram of the block-tilted structure of the Sierra Nevada, showing the gross overall structure of the range (after Bateman and Wahrhaftig, 1966). This block is ~600 km long and 100 km wide, and exhibits little internal deformation, with the exception of the southern Sierra Nevada, which has internal faults (cf. Busby, 2013).



**Figure 2 (on this and following page).** (A) Tectonic setting of the Sierra Nevada microplate (modified from Busby, 2013). The microplate is bound to the east by the north-northwest-south-southeast transtensional Walker Lane belt (cf. Jayko and Bursik, 2012), and to the west by the San Andreas fault, shown in oblique projection of the western Cordillera about the preferred Sierra Nevada–North American Euler pole, following the perspective of Unruh et al. (2003). The east-west extensional Basin and Range province is to the east of the Walker Lane belt, and the present-day Cascades arc is to the north. The Walker Lane belt is a transtensional rift that connects through the Eastern California shear zone (ECSZ) to the Gulf of California transtensional rift. The Mendo-cino Triple Junction (MTJ) has been migrating northward with time, terminating subduction northward (Atwater and Stock, 1998); at 12 Ma, the Sonora Pass–Ebbets Pass area was above the subducting slab, forming part of the Sierra Nevada ancestral Cascades arc (Putirka and Busby, 2007). Note that at 12 Ma, western California was further south than shown (Wakabayashi, 1999). Stipple pattern shows the present-day region of largely unfaulited Cretaceous batholith, and dot pattern is the California Central Valley to the west. Also shown are active transtensional rift volcanic fields at Long Valley and Coso, as well as the southernmost Cascades arc volcano (Lassen), which is in a Walker Lane transtensional basin (cf. Busby, 2013). Active dike swarms at depth north of Lake Tahoe are associated with an interpreted rift system (Smith et al., 2004, 2012). M—Mono Lake, T—Lake Tahoe. In this paper we present a model for the progressive south to north derangement of paleochannels along the Sierra Nevada range front and range crest, from Mono Lake (M) to Lake Tahoe (T), in concert with northward migration of the Mendo-cino Triple Junction.

In this paper we examine the Cenozoic structure and stratigraphy of the central Sierra Nevada to answer the following questions. What can the Cenozoic paleochannels tell us about the paleogeographic and tectonic evolution of the Sierra Nevada? When and how were Sierra Nevada paleochannels beheaded or deranged from their Nevadaplano source, and how may the fill of the Nevadaplano

paleochannels be distinguished from the fill of Walker Lane transtensional grabens? Was derangement of east-west drainage patterns into north-northwest drainage patterns progressive or abrupt, and what were the geologic signals of this reorganization? We also summarize regional data, from Sonora Pass northward to Carson Pass (Busby et al., 2008b; Hagan et al., 2009) to the Lake Tahoe

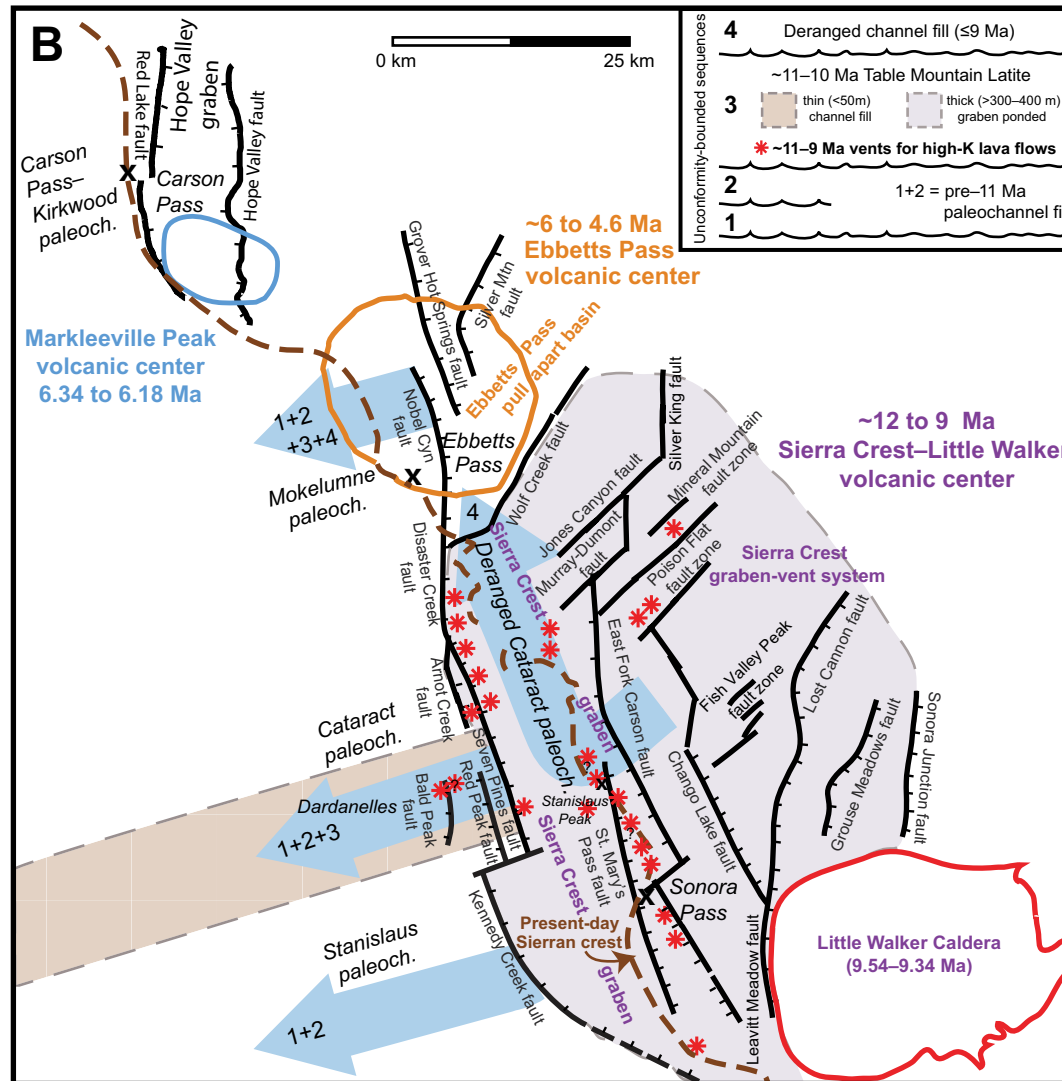


Figure 2 (continued). (B) Tectonic and volcanic setting of the Sonora Pass to Ebbets Pass to Carson Pass region; locality is in Figure 1, and detailed geologic maps are in Figure 5. Paleochannels carved in Cretaceous-Paleocene time contain four unconformity-bound stratigraphic sequences (Fig. 4). 1—Oligocene silicic ignimbrites erupted in central Nevada (Valley Springs Formation). 2—Miocene arc volcanic and volcaniclastic rocks (Relief Peak Formation). 3—11.5–9 Ma high-K arc volcanic rocks (Stanislaus Group). 4—Miocene-Pliocene arc volcanic rocks (Disaster Peak Formation). The high-K volcanic rocks of sequence 3 were erupted from the Sierra Crest–Little Walker volcanic center, which formed a Walker Lane transtensional intraarc graben complex; lavas (mostly Table Mountain Latite, TML, shown in lavender-gray) were erupted from fissures and point sources along faults (red stars), and ignimbrites were erupted from the Little Walker caldera (Busby et al., 2013a, 2013b). All three paleochannels (paleoch.) contain sequences 1 and 2, indicating that they were not deranged prior to ca. 11.5 Ma. The Stanislaus paleochannel contains no TML, so it was beheaded before TML erupted (i.e., prior to the onset of deposition of sequence 3). The Cataract paleochannel continued to function through eruption of sequence 3, including the TML, or flood andesite (Busby et al., 2013a), shown in tan. It was completely beheaded before deposition of sequence 4, and sequence 4 was deposited in a paleochannel that flowed toward the north-northwest in the Sierra Crest graben, referred to as the deranged Cataract paleochannel (ca. 9–5 Ma; see Fig. 12D), along what is now the modern range crest (brown dashed line); this is parallel to modern drainages in the Walker Lane belt. This figure also illustrates structural and geographic relationship between Ebbets Pass and Carson Pass. The Mokelumne paleochannel was beheaded during deposition of sequence 4 at Ebbets Pass (see text and Fig. 12D). New data (work in progress) from the Ebbets Pass volcanic center show that it includes ca. 6 Ma lavas and the ca. 5–4 Ma Ebbets Pass stratovolcano, which formed in a Walker Lane pull-apart basin, beheading the Mokelumne paleochannel ca. 6–5 Ma (see text). At the same time (ca. 6 Ma), to the north, the Markleeville volcanic center formed in the Hope Valley graben, and the east-west Carson-Kirkwood paleochannel became tectonically deranged into the north-northwest-trending Hope Valley graben (Hagan et al., 2009). (For discussion of later derangement of paleochannels further north at Lake Tahoe, see text.)

area (see locations in Figs. 1 and 2), to address whether there is a regional-scale pattern to the paleochannel derangement, and if it bears a temporal relationship to northward migration of the Mendocino Triple Junction (Fig. 2A).

This paper uses detailed geologic mapping to illustrate the interplay between tectonics and drainage development, using techniques that are applicable to a very broad variety of geologic settings.

## PREVIOUS WORK

The central Sierra Nevada is an outstanding place to use paleochannel deposits to reconstruct the paleogeographic and tectonic evolution of the Sierra Nevada. Paleochannel deposits are not preserved in the highest part of the range in the southern Sierra Nevada (note the lack of Cenozoic rocks west

of the range crest in Fig. 1). Paleochannel fills have been very well studied in the northern Sierra, partly because they are extensive (Fig. 1) and contain auriferous Eocene gravels with plant fossils, but also in an effort to understand the age, paleogeography, sedimentology, volcanology, paleoaltimetry, and paleoclimate record (MacGinitie, 1941; Hudson, 1955; Durrell, 1966; Saucedo and Wagner, 1992; Wing and Greenwood, 1993; Deino, 1985; Wagner and Saucedo, 1990; Wolfe et al., 1997; Wagner et al., 2000; Wakabayashi and Sawyer, 2001; Garside et al., 2005; Garrison et al., 2008; Cecil et al., 2006, 2010; Brooks et al., 2008; Cassel et al., 2009a, 2009b, 2012a, 2012b; Mulch et al., 2006; Hinz et al., 2009; Hren et al., 2010; Cassel and Graham, 2011; Wakabayashi, 2013). In contrast, relatively few studies have dealt with paleochannel rocks of the central Sierra Nevada, and many of those have been part of regional-scale studies, or mapping, geochronologic, and paleomagnetic studies that did not focus specifically on the paleochannels (Whitney, 1880; Ransome, 1898; Lindgren, 1911; Slemmons, 1953, 1966; Axelrod, 1957; Dalrymple, 1963, 1964; Bateman and Wahraftig, 1966; Dalrymple et al., 1967; Huber, 1981, 1983a, 1983b, 1990; Keith et al., 1982; Wagner et al., 1987; Wakabayashi and Sawyer, 2001). Exposure of the central Sierran paleochannels is much better than northern Sierra Nevada exposures, which are at lower elevations and are forested.

Only in the past few years have studies focused on central Sierra Nevada paleochannels (Busby et al., 2008a, 2008b; Gorni et al., 2009; Koerner et al., 2009; Busby and Putirka, 2009; Hagan et al., 2009). Paleochannels in the central Sierra have probably been less well studied because access is much more difficult, relative to the northern Sierra: it is largely roadless, and it is rugged, due to greater offset on range front faults. However, exposure is improved due to glaciation in the crestal parts of the range, and the range front is more arid due to a greater rain shadow effect, making three-dimensional exposures of paleochannels and grabens much more complete, relative to the northern Sierra Nevada. The relief on the central Sierra Nevada crest and front is ~2000 m, providing outstanding three-dimensional exposures of the paleochannels and their relationships to faults. This makes detailed mapping worth the effort.

Previous work in central Sierran paleochannels focused in the Carson Pass–Kirkwood paleochannel along the range crest at Carson Pass (Busby et al., 2008b; Hagan et al., 2009), but the less-well-exposed down-paleochannel equivalents at lower elevations to the west have not been mapped in detail because they lack distinctive stratigraphic markers or dateable primary volcanic rocks. In contrast, paleochannels in the Sonora Pass area have been studied a long distance down-paleochannel for >100 yr (Fig. 3), because they contain widespread, dateable, distinctive high-K volcanic rocks of the Stanislaus Group (Ransome, 1898). The distribution of the distinctive high-K volcanic rocks is summarized in Figure 3, and the stratigraphy of paleochannels in Sonora Pass region is summarized in Figure 4.

Much of the previous work in the northern Sierra focused on basal Eocene placer gold-bearing sedimentary paleochannel fills (Lindgren, 1911). These appear to be absent in the central Sierra Nevada; instead, the Oligocene to

earliest Miocene Valley Springs Formation (Fig. 4) forms the oldest paleochannel fills in the central Sierra (Slemmons, 1953). No Eocene conglomerate-sandstone units have been reported in the crestal to range front areas between Sonora Pass and Carson Pass (Busby et al., 2008a, 2008b), nor have they been reported from the Lake Tahoe area. Basal placer gold-bearing sedimentary paleochannel fills occur in a few localities in the western Sierra foothills of the central Sierra. Two localities are in the Cataract paleochannel, near Chinese Camp (which was rich in gold), and beneath the Table Mountain Latite (TML) at Table Mountain (which never proved very remunerative; locations in Fig. 3; Lindgren, 1911). A third locality is ~40 km upstream of Chinese Camp in the Tuolumne paleochannel (not shown in Fig. 3), which is south of the Cataract paleochannel and feeds into it at Chinese Camp (Huber, 1990). However, it is unclear if these basal auriferous gravels are Eocene, Oligocene, or Miocene, because no fossils are reported from them (Lindgren, 1911; Huber, 1990).

The basal paleochannel fill in the central Sierra Nevada consists of Oligocene to early Miocene Valley Springs Formation rhyolitic ignimbrites (sequence 1, Fig. 4). Slemmons (1953) described three main ignimbrites in the Sonora Pass region, based largely on mineralogy, but did not map them separately; he inferred that they were erupted locally. It was later shown that Oligocene to earliest Miocene ignimbrites in the Sierra Nevada are restricted to paleochannels, and were erupted far to the east from calderas in Nevada, in a subduction setting on thick continental crust of the Nevadaplano (cf. Henry et al., 2012; Henry and John, 2013). In this paper we have not attempted to divide the Valley Springs Formation; however, in our description of individual paleochannels here, we point out places where C.D. Henry recognized specific ignimbrites (publications or written communications provided in following). Each ignimbrite of the Valley Springs Formation presumably once formed a nearly continuous channel fill back to its caldera source area in central Nevada on the crest of the Nevadaplano (cf. Henry et al., 2012); however, present-day Valley Springs Formation outcrops are discontinuous due to postdepositional reincision within the paleochannels (cf. Busby et al., 2008a, 2008b), as well as disruption by Miocene and younger faulting (Busby et al., 2013a, 2013b), and Pliocene to Holocene erosion, discussed in the following.

Previous work has shown that basal Oligocene ignimbrites in the central Sierra (sequence 1) are overlain in erosional unconformity by early Miocene andesitic volcaniclastic and volcanic rocks (sequence 2, Fig. 4; Busby et al., 2008a, 2008b). These formed in response to a westward sweep of arc magmatism, off the thickened continental crust in eastern Nevada (which produced silicic calderas) onto thinner crust in western Nevada and eastern California (which produced andesite volcanoes), in response to slab fallback (cf. Busby, 2013). By 16 Ma, andesite arc magmatism had swept westward into what is now the Sierra Nevada, producing the Sierra Nevada ancestral Cascades arc, described in Putirka and Busby (2007) and Busby and Putirka (2009). Miocene to Pliocene andesitic arc volcanic-volcaniclastic rocks in the central Sierra are generally referred to as the Mehrten Formation (following Curtis, 1954).

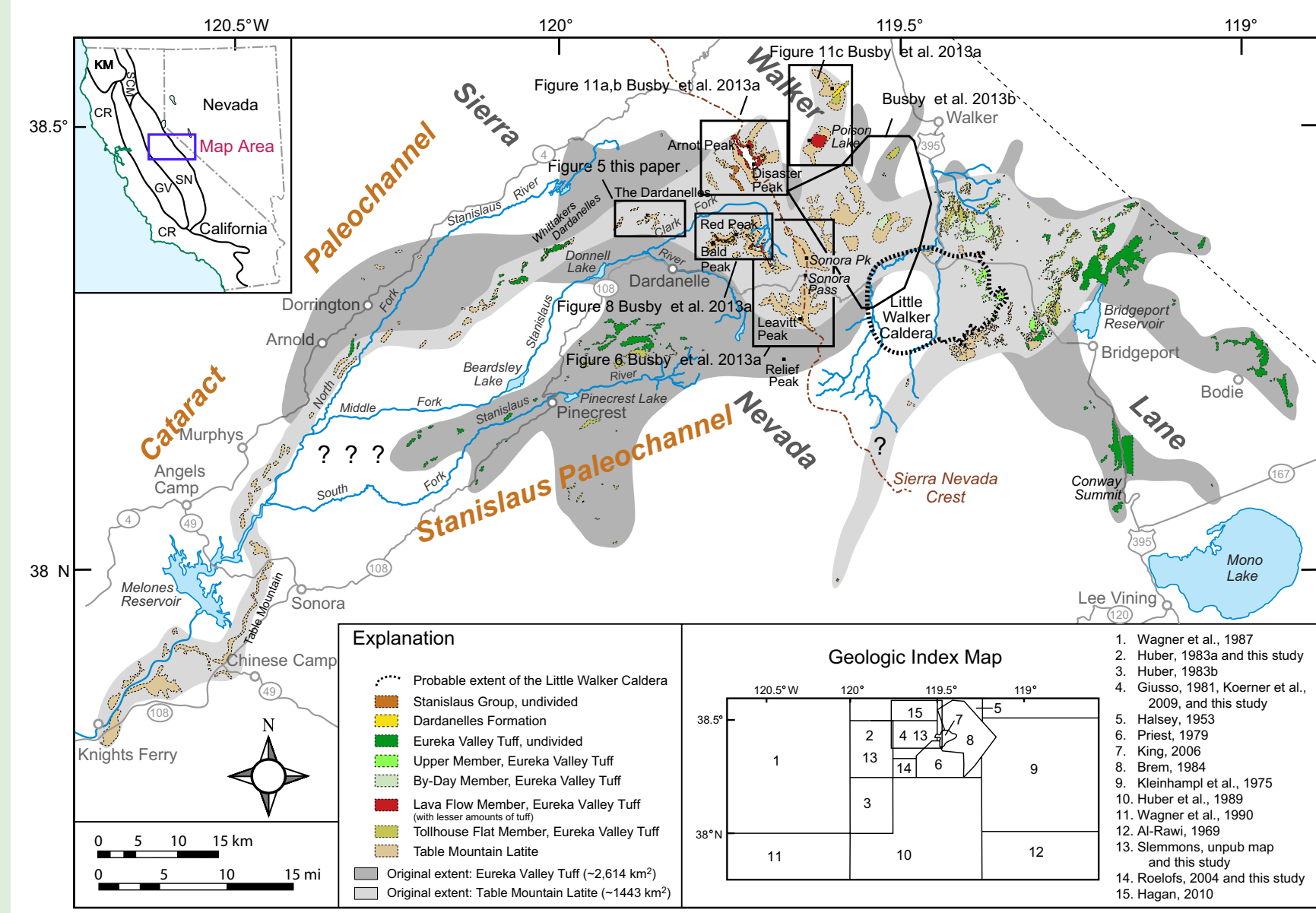


**Figure 3.** Distribution of ca. 11–9 Ma high-K volcanic rocks in the Sierra Nevada and in the adjacent Walker Lane belt east of the Sierra Nevada range crest (revised from Pluhar et al., 2009); stratigraphy is described in Figure 4. We propose herein that two distinct paleochannels (Cataract and Stanislaus) merged downstream into one (Cataract). Basal Stanislaus Group paleochannel fill consists of Table Mountain Latite (TML) lava, which erupted from fissures and was ponded to ~400 m thickness in the Sierra Crest graben-vent system (Fig. 2B). Several TML lavas flowed down the Cataract paleochannel 130 km to Knight's Ferry, shown at the westernmost edge of this figure, but the lavas that escaped down the paleochannel are <80 m thick (Gorni et al., 2013a). The Eureka Valley Tuff includes trachydacite welded ignimbrites (Fig. 4) erupted from the Little Walker caldera (shown here); it is more extensive than the TML lavas because of the much greater mobility of pumice-rich pyroclastic flows (area shaded dark gray). Along the Sierra Nevada crest (brown dashed line) and east of it, the distribution of high-K rocks was largely controlled by grabens, rather than paleochannels. Inset: CR—Coast Ranges; GV—Great Valley; KM—Klamath Mountains; SCM—southern Cascade Mountains; SN—Sierra Nevada. Modified from King et al. (2007), Pluhar et al. (2009), and Busby et al. (2013a).

## Sonora Pass Stratigraphy

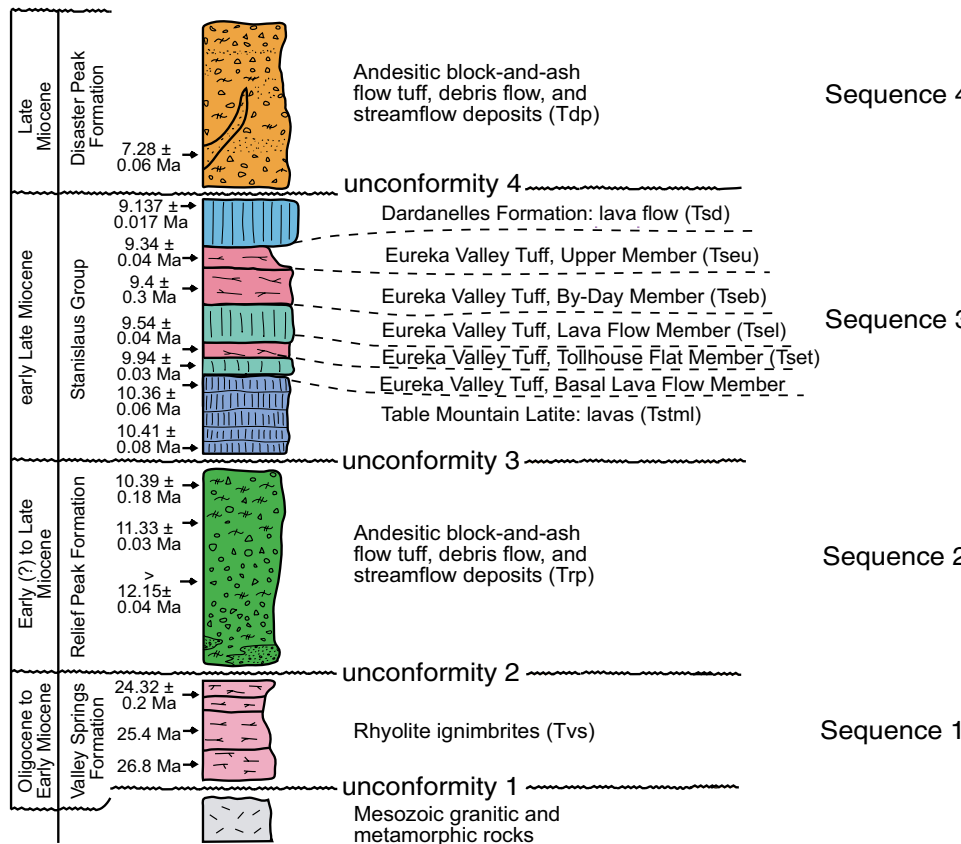


**Figure 4.** Composite stratigraphy of Cenozoic rocks of the Sonora Pass region, central Sierra Nevada, California (modified from Busby et al., 2013a; more detailed stratigraphy is presented in Fig. 5). Thicknesses of units are variable and not shown to scale. Mappable erosional unconformities divide the section into four sequences that have been correlated with unconformities in other central Sierra Nevada paleochannels (Busby et al., 2008a, 2008b; Busby and Putirka, 2009; Busby, 2012). Ages are recalculated from Busby et al. (2008b) and Busby and Putirka (2009), except for the Dardanelles Formation, which consists of a single lava flow  $^{40}\text{Ar}/^{39}\text{Ar}$  whole-rock dated as  $9.137 \pm 0.017$ ; the newly defined Basal Lava Flow Member of the Eureka Valley Tuff dated as  $9.94 \pm 0.03$  Ma by hornblende; and a Relief Peak Formation block-and-ash flow tuff from the north end of the Sierra Crest graben dated as  $11.33 \pm 0.03$  by hornblende (complete age data presented elsewhere). In addition, a sill that intrudes the Relief Peak Formation on the eastern range front by Grouse Meadows fault (Fig. 5A) provides a minimum age of  $12.15 \pm 0.04$  Ma on hornblende (Busby et al., 2013b). The two older ages on the Valley Springs Formation are based on correlations made by C. Henry (2013, written commun.) on ignimbrites in the Stanislaus paleochannel (see text). Tvs—Valley Springs Formation; Trp—Relief Peak Formation andesitic volcaniclastic rocks, divided herein into debris flow deposits (Trpdf), fluviatile deposits (Trpf), and block-and-ash flow tuffs (Trpba); Ts—Stanislaus Group high-K volcanic rocks, divided here into Table Mountain Latite lava flows (Tstml), Eureka Valley Tuff basal Lava Flow Member, Eureka Valley Tuff Tollhouse Flat Member welded ignimbrite (Tvset), Eureka Valley Tuff Lava Flow Member (Tsel), Eureka Valley Tuff By-Day Member welded ignimbrite (Tselb), Eureka Valley Tuff Upper Member nonwelded ignimbrite (Tsue), and Dardanelles Formation shoshonite lava flow (Tsd), which also includes intrusions (Tsdi); Tdp—Disaster Peak Formation andesitic volcanic and volcaniclastic rocks and intrusions.

However, in the Sonora Pass region, distinctive high-K volcanic rocks, referred to as Stanislaus Group (sequence 3, Fig. 4), are in the middle of the stratigraphic section, with andesitic rocks below referred to as the Relief Peak Formation (sequence 2), and andesitic rocks above referred to as the Disaster Peak Formation (sequence 4; following Slemmons, 1953). The Stanislaus Group has since been further divided into formations and members (Fig. 4; cf. Busby et al., 2013a).

Prior to the past few years, it was inferred that faulting in the central Sierra Nevada was younger than volcanism there (younger than ca. 6–3.5 Ma), was restricted to the range front, and was caused by east-west Basin and Range extension (cf. Busby, 2013). However, it was demonstrated (Busby et al., 2013a, 2013b; Busby, 2013) that synvolcanic faulting

began by 12 Ma in the Sonora Pass area and by 6 Ma in the Ebbetts Pass area, extended 20 km or more into the Sierra from the modern range crest, and was caused by Walker Lane northwest-southeast transtension. This paper focuses on the evolution of central Sierran paleochannels prior to, during, and after their derangement by Walker Lane transtensional faults and basins.

## TERMINOLOGY

To avoid confusion, two terms used in this paper are discussed here, paleochannels and derangement.

## Paleochannels

The Sierra Nevada paleochannels of Lindgren (1911) have been variably referred to as paleorivers, paleovalleys, or paleocanyons (cf. Cecil et al., 2010; Cassel et al., 2012a; Henry et al., 2012). The term “paleocanyons” was previously used (Busby et al., 2008a, 2008b; Busby and Putirka, 2009) to emphasize the fact that, in the central Sierra Nevada, these features show very steep relief on the contact with granitic basement (unconformity 1) as well as on internal unconformity surfaces (unconformities 2–4, Fig. 4), and contain abundant fluvial boulder conglomerates, which indicate high axial gradients. However, since those papers were published, others have emphasized that the same features typify northern Sierra Nevada paleochannels (e.g., Cassel et al., 2012a). Most have referred to these features as paleochannels; we do the same, while alerting the reader to the fact that they were probably not much different in gradient from the modern river canyons.

## Derangement

The *Glossary of Geology* (Neuendorf et al., 2005) defined derangement as the process by which changes in a stream course are effected by agents other than the stream, such as by glaciation, wind, deposition, or diastrophism (deformation). The earliest use of “deranged drainage” is in the *Encyclopedia of Geomorphology* (chapter titled Drainage Patterns; Fairbridge, 1968). The term was used with the same meaning in Andrews et al. (2012). In this paper we provide geologic maps that document the derangement of streams by diastrophism (in our case, transtensional deformation).

### ■ NEWLY DEFINED STANISLAUS, CATARACT, DERANGED CATARACT, AND MOKELUMNE PALEOCHANNELS

In Figure 5, we present new geologic mapping over a much broader area than shown in our recent papers on Sonora Pass (Busby et al., 2013a, 2013b) in order to describe the evolution of the paleochannels we recognize in the present-day Sonora Pass to Ebbetts Pass region. From south to north, these are the Stanislaus paleochannel, the Cataract paleochannel, the deranged Cataract paleochannel, and the Mokelumne paleochannel (Fig. 2B). These paleochannels are briefly described here to provide a framework for more detailed descriptions that form the body of this paper.

Prior to this study, the Sonora Pass area was inferred to contain a single paleochannel that roughly coincides with the modern Stanislaus River, which we herein divide into two paleochannels, the Stanislaus and Cataract paleochannels (Figs. 2B and 3). These two distinct paleochannels were previously inferred to represent a single paleochannel, referred to as the Cataract paleochannel by Ransome (1898) and Lindgren (1911), and as the Stanislaus paleo-

channel by Slemmons (1953). Bateman and Wahrhaftig (1966) reported black chert clasts from what they referred to as the Stanislaus paleochannel, and inferred that its headwaters were to the east in Nevada where sources are present. Although Bateman and Wahrhaftig (1966) were not specific about the chert clast locality, these were also described by Roelofs (2004) in what we define herein as Stanislaus paleochannel *sensu stricto*. As described here, more recent studies of the Valley Springs Formation support the Bateman and Wahrhaftig (1966) inference that the head of the paleochannel must have originally existed far to the east of Sonora Pass in Nevada, where caldera sources for the Valley Springs Formation are; however, the Sonora Pass region was still inferred to represent one paleochannel by King et al. (2007), Henry et al. (2012), and Wakabayashi (2013).

We believe that previous workers were misled into thinking that a single paleochannel extends through the Sonora Pass area (rather than two) because that is the lateral extent of continuous TML outcrops along the modern range crest at Sonora Pass (Fig. 5C). However, we now know that the TML there is within the southern half of the Sierra Crest graben, the northern half of which is preserved on the crest north of the Clarks Fork canyon (Busby et al., 2013a; Figs. 2B, 5B, and 5C). Not only is a width of >20 km at least 3 times too great when compared to the width of other Sierran paleochannels, but the thickness of the section in the Sierra Crest graben (1.3 km) is 2–3 times greater than the fill of Sierra Nevada paleochannels (see paleochannel measurements given in Wakabayashi and Sawyer, 2001; Wakabayashi, 2013). For example, the next paleochannel north of those described herein, the Carson Pass–Kirkwood paleochannel in the central Sierra (location in Fig. 1A), is ~5 km wide and <600 m deep (Busby et al., 2008b). Similarly, Henry et al. (2012) described the width of Nevadaplano paleochannels as typically <6 km. Slemmons (1953) recognized that his Stanislaus paleochannel, as defined by discontinuous Valley Springs Formation outcrops at Sonora Pass, was unusually broad (>20 km wide). We instead define two paleochannels, of reasonable width, using features of the Oligocene Valley Springs Formation and the overlying Miocene formations (described in detail in the following): the Stanislaus paleochannel (to the south) and the Cataract paleochannel (to the north) (Figs. 2B, 3, and 5). It appears that these two paleochannels merged downstream, just above the present-day Melones Reservoir, where the Stanislaus paleochannel probably fed into the Cataract paleochannel (although erosional remnants of paleochannel deposits have not yet been located in this area; see Fig. 3). These two distinct paleochannels are best preserved west of the Sierra Crest graben, because within it and to the east of it, paleochannel fill was largely cannibalized by synvolcanic transtensional faulting in the ca. 12–9 Ma Sierra Crest–Little Walker volcanic center (Fig. 2B), where the Valley Springs and fluvial Relief Peak Formations mainly occur as avalanche blocks (Busby et al., 2013a). However, our mapping shows that *in situ* Valley Springs Formation is preserved along the eastern margin of the Sierra Crest–Little Walker volcanic center, marking the position of the Cataract paleochannel in the north (just west of Highway 395; Fig. 5A) and the Stanislaus paleochannel in the south (at the east margin of Fig. 5C; south of Highway 4).

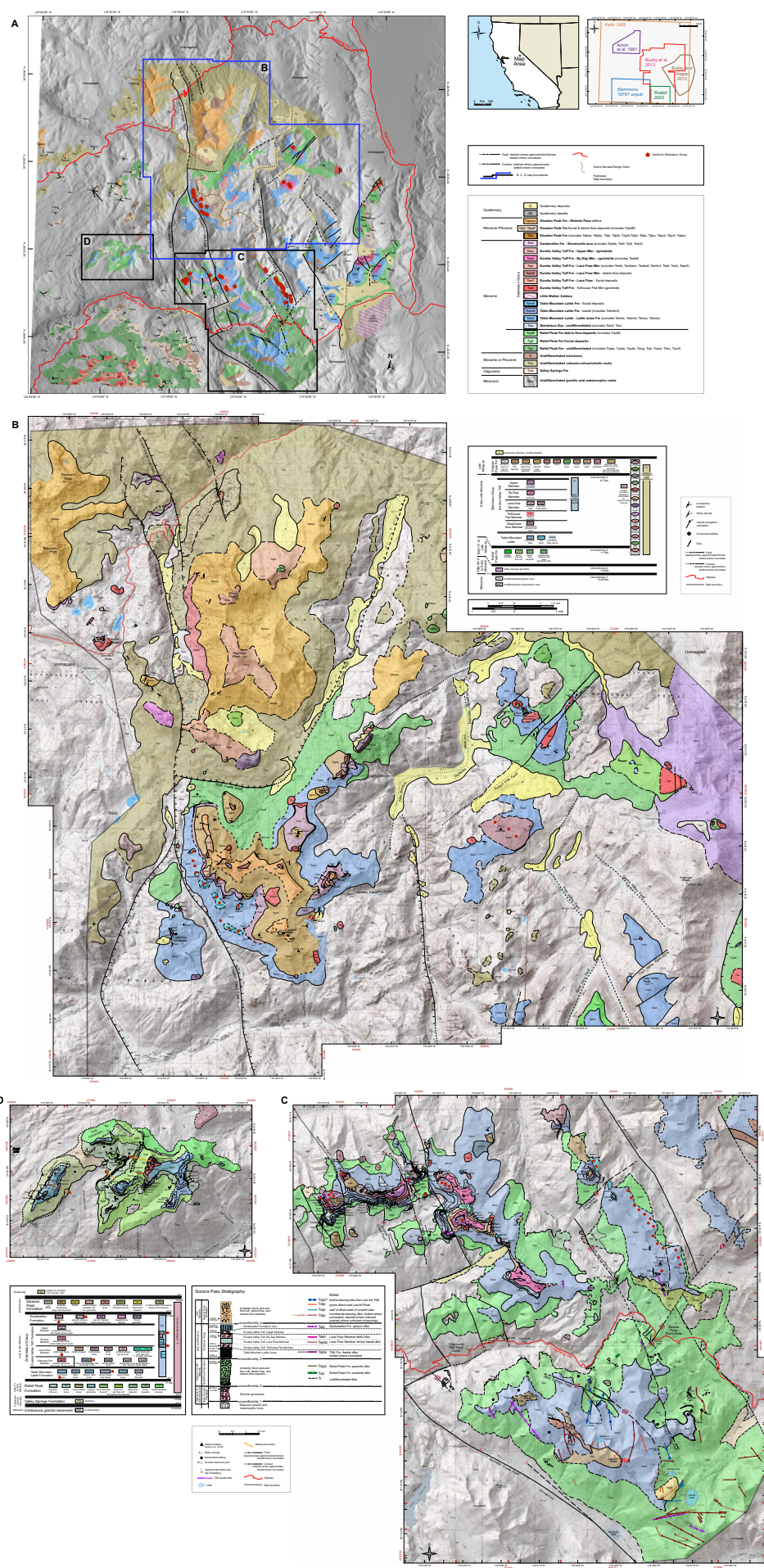


**Figure 5. Geologic maps of Tertiary rocks of the Sonora Pass to Ebbetts Pass area, central Sierra Nevada, and detailed maps and corresponding keys. Detailed maps are presented separately to focus on the Tertiary volcanic rocks (Mesozoic basement, largely granitic, is not divided). Although ~66% of this mapping was published piecemeal (Busby et al., 2013a, 2013b), this map brings all the data together into one regional-scale map for interpretation of the paleochannels and their disruption by Walker Lane faults. All mapping was done between 2001 and 2012 (by Busby and graduate students Jeanette Hagan, Alice Koerner, Ben Melosh, Dylan Rood and postdoctoral researcher Graham Andrews) and draws on work by Slemmons (1953), Keith et al. (1982), and Huber (1983a, 1983b). (A) Generalized geologic map of Tertiary volcanic rocks, showing locations of more detailed maps; major map units shown on this key are further divided in the keys to the detailed maps. Insets on upper right show location and previous mapping. Red stars highlight vents for Stanislaus Group volcanic rocks. Geology along the southwestern part of this map (to the west of map in C) is based partly on Roelofs (2004) between Kennedy Creek and Relief Reservoir, and to the west of that (west of Relief Reservoir south of Highway 108) is based on an unpublished map made by Slemmons in 1979 and provided to us by David Wagner (California Geological Survey), with field modifications made by Busby. Geology along the northwest margin part of this map, west of map in B, is based largely on mapping by Keith et al. (1982) (field modifications made by Busby). Geology along the eastern margin of the map, to the east of maps B and C, was described in detail in Busby et al. (2013a). (B) Detailed geologic map of Ebbetts Pass region. The geology in the north half of the map (Highland Peak–Ebbetts Pass–Raymond Peak area) has not been previously published, and is modified from Hagan (2010). The geology of the Lightening Mountain–Arnot Peak–Disaster Peak–Mineral Mountain area was described in detail in Busby et al. (2013a). (C) Detailed geologic map of the Sonora Pass region (described in Busby et al., 2013a). (D) Detailed geologic map of The Dardanelles area, not previously published, modified from Koerner (2010). TML—Table Mountain Latite; u/c—unconformity; hbl—hornblende. To view the map at full size (poster size), please visit <http://dx.doi.org/10.1130/GES01182.S1> or the full-text article on [www.gsapubs.org](http://www.gsapubs.org).**

In this paper we show for the first time that the Cataract paleochannel became deranged during the development of the Sierra Crest graben, and flowed northward within the graben during deposition of sequence 4 (ca. 9 Ma or younger), as the deranged Cataract paleochannel (Fig. 2B; see Disaster Peak Formation [Tdp] in the Disaster Peak–Arnot Peak area of Fig. 5B). Also for the first time, we present geologic mapping of the Mokelumne paleochannel (Fig. 2B), which crosses the modern Sierra Nevada range crest at Ebbetts Pass (Figs. 2B and 5). Henry et al. (2012) inferred that a Nevadaplano paleochannel crosses here because of the presence of Valley Springs Formation at the pass (Tvs, Fig. 5), and Wakabayashi (2013, fig. 2 therein) indicated a paleochannel here on a Sierra-wide image. Our study is the first to describe the width, length, and fill of this paleochannel using Oligocene to Pliocene deposits (Fig. 5A, described in the following).

## ■ APPROACH TO PALEOCHANNEL DESCRIPTION

Our description of the newly recognized paleochannels is divided into two main parts. In part I, we provide detailed descriptions of the best-exposed paleochannel segments, in order to give a clear picture of their volcanic-volcaniclastic fill, focusing on features that allow distinction of paleochannel fill. In part II, we provide an overview of the paleochannels, describing their history and their derangement, from south to north, in the order they were deranged.

## ■ PART I. CATARACT PALEOCHANNEL AND DERANGED CATARACT PALEOCHANNEL

Our description of the Sonora Pass–Ebbetts Pass region begins with the Cataract paleochannel, because it is the best exposed and best preserved and has therefore been given the most attention (Figs. 5–10). First, we describe a segment of the Cataract paleochannel at The Dardanelles (Fig. 2B) because that segment has not been disrupted by faults or vents, and preserves a nearly complete Oligocene to Miocene (older than 9 Ma) stratigraphy (cf. Fig. 5D legend and Fig. 4 stratigraphy). The Dardanelles map and description were not previously published. Second, we provide a summary of the Cataract paleochannel in the Red Peak–Bald Peak area (Fig. 2B) in order to document the effects of faulting and fault-controlled volcanic venting on Oligocene to Miocene (older than 9 Ma) stratigraphy in the Cataract paleochannel, during the onset of paleochannel derangement (Figs. 5C, 9, and 10). Although these faults were described elsewhere (Busby et al., 2013a), the volcanosedimentary record of the onset of paleochannel derangement have not. Third, we provide for the first time a description of the deranged north-northwest Cataract paleochannel (Fig. 2B), which contains fill younger than that of the east-west Cataract paleochannel (younger than 9 Ma).

## Undisrupted East-West Cataract Paleochannel at The Dardanelles

This area contains a nearly complete, unfaulted stratigraphic section through the distinctive, regionally extensive, well-dated units of the high-K Stanislaus Group (Figs. 4 and 5), preserved in the Cataract paleochannel (Fig. 2B). As Ransome (1898, p. 24) wrote, “Probably no known area in the Sierra Nevada presents a more interesting succession of volcanic rocks than the cluster of peaks known as The Dardanelles.” However, no detailed geologic maps and descriptions were made of the area before our study (Fig. 5D).

### Unconformity 1 and Sequence 1

The Oligocene to early Miocene Valley Springs Formation (Tvs) overlies Mesozoic (mainly Cretaceous) mesozonal granitic rocks unroofed in Late Cretaceous to Paleocene time, producing unconformity 1 (Fig. 6A). The Valley Springs Formation here consists largely of nonwelded to welded rhyolite ignimbrites (Fig. 6A) deposited on unconformity 1; fluvially reworked rhyolite tuff is locally present, and together these deposits form sequence 1 (Fig. 8A). The Valley Springs Formation is visible from a distance because it forms the whitest rocks in the region (Figs. 7C, 7D). To our knowledge, the Valley Springs Formation has not been dated at The Dardanelles.

### Unconformity 2 and Sequence 2

The Valley Springs Formation is deeply incised along unconformity 2, which is overlain by sequence 2 andesitic volcaniclastic rocks of the Relief Peak Formation (Figs. 4 and 5D). Unconformity 2 is an extremely irregular surface, with as much as 600 m paleorelief, and in most of The Dardanelles, it merges with unconformity 1 (Figs. 5D and 6B). The Relief Peak Formation is defined as andesitic volcaniclastic rocks underlain by the Valley Springs Formation and overlain by high-K volcanic rocks of the Stanislaus Group (Slemmons, 1953; Fig. 4).

The basal Relief Peak Formation at The Dardanelles (Figs. 5D and 6B) consists of interstratified fluvial deposits (Trpf) and debris flow deposits (Trpdf), shown as undifferentiated (Trpu) where fluvial and debris flow units were not mapped individually. These form the well-stratified basal deposits in the oblique aerial photos of Figures 7A and 7B. The debris flow deposits are crudely stratified, with dominantly angular clasts and poor sorting (Fig. 6B), while the fluvial deposits are well stratified, with rounded clasts, forming relatively well sorted clast-supported conglomerates, pebbly sandstones, and sandstones, locally with petrified wood (Figs. 6B, 8B–8C). In this segment of the Cataract paleochannel, the Relief Peak Formation has a much higher proportion of fluvial deposits (relative to debris flow deposits) than it does up-paleochannel in the Red Peak–Bald Peak section (described in the following).

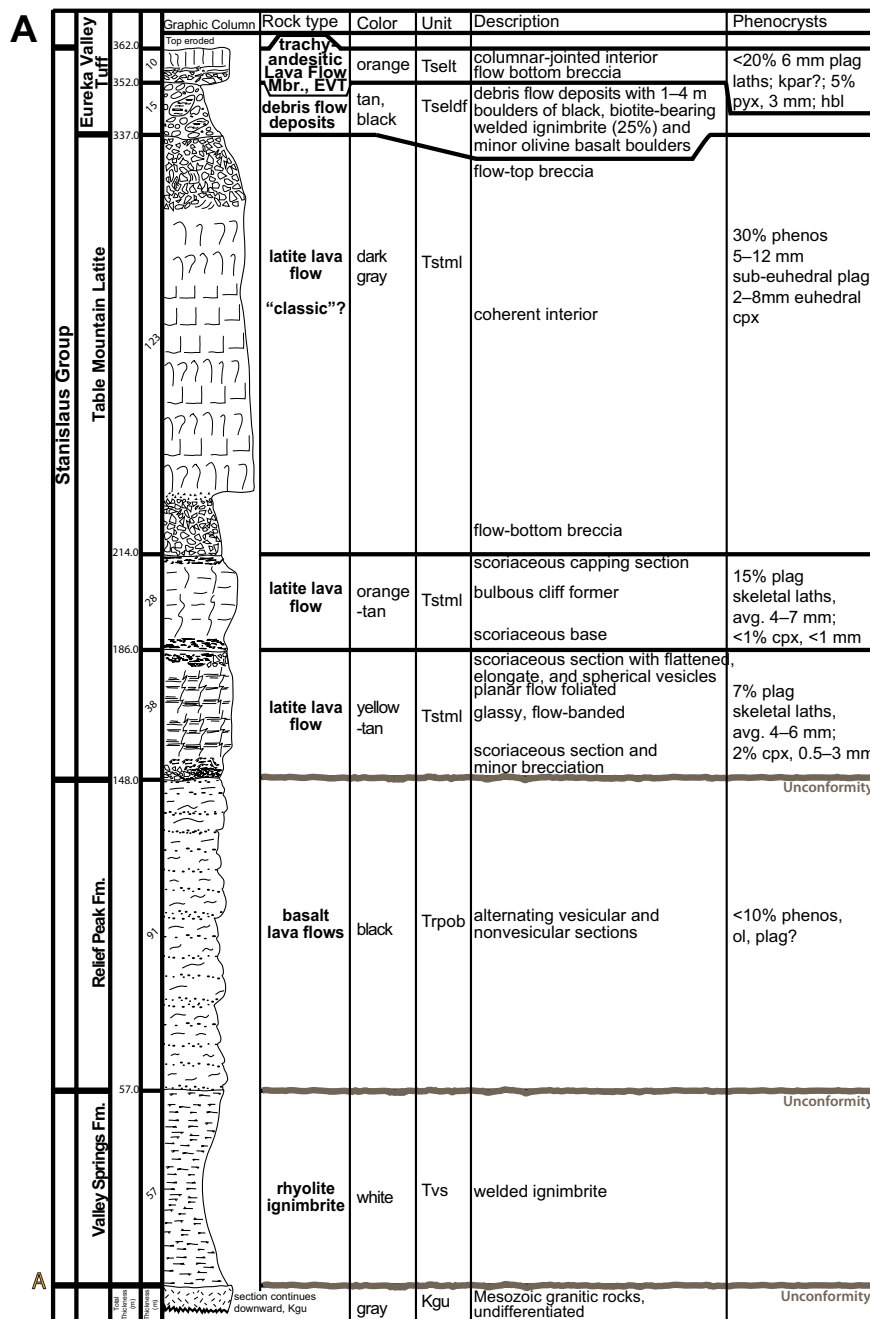


**Figure 6 (on this and following two pages).**  
Measured sections through Cataract paleo-channel fill. (A) The Dardanelles. (B) Dardanelles Cone (1—base, 2—top). Lines of section are plotted in Figure 5D. Measured by Koerner (2010). Plаг—plagioclase; cpx—clinopyroxene; pyx—pyroxene; ol—olivine; hbl, hb—hornblende; kpar—potassium feldspar; avg—average; xtal—crystal; phenos—phenocrysts; EVT—Eureka Valley Tuff; Mbr.—member; Fm.—formation; ss—sandstone.

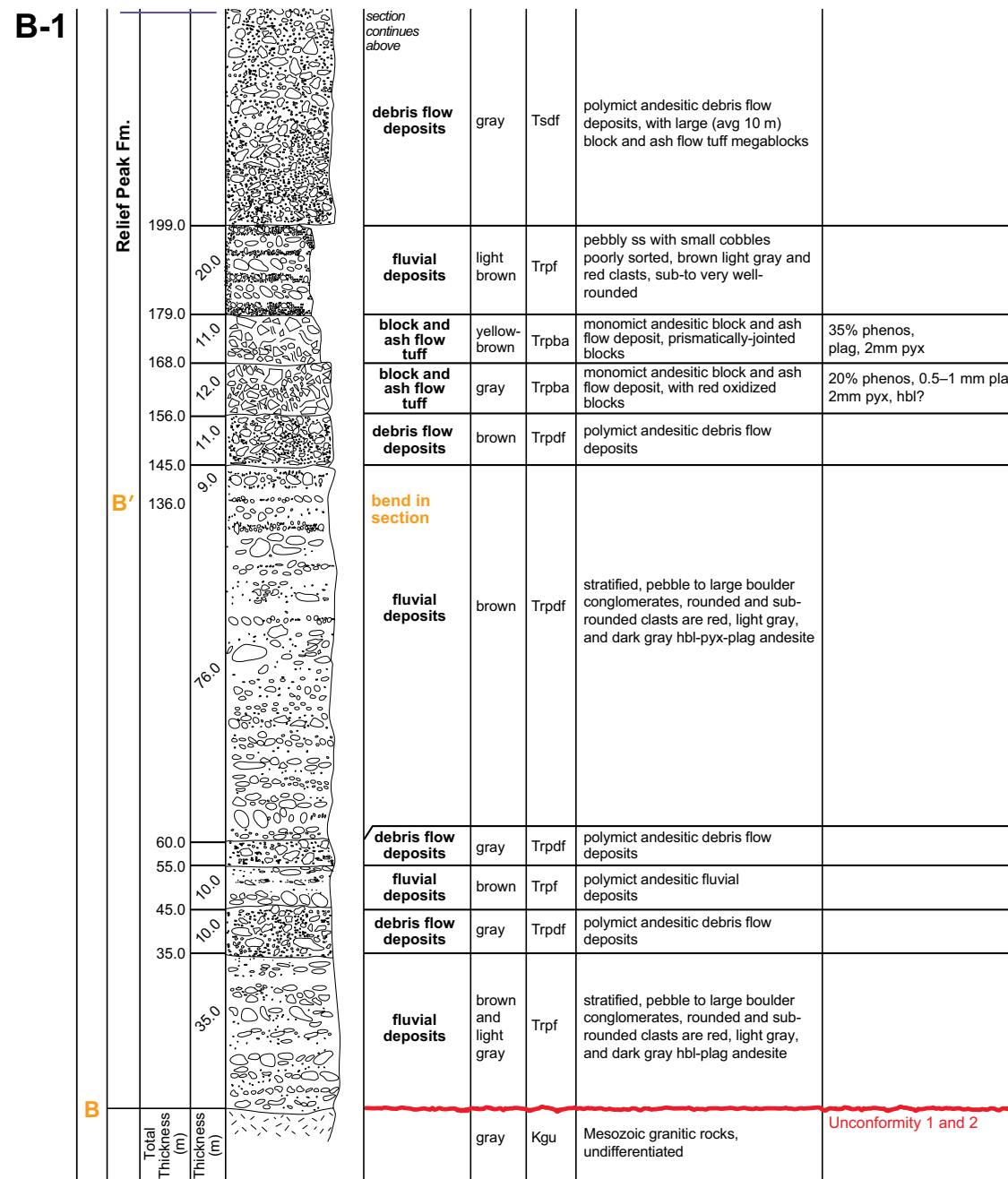


**Figure 6 (continued).**

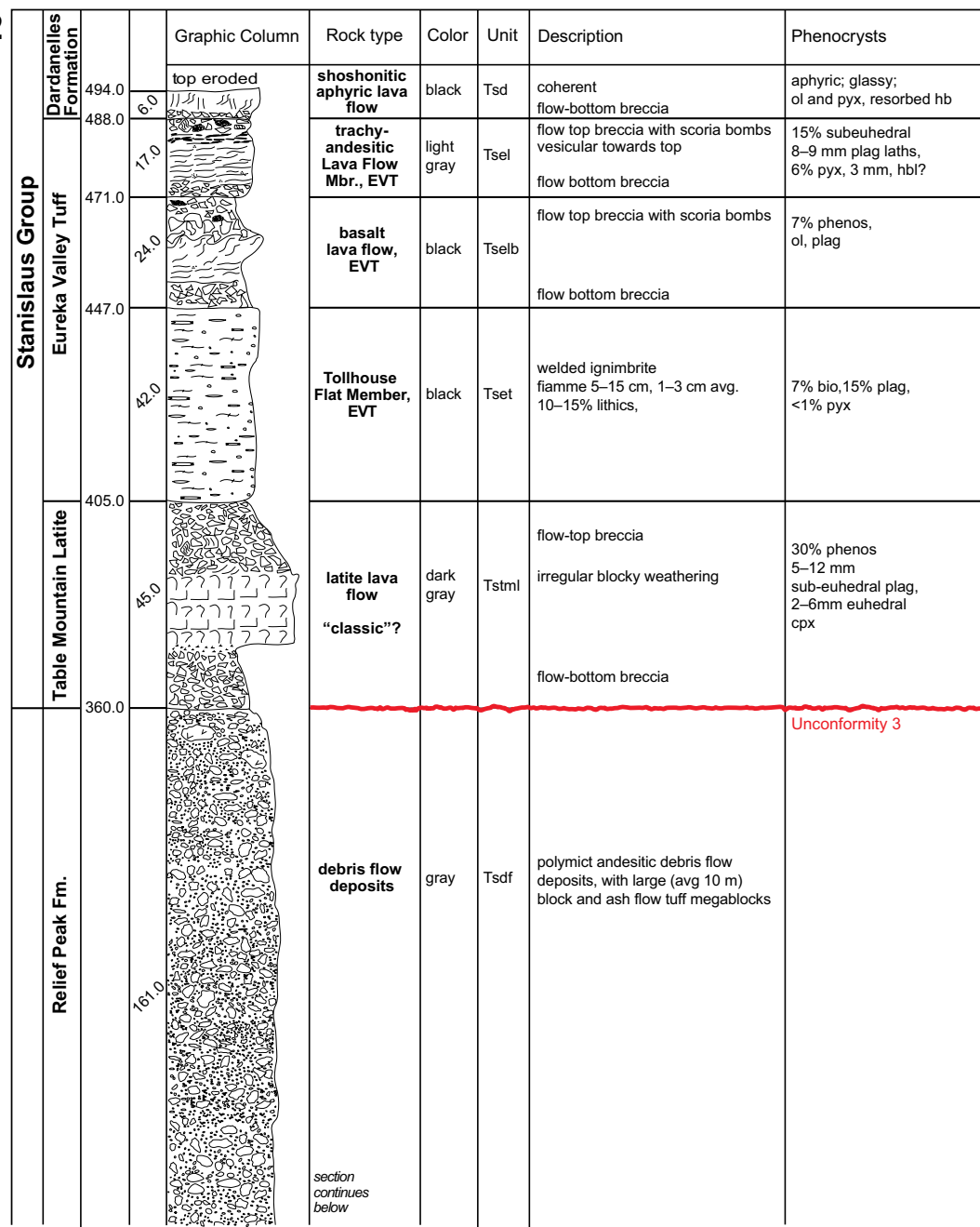
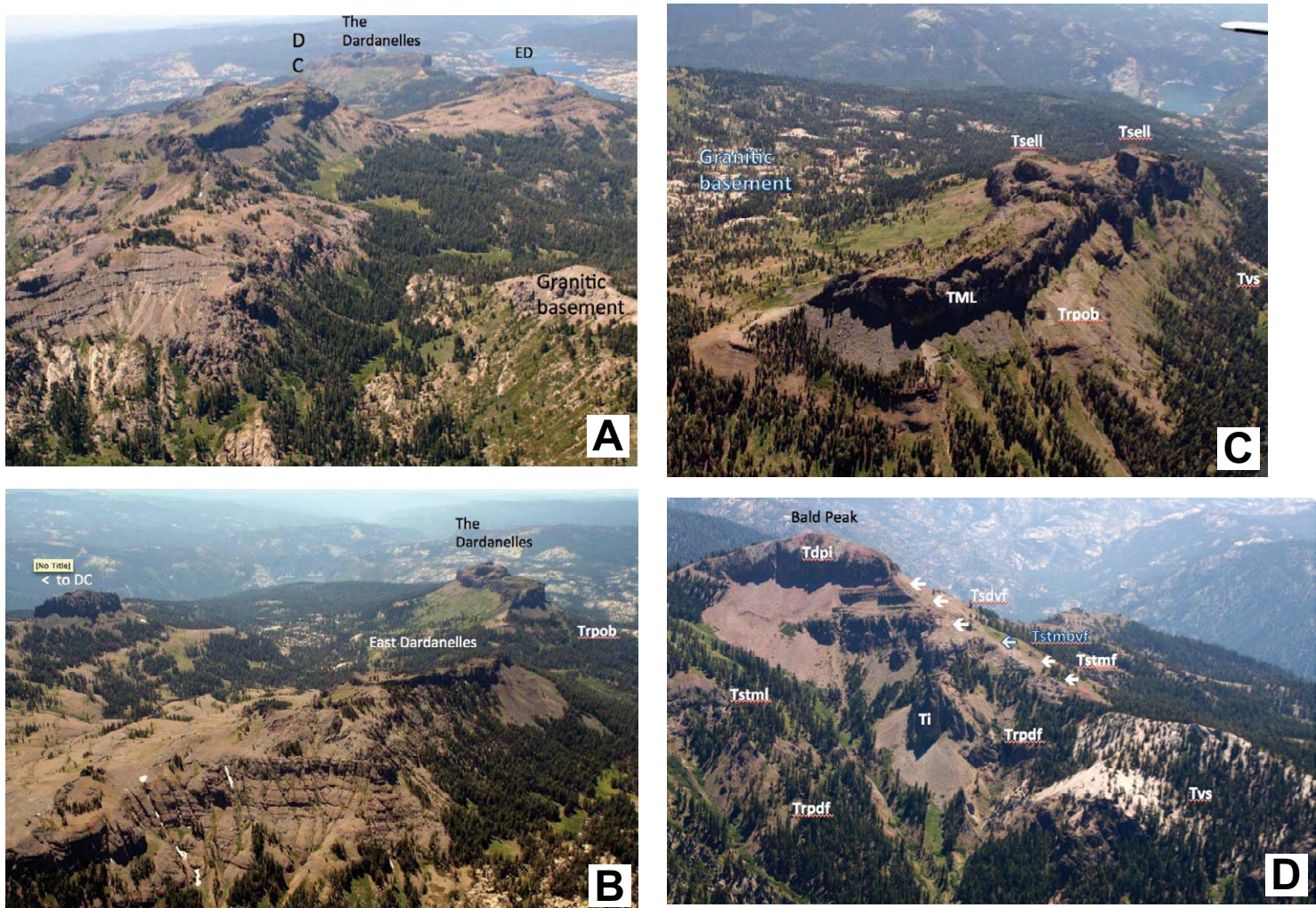
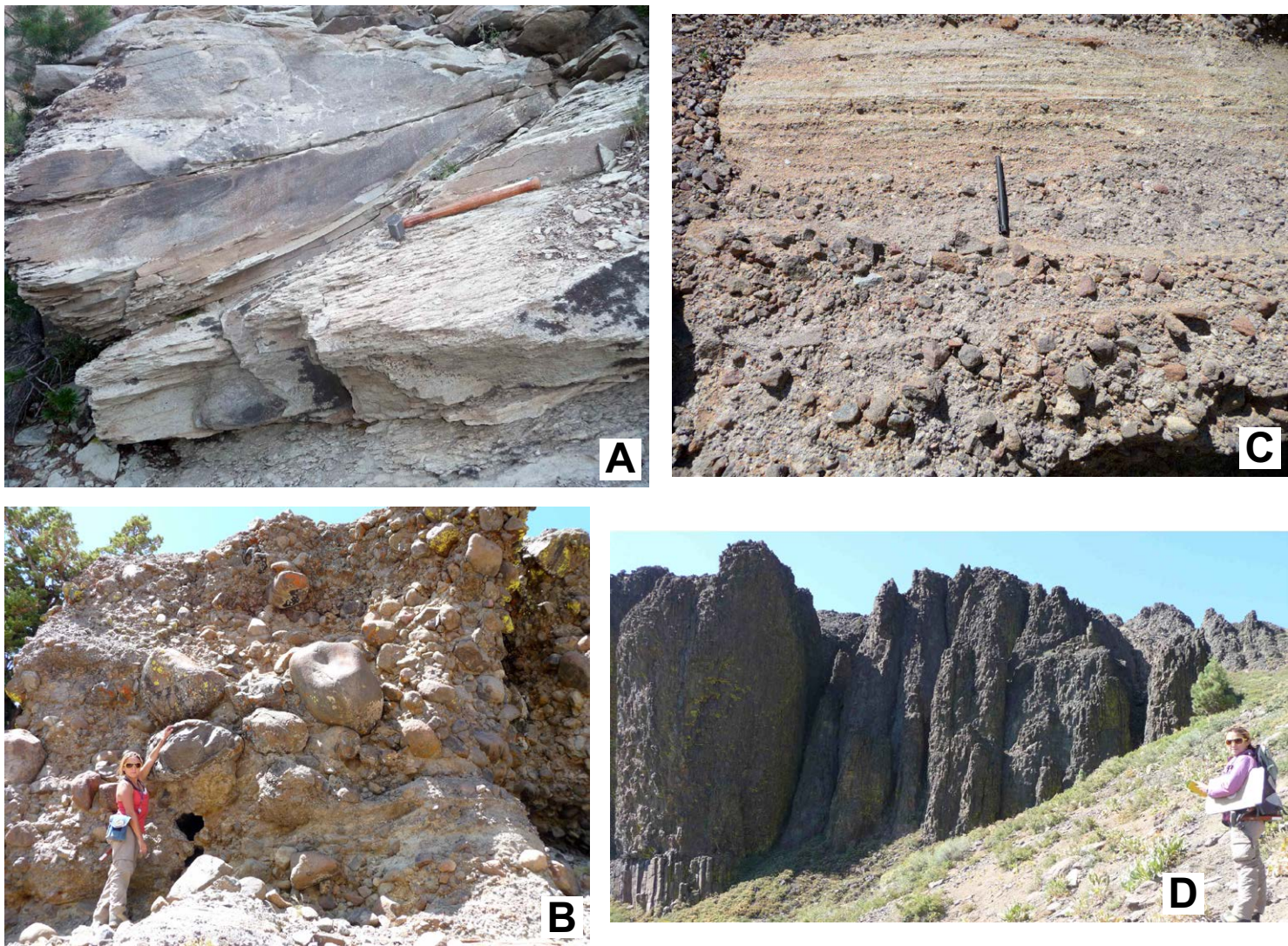
**B-2**

Figure 6 (continued).

**Figure 7.** Oblique aerial photos of the Cataract paleochannel (Fig. 3) in the central Sierra Nevada. (A) View toward the west down the Cataract paleochannel, toward Dardanelles Cone (DC); ED—East Dardanelles and The Dardanelles, mapped in Figure 5D. Dark-colored Miocene volcanic-volcaniclastic rocks overlie light-colored Mesozoic granitic basement with obvious erosional relief. In this view, basal paleochannel fill consists of stratified Relief Peak Formation fluvial and debris flow volcaniclastic rocks (shown in measured section in Fig. 6B). These are overlain by cliff-forming lavas of the Table Mountain Latite (Stanislaus Group, Fig. 4; measured section in Fig. 6B). Above, Dardanelles Cone consists of the Tollhouse Flat Member of the Eureka Valley Tuff and the peak is made of one of the few erosional remnants of the Dardanelles Formation (see Fig. 6B), a single shoshonite lava flow at the top of the high-K Stanislaus Group (Fig. 4), erupted from the western margin of the Sierra Crest graben (Peak 9798, Peak 10244 in Fig. 5C; Busby et al. 2013a). (B) View toward the southwest down the Cataract paleochannel, looking toward the East Dardanelles and The Dardanelles (Fig. 5D), showing stratified Relief Peak Formation fluvial and debris flow volcaniclastic rocks in the near foreground, overlain by cliff-forming trachyanesite and trachybasaltic andesite lavas of the Table Mountain Latite (TML) (Stanislaus Group, Fig. 4) on the East Dardanelles, The Dardanelles, and the unnamed ridge to the west-southwest of Dardanelles Cone, off the photo to the left. In the saddle between the East Dardanelles and The Dardanelles, soft, white rhyolite ignimbrites of the Valley Springs Formation (measured section in Fig. 6A) are overlain by stratified Relief Peak Formation (map unit Trpob; see Fig. 5D), which is here dominated by olivine basalt lavas (Fig. 6A; unit Trpob, Fig. 5D), in turn overlain by cliff-forming sheet-like lavas of the TML (Fig. 6A). These are overlain by erosional remnants of the Tollhouse Flat Member of the Eureka Valley Tuff (Fig. 4; not visible here), in turn capped by bulbous trachyanesite-trachydacite lavas we assign to the Lava Flow Member of the Eureka Valley Tuff (Figs. 4, 5, and 6A); these flows were previously erroneously assigned to the Dardanelles Formation. (C) Close-up of The Dardanelles (view toward southwest; Donnells Reservoir in distance). White rocks on the far left are Mesozoic granitic basement rocks exposed in McCormick Creek (Fig. 5D), with The Dardanelles ridge formed of volcanic rock through topographic inversion. The relatively soft, partly talus-covered section below the cliffs is made of multiple thin olivine basalt lava flows of the Relief Peak Formation (map unit Trpob; see Figs. 5D and 6A), overlying in erosional unconformity the Valley Springs Formation. Cliff-forming lavas of the TML are sheet like, whereas overlying trachyanesite-trachydacite lavas of the Lava Flow Member of the Eureka Valley Tuff are more bulbous (Tsell, Fig. 5D; also shown in Fig. 6A). A small remnant of the basal Valley Springs Formation is visible at the base of the section in the light colored area above Tvs (mapped in Fig. 5D); this soft material partly gave way in a debris flow (not mapped) produced during the 1996–1997 El Niño year rain-on-snow event, which may have enhanced rainfall here by orographic lifting along the vertical cliff above (Tollhurst, 2012). (D) Cataract paleochannel fill at Bald Peak (west end of Fig. 5C), up-paleochannel from The Dardanelles (Fig. 5D); view is toward the south, of the north face of Bald Peak. This is in a syndepositionally faulted part of the paleochannel fill (see text; see also Busby et al., 2013a). In contrast to the unfaulted paleochannel fill at The Dardanelles, the faulted paleochannel fill in the Red Peak–Bald Peak area contains vent facies deposits of the Stanislaus Group (red stars in Figs. 5A, 5C). The two major cliffs are formed of younger intrusions; the one that forms Bald Peak (Tdpi) is assigned to the Disaster Peak Formation because it intrudes the Stanislaus Group and is dated as  $7.28 \pm 0.06$  Ma (Fig. 4), although no strata of Disaster Peak Formation age occur in the Cataract paleochannel (sequence 4 of Fig. 4) because it was beheaded by that time. The intrusion lower on the slope (Ti) is undated. Well-stratified light gray fluvial deposits formed of TML clasts (Tstmf) directly overlie the Valley Springs Formation (i.e., unconformities 2 and 3 are merged, Fig. 4) at the base of a narrow, small paleochannel cut into Relief Peak Formation debris flow deposits (Trpdf) along unconformity 3. The base of this small channel cuts upsection around the west flank of the mountain, to overlie TML lavas (Fig. 5C); there the TML fluvial deposits are overlain by a basalt lava, which maps around to the north face (visible here) into basalt cinder cone deposits, mapped as TML vent facies (Tstmbvf). More fluvial deposits are above that on the south side of Bald Peak, indicating that the Cataract paleochannel continued to function despite the volcanism, and an ignimbrite sourced from the Little Walker caldera (Tollhouse Flat Member of the Eureka Valley Tuff, the most widespread ignimbrite) flowed down the channel (not visible in this photo). That is overlain by a Dardanelles Formation lava flow that is overlain by, and strikes into, a 200-m-thick section of Dardanelles Formation cinder cone deposits mapped as Dardanelles Formation vent facies (Tsdvf, visible here). This signals the demise of the Cataract paleochannel, because Dardanelles Formation lava forms the top of the fill down-paleochannel at Dardanelles Cone (Figs. 5D, 7A), and no younger units (Disaster Peak Formation) occur as inset paleochannel fill anywhere down the paleocanyon.





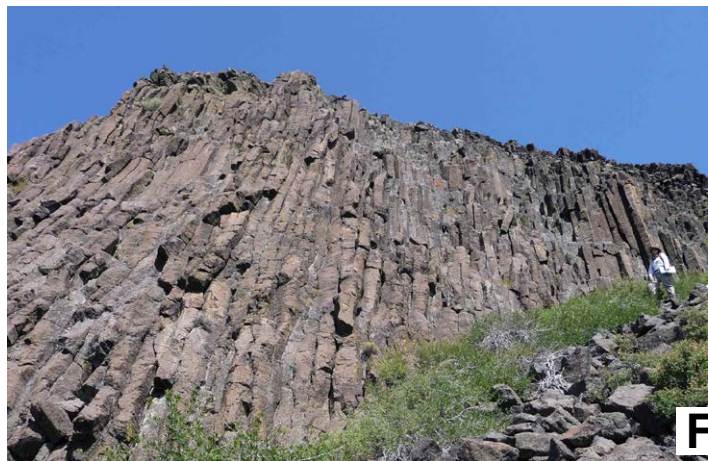
**Figure 8 (on this and following three pages).** Outcrop photos of paleochannel deposits, shown to illustrate the stratigraphic sequence shown in Figure 4. (A) Sequence 1: Fluvial cross beds in white rhyolite tuff of the Valley Springs Formation (Tvs, Sequence 1, Fig. 4); this is unusual because the Valley Springs Formation is dominated by welded ignimbrites. This fluvially reworked Valley Springs Formation is *not in situ*; the photo comes from a 200-m-long slide block within the Sierra Crest graben (near Sardine Falls, southeast corner of Fig. 5C). The slide block also contains nonwelded and welded white rhyolite ignimbrite. (B) Sequence 2: Relief Peak Formation andesitic boulder conglomerate in the Cataract paleochannel at East Dardanelles, showing clast-supported fluvial deposits with rounded clasts (Trpf, Fig. 5D). (C) Sequence 2: Relief Peak Formation andesitic cobble-breccia conglomerate, pebbly sandstone, and sandstone in the Cataract paleochannel at East Dardanelles, showing stratification, clast-supported textures, and cut and fill structures typical of fluvial deposits. (Trpf, Fig. 5D). (D) Sequence 2: Cliff-forming block-and-ash-flow tuff at the top of the Relief Peak formation in the Cataract paleochannel at East Dardanelles (Trpba, Fig. 5D), showing its massive character.



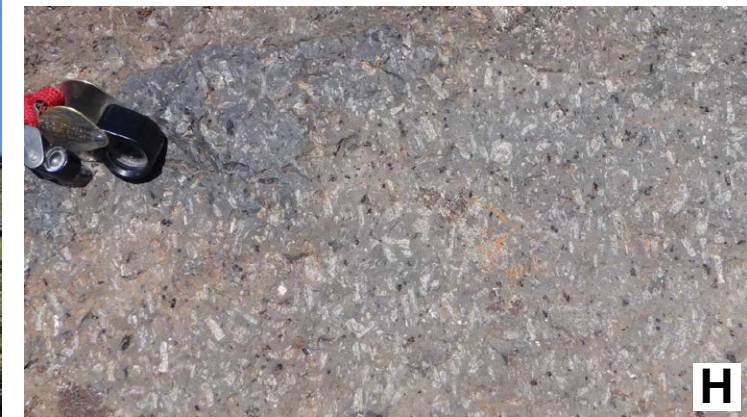
E



G



F



H

**Figure 8 (continued).** (E) Sequence 2: Closeup of the cliff-forming block-and-ash-flow tuff shown in Figure 8D (boot for scale). Massive, unsorted monomict angular andesite tuff breccia is interpreted to represent a lava dome collapse deposit. (F) Sequence 3: Table Mountain Latite lava ponded in a channel within the larger Cataract paleochannel at The Dardanelles (Tstml, Fig. 5D); person on right side for scale. This lava is 123 m thick on the measured section shown in Figure 6A. (G) Sequence 3: Kuppaberg texture on the top of a TML lava on The Dardanelles (Tstml, Fig. 5D). We find no kuppaberg texture in TML lavas ponded in grabens, only in those within paleochannels, which presumably had water flowing over the top of them. (H) Sequence 3: Distinctive outcrop appearance of TML lavas, with large, sieve-textured plagioclase and smaller black pyroxene (hand lens for scale).

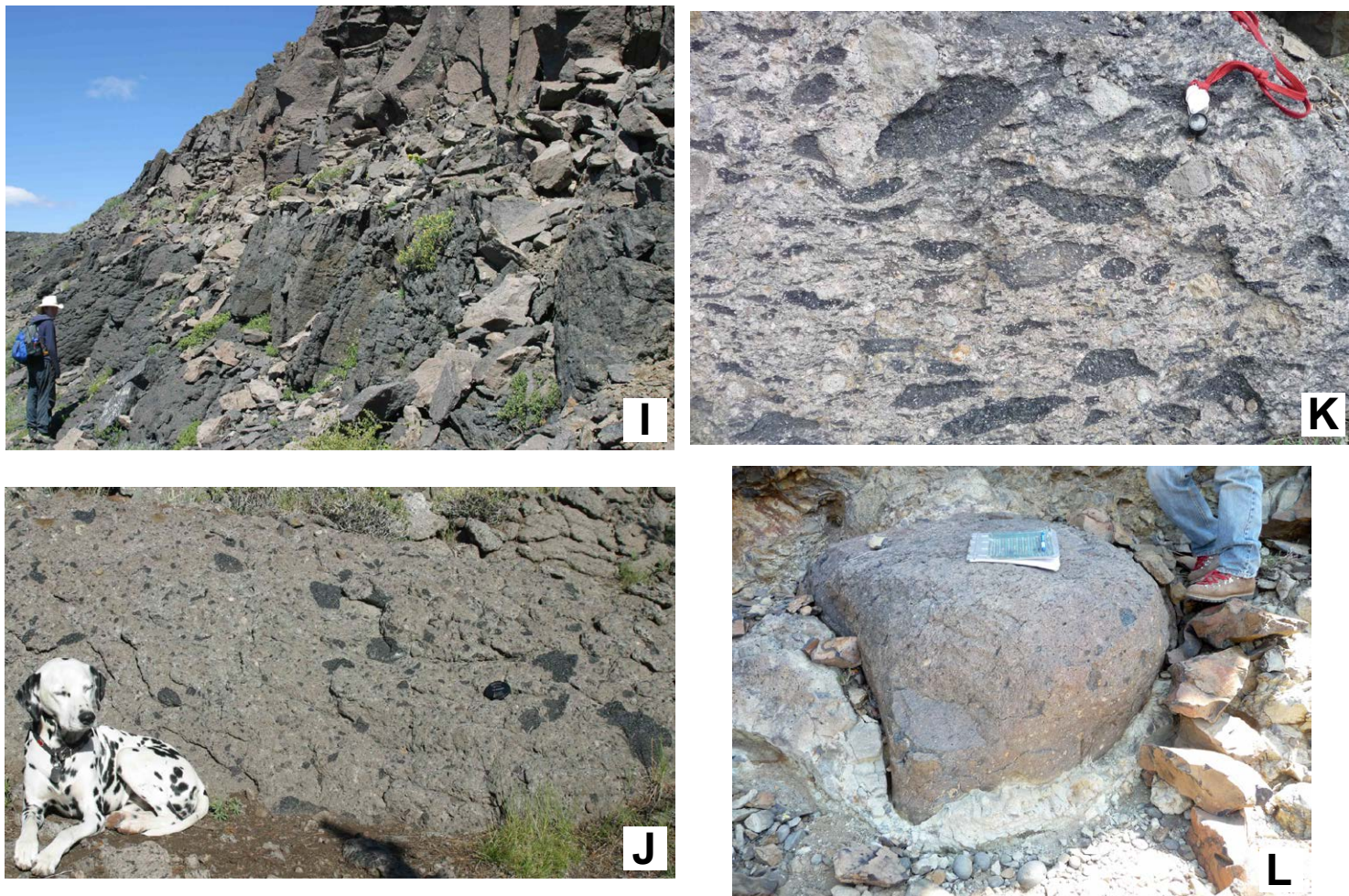


**Figure 8 (continued).** (I) Sequence 3: Basal black basal vitrophyre in densely welded ignimbrite, which is present at the base of both the Tollhouse Flat Member and the By-Day Member of the Eureka Valley Tuff (Fig. 4), each of which form a single cooling unit. In this photo, the basal black densely welded vitrophyre passes upward into gray moderately welded ignimbrite, but in many places, only the black basal vitrophyre is preserved. (J) Sequence 3: Typical outcrop photo of a moderately welded part of the most widespread unit of the high-K Stanislaus Group (Fig. 3), the Tollhouse Flat Member of the Eureka Valley Tuff (Fig. 4). This ignimbrite was erupted at the Little Walker caldera and flowed down both the Stanislaus and Cataract paleochannels (Fig. 2B), while less mobile lavas of the underlying TML did not flow down the Stanislaus paleochannel (Fig. 5A). The black fragments are nonflattened obsidian fragments erupted together with white pumice and black glassy blocks that were hot enough to become flattened. (K) Sequence 3: Closeup of strongly welded Tollhouse Flat Member of the Eureka Valley Tuff, showing flattening of glassy blocks, with accordion terminations, and angular white silicic volcanic rock fragments. Hand lens for scale. (L) Sequence 3: Close-up of the boulder of Tollhouse Flat Member in the boulder conglomerate shown in Figure 8M. Welding of the ignimbrite instantaneously made it into a rock that could be eroded into boulders by reincision within the paleochannel.

**Figure 8 (continued).** (M) Sequence 3: Lava Flow Member trachydacite lava overlying ~20 m thick boulder conglomerate with boulders of welded Tollhouse Flat Member. The bulbous nature of the trachydacite lava contrasts with the sheet-like character of TML trachyandesites and trachybasaltic andesites (contrast also evident from oblique air photo, Fig. 7C). The top of the lava has kuppaberg joints, like those in the TML (see Fig. 8G), consistent with emplacement into a river channel. (N) Sequence 3: Bulbous nature of Lava Flow Member trachydacite lava, which forms the top of The Dardanelles (Fig. 5D).

Like the paleo-upstream equivalents, the debris flow deposits commonly contain megablocks of block-and-ash flow tuff as much as 10 m in diameter; this suggests a steep axial gradient for the paleochannel (whereas megablocks in the syndepositionally faulted paleochannel reach at Red Peak–Bald Peak could be attributed to intrachannel faulting). Approximately 1.6 km west of Dardanelles Cone (Fig. 5D), the debris flow deposits contain 20-m-long slide blocks of andesite with globular peperite margins encased in fluvial sandstone, suggesting intrachannel remobilization by the intrusive process (see examples in Busby et al., 2008b). The anomalous dip in the Relief Peak Formation below the East Dardanelles ( $15^{\circ}$ E; Fig. 5D) is a soft-sediment slump.

An ~200-m-deep erosional surface is cut into the Relief Peak Formation fluvial-debris flow sections and into the underlying Valley Springs Formation, and overlain by a section of olivine basalt lavas as much as 200 m thick (Trpob), first recognized by Ransome (1898), which we assign to the Relief Peak Formation (Figs. 5D, 6A, 7B). Basalts are very rare in the Relief Peak Formation (but common in all younger formations, as described in the following). Gilbert et al. (1968) reported small-volume basalts intercalated with Relief Peak Formation andesites in the Mono Basin area, and Priest (1979) found olivine basalts below and within the Relief Peak Formation in the Devil's Gate area near Bridgeport (Fig. 3). However, the olivine basalt lavas at The Dardanelles are the only ones that have been found so far within the Relief Peak Formation in the Sierra Nevada, and the vent for them has not been found.

The Relief Peak Formation basalt lavas directly overlie Valley Springs Formation ignimbrites and granitic basement at an elevation of 2377.4 m (7800') at the head of McCormick Creek (see map unit Trpob with horizontal dip symbol; Fig. 5D). They are also deeply inset into Relief Peak Formation fluvial deposits on the lower slopes of The Dardanelles, but that erosional surface rises quickly in elevation to the northeast toward the East Dardanelles, from 2273.8 m to 2560.3 m (7460' to 8400'), with relief of 287 m over a horizontal distance of <700 m, showing the complexity of the reincision surfaces in the paleochannel (Fig. 5D). Andesitic volcaniclastic rocks (Trpu, Fig. 5D) intervene as lenses between the olivine basalt lavas and the TML (of sequence 3), which is why we assign the basalts to the Relief Peak Formation rather than the Stanislaus Group (where basalts are common, Fig. 5); andesitic “conglomerate” lenses (actually volcanic breccia; see photo in Ransome, 1898, p. 25) were also described at this stratigraphic position by Ransome. The Relief Peak Formation olivine basalt sequence has as many as



M



N

17 lavas, separated by vesiculated tops (Fig. 6A). The lavas are porphyritic to nearly aphyric, with plagioclase and olivine (locally altered to iddingsite). The 200-m-thick section of basalt lavas on the lower slopes of The Dardanelles is not well exposed, but at the head of McCormick Creek, the basal basalt lava is spectacularly well exposed. There, columnar joints in this flat-lying lava plunge  $60^{\circ}$ NNE against the cooling surface formed by the deep erosional surface (unconformity 2) cut into Valley Springs Formation within the paleochannel.

The upper part of the Relief Peak Formation has a variety of block-and-ash flow tuffs, at several stratigraphic levels, mapped individually at the head of McCormick Creek and on either side of it (Trpba, Fig. 5D; see Figs. 6B, 8D, 8E).

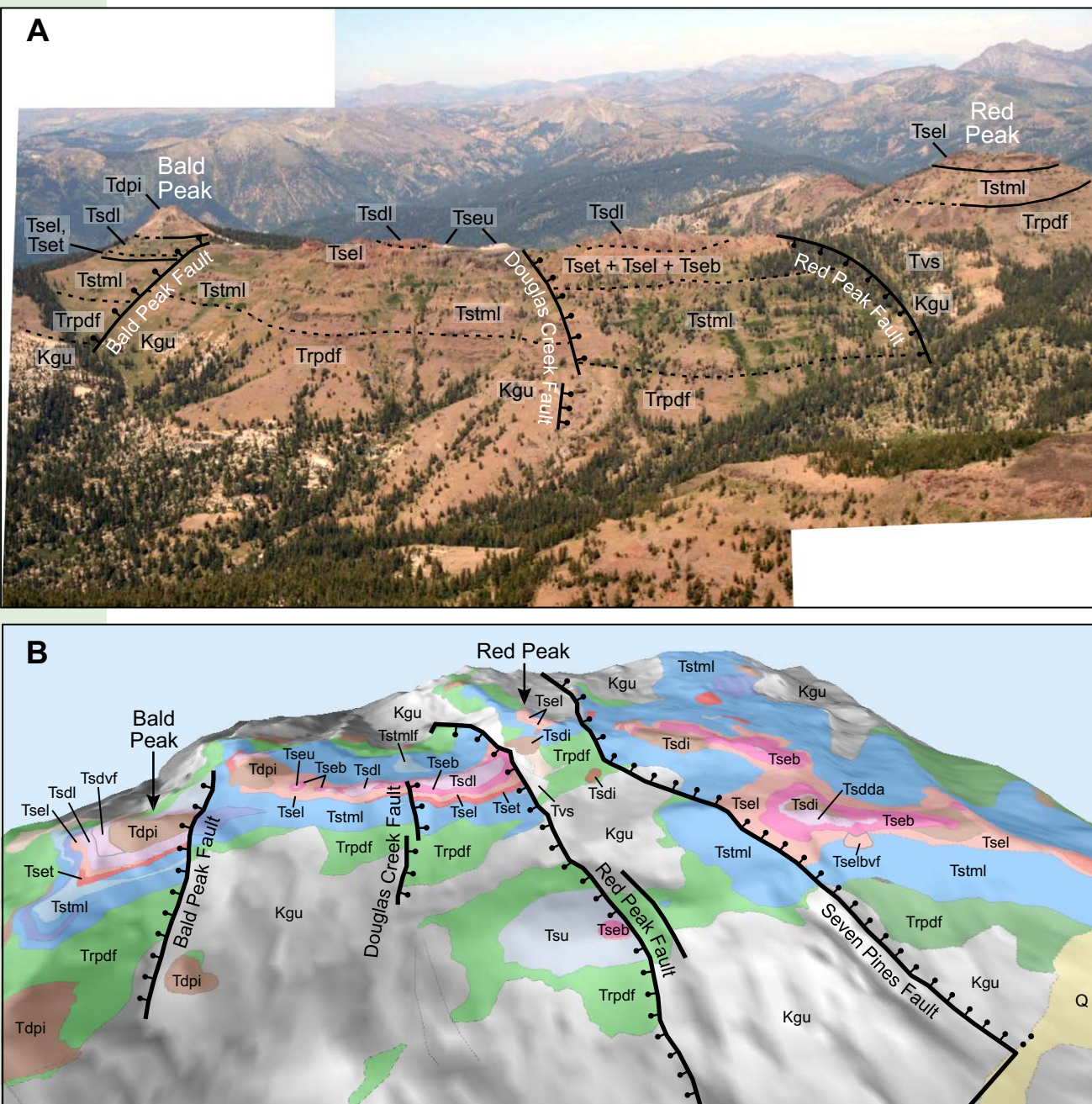


**Figure 9.** (A) View of the syndepositionally faulted Cataract paleochannel fill on the east-west ridge between Bald Peak and Red Peak, immediately west of the Sierra Crest graben (Fig. 2B), showing superior exposure of stratigraphy and faults. (B) Oblique map view of Bald Peak–Red Peak ridge, which extends further eastward to include the Seven Pines fault, which forms the western boundary of the Sierra Crest graben (geology simplified from Fig. 5C; see text for description). Tvs—Valley Springs Formation. Trpdf—Relief Peak Formation andesitic debris flow deposits. Ts—Stanislaus Group high-K volcanic rocks, divided here into Table Mountain Latite lava flows (Tsmf), Eureka Valley Tuff Tollhouse Flat Member welded ignimbrite (Tvset), Eureka Valley Tuff Lava Flow Member (Tsel) that includes basalt vent facies (Tselbvf), Eureka Valley Tuff By-Day Member welded ignimbrite (Tseb), and Eureka Valley Tuff Upper Member nonwelded ignimbrite (Tseu). Td—Dardanelles Formation shoshonite, including lava flow (Tsdl), intrusions (Tsdi), vent facies deposits (Tsdvf), and a debris avalanche deposit (Tdd). Tdp—Disaster Peak Formation andesitic intrusions.

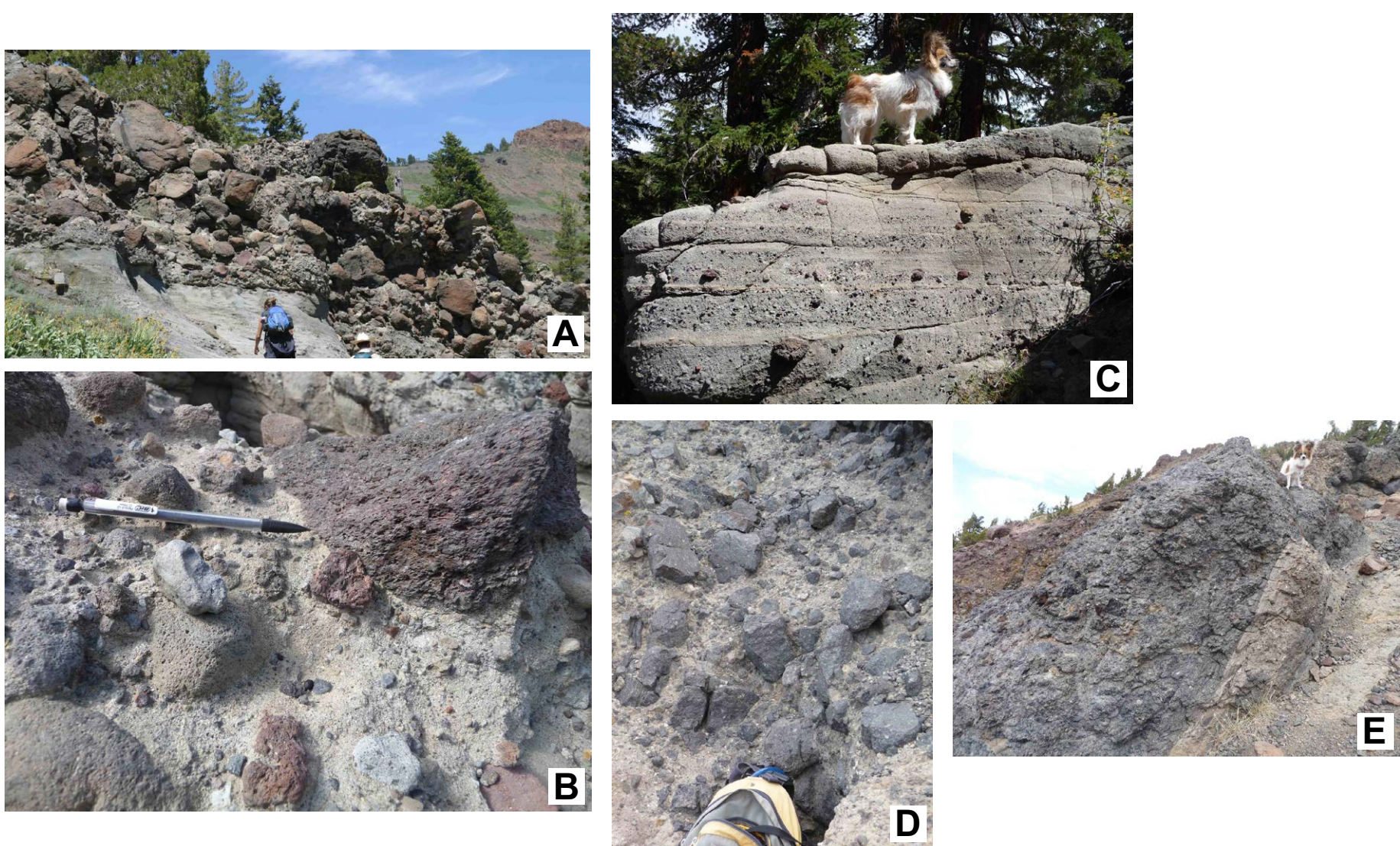


**Figure 10.** Outcrop photos of paleochannel deposits in the syndepositionally faulted Bald Peak–Red Peak segment of the Cataract paleochannel (Figs. 2B and 5C). (A) 1–2-m diameter boulders deposited on a syndepositionally downthrown block in the Relief Peak Formation (sequence 2), on the hanging wall of the Bald Peak fault (Figs. 2B, 5C, 9). The Relief Peak Formation thickens dramatically into the hanging-wall graben (Fig. 5C; Busby et al., 2013a). We infer that these very large boulders mark the position of a plunge pool at the base of a fault-controlled waterfall in the Cataract paleochannel. (B) Typical debris flow deposit in Relief Peak Formation (Trpd, sequence 2, Fig. 4), with a variety of intermediate-composition volcanic clasts supported in a pebbly sandstone matrix. (C) Typical Relief Peak Formation (sequence 2) fluvial deposits, with relatively poor sorting and crude stratification typical of hyper-concentrated flood flow (2.2 kg Papillon for scale). (D) Fault-talus breccia composed of clasts of Tollhouse Flat Member of Eureka Valley Tuff, formed by syndepositional faulting within the Cataract paleochannel (mapped as Tseldf on Red Peak, Fig. 5C); compare these angular clasts with the rounded boulders of Tollhouse Flat Member in the nonfaulted paleochannel at The Dardanelles (Fig. 8L, 8M). This surrounds larger slabs shown in (E). Part of backpack for scale. (E) Avalanche slab of Tollhouse Flat Member of Eureka Valley Tuff formed by syndepositional faulting within the Cataract paleochannel (mapped as Tseldf on Red Peak, Fig. 5C). Stratigraphy is preserved within the slab (note tan bed at right), but the welded ignimbrite (black) is shattered, typical of slabs in a hard-rock avalanche.

These are generally more resistant than the debris flow or fluvial deposits (Fig. 8D). The block-and-ash flow deposits are massive, unsorted, nonstratified monomict angular andesite tuff breccias, interpreted to represent lava dome collapse deposits funneled down the paleochannel from domes somewhere upslope. Most have the hornblende and plagioclase phenocrysts typical of Relief Peak Formation, but there is also an unusual variety with sieve-textured plagioclase, pyroxene, and possible olivine, which is more typical of the Stanislaus Group (sequence 3, Fig. 4). One of these, a 10 m thick block-and-ash flow tuff near the top of the Relief Peak Formation on the south face of the East Dardanelles (Fig. 5D), is underlain by 2–3 m of white pumiceous deposits, which are very rare in the Relief Peak Formation; the only similar deposit is present in the Sierra Nevada range front at Sonora Pass (see fig. 9B of Busby et al., 2013b).

Block-and-ash flow tuffs at The Dardanelles could be sampled for dating by  $^{40}\text{Ar}/^{39}\text{Ar}$  to provide age controls on the Relief Peak Formation, which is generally only broadly constrained to be between the Valley Springs Formation (older than ca. 18 Ma) and the TML (younger than ca. 11 Ma) in age. There are no dates on Relief Peak Formation paleochannel fill, and the only dates on Relief Peak Formation graben fills are (1) a block-and-ash flow tuff within an avalanche deposit in the Sierra Crest graben at Sonora Pass ( $10.39 \pm 0.18$  Ma,  $^{40}\text{Ar}/^{39}\text{Ar}$ , Fig. 4; Busby et al., 2008a); (2) a minimum age on a Relief Peak debris flow section in the Grouse Meadows fault block on the range front, provided by an  $^{40}\text{Ar}/^{39}\text{Ar}$  hornblende date on a sill ( $12.15 \pm 0.04$  Ma; Busby et al., 2013b); and (3) a block-and-ash flow tuff within a debris flow section at the northernmost end of the Sierra Crest graben, with an  $^{40}\text{Ar}/^{39}\text{Ar}$  age of  $11.33 \pm 0.03$  (Busby et al., 2013c).

### Unconformity 3 and Sequence 3

At The Dardanelles (Fig. 5D), the unconformity beneath the TML (unconformity 3) does not have as much relief (~60 m) as it does regionally (the pre-Latite unconformity of Slemmons, 1953, 1966; unconformity 3 of Busby et al., 2008a, 2008b; Hagan et al., 2009; Busby and Putirka, 2009; Busby, 2012). Sequence 3 consists of high-K volcanic rocks of the Stanislaus Group (Fig. 4).

**Table Mountain Latite (sequence 3).** The basal formation of the high-K Stanislaus Group, the TML (sequence 3, Tstml, Fig. 5D), was referred to as a flood andesite in Busby et al. (2013a) because it is so voluminous, and because it erupted from fissure vents (Fig. 2B). It consists mainly of trachyandesite and trachybalsatic-andesite lavas, with minor basalt lavas (Busby et al., 2013a, 2013b). The TML is the major cliff former on Dardanelles Cone, East Dardanelles, and The Dardanelles (Figs. 7A, 7B, 7C, 8F). The TML is easily recognized by its sheet-like lavas with large, sieve-textured plagioclase and smaller black pyroxene (Fig. 8H), although some lavas in a section of the TML may lack pyroxene phenocrysts, or be phenocryst poor.

The TML lavas are mapped individually and correlated across The Dardanelles map area (Fig. 5D). The TML here has four lavas (Tstml 1–4) overlain

by a lava we informally mapped as classic TML (Tstmlc; Figs. 6A, 6B), which in places directly overlies the Relief Peak Formation (Fig. 5D). The classic TML is distinctive for its unusually abundant (~40%) phenocrysts of large (13 mm) euhedral skeletal plagioclase, with smaller euhedral clinopyroxene and minor altered olivine (Figs. 6A, 6B). This resembles the 44-m-thick lava with classic TML paleomagnetic remanence direction (Pluhar and Cox, 1996), which was vented 18 km to the east at Sonora Peak, and extends 120 km to the west from The Dardanelles to Knight's Ferry (Fig. 3), a total distance of nearly 140 km (Busby et al., 2008a, 2013a; Pluhar et al., 2009; Gorni et al., 2009). However, paleomagnetic studies at The Dardanelles are needed to confirm this correlation. The classic lava is by far the thickest lava in The Dardanelles map area (50–150 m thick, Tstmlc; Fig. 5D) and is a major cliff former (Fig. 8F). It forms the only TML lava on the East Dardanelles (Peak 8948' informally named in Fig. 5C). It has thick (~10 m) lower and upper breccias (Figs. 6A, 6B), and much of the coherent interior has columnar joints (Fig. 8F), commonly subvertical but in places inclined due to cooling against the sides of erosional surfaces within the paleochannel. The columnar-jointed basal section passes upward into a >10-m-thick cobble-jointed entablature referred to as kuppaberg jointing (Fig. 8G); this style of cooling joints is inferred to form when water penetrates vertical joints along the top of a cooling lava, causing secondary joints to form perpendicular to them (Walker, 1993). It is a feature of lava quenched by flowing water above. We infer that the lava was emplaced into the paleochannel in the presence of a river that was subsequently displaced onto the top of the cooling lava. In addition, river cobbles are entrained in the basal part of the TML on the south end of The Dardanelles.

The third latite lava in the TML in Dardanelles Cone area (Tstml3, Fig. 5D) is correlated with the second lava at The Dardanelles (also mapped as Tstml3) on the basis of lithology (see Koerner, 2010), including ~7%–10% pyroxene-olivine glomerocrysts that have not been observed elsewhere in the TML. This latite lava is also distinctive in chemical composition, because it borders on trachydacite in composition (but is a silicic latite; sample DC065, Busby et al., 2008a). The TML lavas beneath the classic lava generally lack breccia (Fig. 6A), and locally have basal tree molds as much as 1 m in diameter.

**Eureka Valley Tuff (sequence 3).** The TML is overlain by the Eureka Valley Tuff (also in sequence 3; Fig. 4). A brief general description of the Eureka Valley Tuff is given here, before the details of its features at The Dardanelles are described (Fig. 4). The Eureka Valley Tuff has three trachydacite ignimbrite members (Fig. 4): the Tollhouse Flat Member, the By-Day Member, and the Upper Member (cf. Busby et al., 2013a). The lower two trachydacite ignimbrites (Tollhouse Flat and By-Day Members) are welded, and each consists of a single cooling unit with a distinctive black basal vitrophyre (Fig. 8I); in many places, only the black basal vitrophyre is preserved, making a distinctive black sheet that can be recognized from great distances. In other places, the black vitrophyre passes upward into gray moderately welded ignimbrite (Figs. 8J) with black obsidian fragments of the same composition, and white silicic rock fragments (Fig. 8K). Some obsidian fragments are angular and not flattened, while others are flattened (Fig. 8K), sometimes with rigid and plastically deformed

blocks mixed together. The lower welded ignimbrite (Tollhouse Flat Member, Tset) is easily distinguished from the upper welded ignimbrite (By-Day Member, Tseb) by its abundant, large biotite crystals. The third ignimbrite of the Eureka Valley Tuff, referred to as the Upper Member (Tseu; Fig. 4; cf. Busby et al., 2013a), is a white nonwelded ignimbrite. All three ignimbrites of the Eureka Valley Tuff were erupted from the Little Walker caldera (Figs. 3 and 5A; cf. King et al., 2007).

Lavas between the Tollhouse Flat Member and the By-Day Member in the vicinity of the Little Walker caldera were referred to as the Latite Lava Flow Member by Priest (1979), but when Koerner et al. (2009) found trachydacite lavas at this stratigraphic level in the Stanislaus Group reference section at Bald Peak, the name was revised to Lava Flow Member (Tsel), to include trachydacites as well as trachyandesites and trachybasaltic andesites. Lavas of the Lava Flow Member were erroneously identified as Dardanelles Formation previously (cf. Koerner et al., 2009), but that formation is above the Upper Member (Fig. 4), and consists of a distinctive single glassy black aphyric lava (described in the following). Although the Lava Flow Member is commonly trachydacite, and thus relatively easily distinguished from the TML, it includes trachyandesites, trachybasaltic-andesites, and basalts, which can only be distinguished from the TML if the Tollhouse Flat Member (or detritus thereof) intervenes (Koerner et al., 2009; Busby et al., 2013a). The Lava Flow Member also includes basalt lavas (Busby et al., 2013a), including a basalt described here at The Dardanelles (Figs. 5D and 6B).

Another lava member has been recently identified at the base of the Eureka Valley Tuff (Fig. 4), referred to as the Basal Lava Flow Member (Fig. 4; Busby et al., 2013a); it is distinguished from the TML and the Lava Flow Member of the Eureka Valley Tuff by being a trachydacite lava that overlies the TML and is overlain by the Tollhouse Flat Member in the Bald Peak reference section (Chris Pluhar, 2013, written commun.). Because the TML has no trachydacite within it and the Eureka Valley Tuff Formation does, the trachydacite lava is assigned to the Eureka Valley Tuff. As described in Busby et al. (2013a), trachydacite lava of the Basal Lava Flow Member has an  $^{40}\text{Ar}/^{39}\text{Ar}$  age of  $9.94 \pm 0.03$  Ma (Fig. 4), which is older than the Tollhouse Flat Member ( $^{40}\text{Ar}/^{39}\text{Ar}$  age of  $9.54 \pm 0.04$  Ma), so it cannot be part of the Lava Flow Member. We have found no lavas between By-Day Member and Upper Member ignimbrites, which also appear to overlap in age (although the error on the By-Day Member is large; see Pluhar et al., 2009). Many lavas in the Eureka Valley Tuff were erupted from fault-controlled vents in the Sierra Crest graben-vent complex (Fig. 2B; Busby et al., 2013a), although some are closely associated with the Little Walker caldera, as noted here (Priest, 1979).

**Tollhouse Flat Member, Eureka Valley Tuff.** In The Dardanelles segment of the Cataract paleochannel (Fig. 5), the Tollhouse Flat member of the Eureka Valley Tuff overlies the TML (i.e., there is no Basal Lava Member; Fig. 6B). The Tollhouse Flat Member forms the most regionally extensive unit of the Stanislaus Group, and occurs from Nevada to the Sierra foothills (Fig. 3). However, within the paleochannels of the Sierra Nevada, it is commonly preserved within smaller channels, forming a horizon of lenses like a string of pearls.

In The Dardanelles segment of the Cataract paleochannel (Fig. 5D), erosional remnants of the Tollhouse Flat Member are only present on Dardanelles Cone, and in a single small channel fill on top of The Dardanelles. However, on The Dardanelles, at the stratigraphic position where the Tollhouse Flat Member should be (above the TML; Fig. 6A), fluvial and debris flow deposits contain abundant rounded boulders, cobbles, and pebbles of Tollhouse Flat ignimbrite (not mapped separately but shown in measured section in Fig. 6A; see Figs. 8L–8M). This indicates up-paleochannel erosion of Tollhouse Flat Member welded ignimbrite, and fluvial transport sufficient to round the clasts before they became incorporated in the debris flow. The debris flow deposit also contains olivine basalt boulders (Fig. 6A), similar to the olivine basalt lava (sample DC036, Busby et al., 2008a) that is at the base of the Lava Flow Member on Dardanelles Cone (Tselb, Figs. 5D and 6B), overlying Tollhouse Flat ignimbrite.

**Lava Flow Member, Eureka Valley Tuff.** The Lava Flow Member on Dardanelles Cone is distinguishable from the TML only by its stratigraphic position above the Tollhouse Flat Member, not by composition, because it here has no trachydacite lava; instead it is a basalt lava overlain by a trachyandesite lava (Figs. 5D and 6B).

The olivine basalt at the base of the Lava Flow Member on Dardanelles Cone has subhedral embayed olivine with iddingsite rims, euhedral to subhedral clinopyroxene, rare euhedral to anhedral sieve-textured plagioclase, and opaque oxide microcrysts set in an aphanitic, fine-grained, trachytic-textured groundmass (Fig. 6B). Its flow top breccia contains delicate plastically deformed scoria clasts, perhaps suggestive of a proximal source, although these can be rafted moderate distances; a nearby olivine basalt dike (Tselbi dike by Dardanelles Cone, Fig. 5) may represent a feeder, although no vent deposits are preserved in the paleochannel. The Dardanelles segment of the Cataract paleochannel is unfaulted; it also lacks intrusions (except for the single dike), in marked contrast to faulted rocks at the range crest and range front; thus, although the Lava Flow Member basalt on Dardanelles Cone may have vented locally, that was an unusual occurrence.

The Lava Flow Member on The Dardanelles consists of a trachydacite lava (geochemistry sample DC064 of Busby et al., 2008a) that is easy to distinguish from the TML because (1) it is underlain by the Tollhouse Flat Tuff and detritus derived from it, and (2) it exhibits a bulbous profile (high-aspect ratio) typical of silicic lavas rather than being sheet-like (Figs. 8M, 8N). The 60-m-thick trachydacite lava on the top of The Dardanelles has ~10%–20% phenocrysts, including euhedral skeletal plagioclase laths, lesser anhedral pyroxene, and subhedral oxidized hornblende. Kupparberg entablature occurs in the top ~5 m (Fig. 8M), showing (like the TML, Fig. 8G) that river water flowed over the top of the lava while it was cooling. The lava is commonly flow banded, with a dark blue-gray, vitreous interior, and it has very well developed perlitic fracture suggestive of quenching by stream water.

The Lava Flow Member trachydacite lava on The Dardanelles was referred to as Dardanelles flow by Ransome (1898) and mapped as the Dardanelles Formation by Huber (1983a), but there is no Dardanelles Formation on The Dardanelles.

**Dardanelles Formation (sequence 3).** We report here for the first time that Dardanelles Formation is on the top of Dardanelles Cone (sequence 3; Tsdl, Fig. 5D) on top of the Lava Flow Member (Fig. 6B), although it is a very small ( $16 \times 8$  m) erosional remnant. There is no intervening By-Day Member and Upper Member that would enable one to recognize it by stratigraphic position; however, that is not necessary, because the Dardanelles Formation is very distinctive, in the field, in mineralogy, and in chemistry. It is a jet-black, unusually glassy lava; although it is nearly aphyric, it is distinctive for having resorbed hornblende in addition to clinopyroxene and olivine, and it is the only shoshonite we have found in the Stanislaus Group (sample DCO32 of Busby et al., 2008a).

#### **Unconformity 4 and Sequence 4**

There are no sequence 4 rocks (i.e., the Disaster Peak Formation) in The Dardanelles segment of the Cataract paleochannel, nor have any been found in the syndepositionally faulted segment of the Cataract paleochannel. One could argue that sequence 4 rocks have been eroded off the top of the Stanislaus Group (sequence 3), but that is not consistent with the inset nature of all other units in the paleochannel fills. Sequence 4 rocks are inset into sequence 3 rocks along unconformity 4 in the deranged north-northwest paleochannel fill along the modern Sierra Crest (described in detail in the following).

#### **Onset of Paleochannel Derangement in East-West Cataract Paleochannel at Red Peak–Bald Peak**

The Red Peak to Bald Peak area is along the western edge of the Sierra Crest graben (Fig. 2B), where the fill of the Cataract paleochannel forms a resistant ridge from Red Peak to Bald Peak (Fig. 9). The slip history for faults of this area was described in detail in Busby et al. (2013a), fault by fault; here we describe the effects of syndepositional faulting on the paleochannel fill, sequence by sequence. Postdepositional faulting is also described elsewhere (Busby et al., 2013a). The fault blocks, from east to west, are (Figs. 5C and 9): (1) the Red Peak horst block, between the east-dipping Seven Pines normal fault to the east, and the west-dipping Red Peak normal fault to the west; (2) the hanging-wall graben of the west-dipping Red Peak normal fault, which contains an east-dipping antithetic normal fault to the Red Peak fault, the Douglas Creek fault; and (3) the hanging-wall graben of the west-dipping Bald Peak normal fault.

In addition to describing the effects of syndepositional faulting on the paleochannel fill, we note features that indicate deposition in a paleochannel, in order to contrast the deposits with graben-filling deposits not associated with any paleochannels.

#### **Unconformity 1 and Sequence 1**

Unconformity 1 (granitic basement below, Valley Springs Formation above) is extremely irregular, due to paleotopographic effects, and it is largely merged with unconformity 2 (Relief Peak Formation above). The Valley Springs Forma-

tion (Tvs) is only preserved at two localities: (1) in the Red Peak horst block, as a 100-m-thick and 150-m-long erosional remnant on a paleoledge on the side of a paleochannel in the granitic basement (Kgu, Figs. 5C and 9); and (2) on the north face of Bald Peak (Figs. 5C and 7D), as a 220-m-thick erosional remnant. Even where sparse, the remnants of the Valley Springs Formation indicate the original courses of the paleochannels, and here mark the Cataract paleochannel in the Bald Peak–Red Peak area.

#### **Unconformity 2 and Sequence 2**

Evidence for deposition of the Relief Peak Formation (Trp) in a paleochannel includes the following. (1) The base of the Relief Peak Formation is locally topographically lower than the base of the Valley Springs Formation in the Red Peak horst block (Fig. 5C), due to a reincision event in the paleochannel, which produced unconformity 2 (Fig. 4). Reincision surfaces are a distinguishing feature of the paleochannels, and they are not present in the transtensional graben fill, which aggraded rapidly. (2) The Relief Peak Formation is here formed mainly of debris flow deposits (Trpdf, Fig. 5C), but they are stratified (not massive), as is obvious on the oblique air photo (Fig. 9). The graben-filling debris flow deposits are massive, with abundant avalanche blocks, indicating catastrophic resedimentation (see following). (3) The paleochannel debris flow deposits have fluvial interbeds throughout (Figs. 10A, 10C), which are absent from the graben fills elsewhere. The fluvial interbeds have clast imbrication and well-developed trough cross-beds that indicate a paleo-transport direction toward  $238^{\circ}$ – $283^{\circ}$ , consistent with transport in the Cataract paleochannel. The higher debris flow/fluvial deposit ratio of this segment of the Cataract paleochannel, relative to The Dardanelles segment, is consistent with its up-paleochannel position, closer to the inferred position of the arc front at this time (just to the east of the area mapped in Fig. 5A; discussed in the following).

The most obvious Cataract paleochannel syndepositional fault in the Relief Peak Formation is the Bald Peak fault (Fig. 9); there, the Relief Peak Formation (Trpdf) thickens from 45 m to 110 m on the downthrown block of the Bald Peak fault, where it also contains avalanche megablocks of pink and white block-and-ash flow tuff. Some of the coarsest boulder conglomerates in the Cataract paleochannel are here (Fig. 10A), adjacent to the Bald Peak fault, perhaps marking the position of a plunge pool at the base of a fault-controlled waterfall in the Cataract paleochannel.

#### **Unconformity 3 and Sequence 3**

**Table Mountain Latite (sequence 3).** The TML here shows abundant evidence for deposition in a fluvial paleochannel. Fluvial sandstone and conglomerate are between flows 2 and 3 in the Red Peak horst block (Tstmf, Fig. 5C), with pebble- to boulder-sized, well-rounded clasts of latite. More fluvial conglomerates, with rounded cobbles and sparse boulders of latite and minor hornblende andesite, occur between the TML lavas and the Lava Flow Member

lavas on the northeast face of Red Peak in the Red Peak horst block (Fig. 5C). Fluvial deposits are also interstratified with the TML on the hanging wall of the Red Peak fault, on the north side of the Red Peak–Bald Peak ridge (Fig. 5C), where they form an ~40-m-thick section of white conglomerate and sandstone that fines upward. Fluvial deposits within the TML on the hanging wall of the Bald Peak fault (Fig. 5C) are at two stratigraphic intervals: a lower one on the north side of Bald Peak (Fig. 7D) and the higher one on the south face of Bald Peak. They are each as much as ~30 m thick, and have a mixture of hornblende-bearing andesitic and latite clasts, with rounded boulders as large as 2 m, indicating high axial gradients in the Cataract paleochannel. The TML lava flow 5 lenses out within a minor channel cut into the upper of these two fluvial deposits (Fig. 5C). These fluvial deposits indicate that water continued to flow down the Cataract paleochannel between TML eruptions. Furthermore, measurements of elongate vesicles in this area (225°; see Koerner et al., 2009, fig. 11 therein) are consistent with the interpretation that this part of the TML is confined within, and was emplaced along, the Cataract paleochannel.

Volcanic fault-controlled venting within the Cataract paleochannel began during deposition of the TML in the hanging wall of the Bald Mountain fault, and continued through deposition of the Dardanelles Formation (see following). Discontinuous, black, olivine-plagioclase-phyric basaltic lavas are between TML flows 3 and 4 on either side of the Bald Peak fault (Tstmb, Fig. 5C). The olivine basalt lava that is west of the fault strikes into olivine basalt vent facies deposits on the northeast side of Bald Peak (Tstmbv, Fig. 5C). An intrusion that may be related to this basalt vent is ~1 km southwest of Bald Peak, along the east side of an unnamed fault; there, an olivine basaltic dike strikes ~315°, parallel to the fault (Tstmbi, Fig. 5C). Thus, fault-controlled volcanic venting played a role in the derangement of the Cataract paleochannel.

**Eureka Valley Tuff (sequence 3).** The Eureka Valley Tuff ignimbrites provide sensitive indicators of paleofault scarps in the paleochannel, because each ignimbrite is an instantaneous event, and the upper surface of an ignimbrite is normally flat, while its base inundates topography, in this case created by the faults (see Tset and Tseb, Fig. 9A). The ignimbrites show rapid thickness changes across faults in the paleochannel, due to syndepositional faulting; in contrast, the ignimbrites are more widespread and even in thickness in the Sierra Crest graben east of the Seven Pines fault (Busby et al., 2013a).

**Tollhouse Flat Member, Eureka Valley Tuff.** The Tollhouse Flat Member is absent from the section in the Red Peak horst block, even though the Lava Flow Member lavas (which should be above the Tollhouse Flat Member) are present; this may mean that the softer ignimbrite was preferentially stripped away by uplift on the horst block, while the lavas resisted erosion. At the stratigraphic level where the Tollhouse Flat Member should be, a very narrow, 25-m-deep paleochannel is mapped (Fig. 5C, map unit Tseldf). This deep narrow paleochannel is filled with a fault talus breccia composed of clasts of the Tollhouse Flat Member, including shattered avalanche blocks up to 3 m long (Figs. 10D, 10E). We interpret this to represent a fault talus accumulation; note the contrast between this fault-related breccia and the rounded Tollhouse Flat Member clasts at the same stratigraphic level in the nonfaulted paleochannel

fill at The Dardanelles (Fig. 8L). The fault talus breccias and landslide blocks are geologic evidence of the paleochannel derangement that was in progress.

The Tollhouse Flat Member thickens from 0 to 25 m onto the downdropped block of the Red Peak fault (Figs. 5C and 9). It maintains an even thickness (25 m) from there to the Douglas Creek antithetic fault, where it thins abruptly to 7 m on the upthrown block. These relatively small scarps were buried by the Tollhouse Flat Member, allowing the paleochannel to continue to function after it was deposited.

**Lava Flow Member, Eureka Valley Tuff.** Lavas in the Eureka Valley Tuff are not as sensitive recorders of paleofault scarps as the ignimbrites, because most of them are silicic (trachydacite) and could therefore stick on steeper slopes (relative to Table Mountain trachyandesites, trachybasaltic andesites, and basalts), and develop irregular upper surfaces. A latite dike interpreted to be a feeder for the Lava Flow Member in the Red Peak horst block (pink with hachures; Fig. 5C) could be taken as an indication that faults were active in the paleochannel during eruption of the Lava Flow Member, but no systematic changes in thicknesses can be demonstrated across faults.

**By-Day Member, Eureka Valley Tuff.** The By-Day Member doubles in thickness toward the footwall of the Red Peak fault, in the short distance between the Douglas Creek fault (30 m) and the Red Peak fault (60 m) (Figs. 5C and 9). Furthermore, the By-Day Member thins abruptly onto the upthrown block of the Douglas Creek fault, from 30 m to 20 m. Like the Tollhouse Flat Member, this ignimbrite buried fault scarps in the paleochannel, but the paleochannel continued to function (see following).

The By-Day Member is not preserved in the Cataract paleochannel at The Dardanelles, but it forms a relatively complete section in the Cataract paleochannel on the hanging wall of the Red Peak fault, so we describe it here. It includes a basal ~5-m-thick white and tan nonwelded to incipiently welded tuff, passing upward through ~20 m of welded tuff, with an ~5-m-thick orange vapor-phase-altered top. This contrasts with the By-Day Formation ignimbrite in the Sierra Crest graben fill, which is welded to the base (see Fig. 13A of Busby et al., 2013a). Perhaps this is due to greater conductive cooling around the surfaces of a channelized ignimbrite. The vitrophyres in both Tollhouse Flat and By-Day Members in the paleochannel have unusually well-developed perlitic fractures, suggesting quenching by running water.

**Upper Member, Eureka Valley Tuff.** This is the least extensive ignimbrite, and is not present at The Dardanelles, so we describe it here. The Upper Member forms distinctive bright white outcrops that can be seen from a long distance. It is preserved at only two localities in the Cataract paleochannel (Figs. 5C and 9). It has a thin (<20 cm) basal fine-grained ash-fall tuff, overlain by a white nonwelded ignimbrite. This in turn is overlain by a lithic-rich tan unit that may either be nonwelded ignimbrite or its equivalent reworked by debris flow, and it has a thin (<20 cm) discontinuous cap of stratified fluvially reworked tuff with pebbles. Because the Upper Member is not welded, it must have had a lower preservation potential within the paleochannel than the welded ignimbrites. Given the fact that the overlying Dardanelles Formation lava was not erupted over the top of it until at least 350 k.y. later (Fig. 4), it is surpris-

ing that any is preserved. This suggests that the paleochannel was basically abandoned by then, although one small outcrop of peperite at the base of the Dardanelles Formation lava suggests that the ground was wet at that locality (described in the following); the paleochannel remained a topographic low that acted as a funnel for the Dardanelles Formation lava, even though stream power had been eliminated. Similarly, lava was accommodated in the Mokelumne paleochannel after it was beheaded and ceased to function as a fluvial system (see following); we refer to this as a relict paleochannel.

**Dardanelles Formation.** Early workers first recognized the Dardanelles Formation on the hanging wall of the Bald Mountain fault, where the By-Day Member and Upper Member are not present, so it could have alternatively been considered a unit within the Eureka Valley Tuff; however, the same distinctive black glassy lava flow occurs above Upper Member on the hanging wall of the Red Peak fault, so the assignment was correct (see discussion in Koerner et al., 2009). It is as much as 60 m thick.

In one erosional remnant, only 8 m × 8 m, the Dardanelles Formation lava has a peperite base. Approximately 5 m of flow bottom breccia at the top of the outcrop passes downward into ~4 m of very irregularly shaped or pillow-like or angular fragments encased in a host of massive sandstone. This indicates that the lava locally burrowed into and interacted with wet sediment in the relict paleochannel. The Dardanelles Formation lava fills erosional surfaces cut less than a few meters down through the soft Upper Member and locally shows 1–2 m of relief on the upper surface of the soft vapor-phase top of the By-Day Member of the Eureka Valley Tuff. This is very modest erosion, given the length of time (>350 k.y.) and the softness of the substrate relative to other erosional surfaces within the Cataract paleochannel. The Dardanelles Formation is overlain by a single small (~20 m long) erosional remnant of fluvial sandstone and conglomerate, <1 m thick, with angular to rounded pebbles and cobbles of probable andesite and latite (no chemical analyses), tentatively assigned to the Dardanelles Formation (Tsdvf?, Fig. 5). However, there are no younger units inset into the Dardanelles Formation along erosional surfaces, even though all older units in the paleochannel have overlying units inset along erosional surfaces. This suggests that enough water continued to flow through the conduit to deposit stream gravels on top, but not enough to erode it and transport new material into the conduit.

Dardanelles Formation vent facies deposits (Tsdvf; Figs. 5C and 7D) are preserved within the paleochannel fill on Bald Peak. In addition to red scoria fall typical of dry Strombolian eruptions, they include white cross-bedded tuff interpreted to represent phreatomagmatic deposits (from wet eruptions). The phreatomagmatic deposits indicate that there was standing water or groundwater in the paleochannel at the time of eruption of the Dardanelles Formation.

#### **Unconformity 4 and Sequence 4**

Like the unfaulted Cataract paleochannel segment at The Dardanelles, there are no sequence 4 strata in the syndepositionally faulted segment of the Cataract paleochannel. Several intrusions are assigned to Disaster Peak

Formation based on crosscutting relations, or a date younger than 9 Ma, but these are not related to paleochannels. As at The Dardanelles segment, one could argue that Disaster Peak Formation strata were once present and have since been eroded; however, in both areas, there are no younger rocks inset into the Stanislaus Group along erosional surfaces, in contrast to older parts of the section, where the Stanislaus Group is inset into the Relief Peak Formation, which is in turn inset into the Valley Springs Formation. This indicates that the paleochannel was abandoned. We show here that sediment that previously came down the east-west Cataract paleochannel was diverted into a new north-northwest paleochannel in the Sierra Crest graben (deranged Cataract paleochannel; Fig. 2B); this paleochannel is represented by the Disaster Peak Formation along the modern range crest in the Arnot Peak–Disaster Peak area (Fig. 5B).

#### **Deranged North-Northwest Cataract Paleochannel on the Sierra Crest at Disaster Peak–Arnot Peak**

The deranged Cataract paleochannel (Fig. 2B) provides a geologic record of the transition from ancient east-west drainages of the Nevadaplano to the north-northwest drainages of the Walker Lane belt. The deranged Cataract paleochannel is in the Sierra Crest graben, a transtensional Walker Lane graben that began to form by 11–12 Ma (Busby et al., 2013a; Busby, 2013). Exposures of the Sierra Crest graben are divided into a northern segment (Fig. 5B) and a southern segment (Fig. 5C) separated by the South Fork Clark River glacial valley (Fig. 5A), which eroded into the Mesozoic basement below the graben. However, some of the graben-bounding faults are continuous between the two areas, and the synvolcanic graben fill has a similar thickness between the two preserved segments, so we infer that the graben was originally continuous between the two areas (Busby et al., 2013a). The northern segment is referred to as the Disaster Peak–Arnot Peak segment of the Sierra Crest graben, named for two major peaks along the modern Sierra Nevada crest (Fig. 5B).

We describe in detail for the first time the Disaster Peak Formation (sequence 4), which consists largely of volcanic debris flow and fluvial deposits that fill a north-northwest-flowing paleochannel (Figs. 11A–11F). These deposits overlie the Stanislaus Group (sequence 3) and the Relief Peak Formation (sequence 2), which here represent graben fill unrelated to a paleochannel; however, they are briefly described here, in order to (1) highlight the differences between graben fill and paleochannel fill, and (2) demonstrate that the north-northwest-deranged Cataract paleochannel was not part of the ancient east-west paleochannel system, but rather was between two of them, the Mokelumne paleochannel to the north, and the Cataract paleochannel to the south (Fig. 2B). In order to demonstrate this, and to facilitate discussion of the Stanislaus and Mokelumne paleochannels, we use a series of time-slice maps that show the distribution of preserved erosional remnants of sequences 1–4 (Fig. 12).

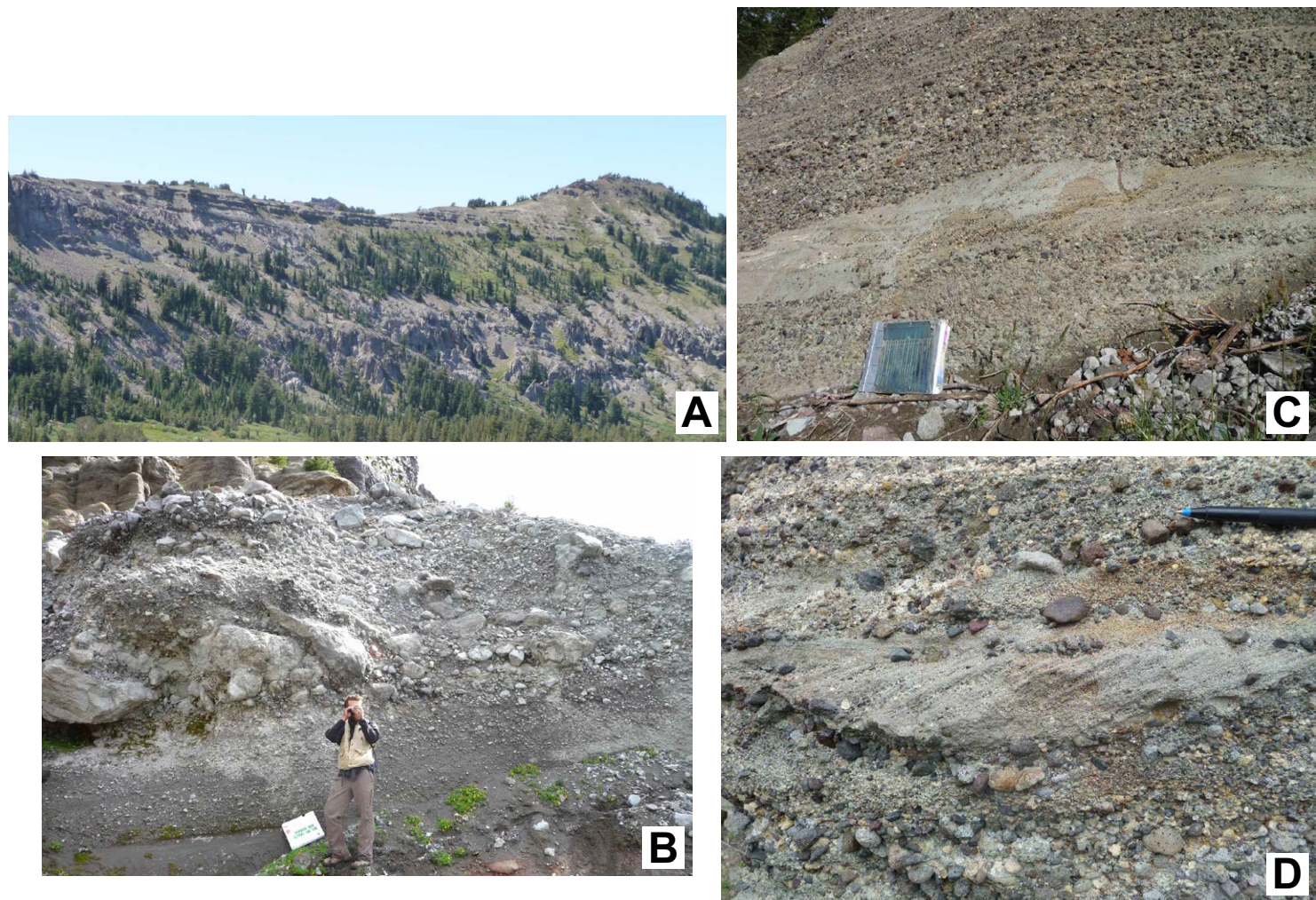


**Figure 11 (on this and following two pages).** Outcrop photos of sequence 4 paleochannel deposits (Disaster Peak Formation, Figs. 4, 5, and 12D), including the north-northwest-deranged Cataract paleochannel and the Mokelumne paleochannel. (A) Northwest-dipping progradational fluvial wedge north-northwest-deranged Cataract paleochannel along the Disaster Peak–Arnold Peak range crest (Fig. 12D), viewed from the east. The wedge consists of an approximately 300 m thick section of crudely-stratified volcanic debris flow deposits and well-stratified fluvial deposits, shown in closeup photos in Figures 11B, 11C, and 11D. (B) Stratified boulder to cobble conglomerate and pebbly sandstone with well-rounded clasts, indicating transport in a paleochannel, but also including outsized angular blocks that were locally derived from within the north-northwest Sierra Crest graben, which contains the NNW-deranged Cataract paleochannel. Slide blocks of distinctive Stanislaus Group strata, as much as 25 m long, occur at several localities in sequence 4 within the graben, indicating that it continued to subside during deposition of sequence 4. (C) Well-stratified fluvial pebbly sandstones and sandstones in the NNW-deranged Cataract paleochannel in the Sierra Crest graben. (D) Cross stratification in fluvial granule sandstone in the NNW-deranged Cataract paleochannel in the Sierra Crest graben, indicating paleocurrent direction toward the north (to left).

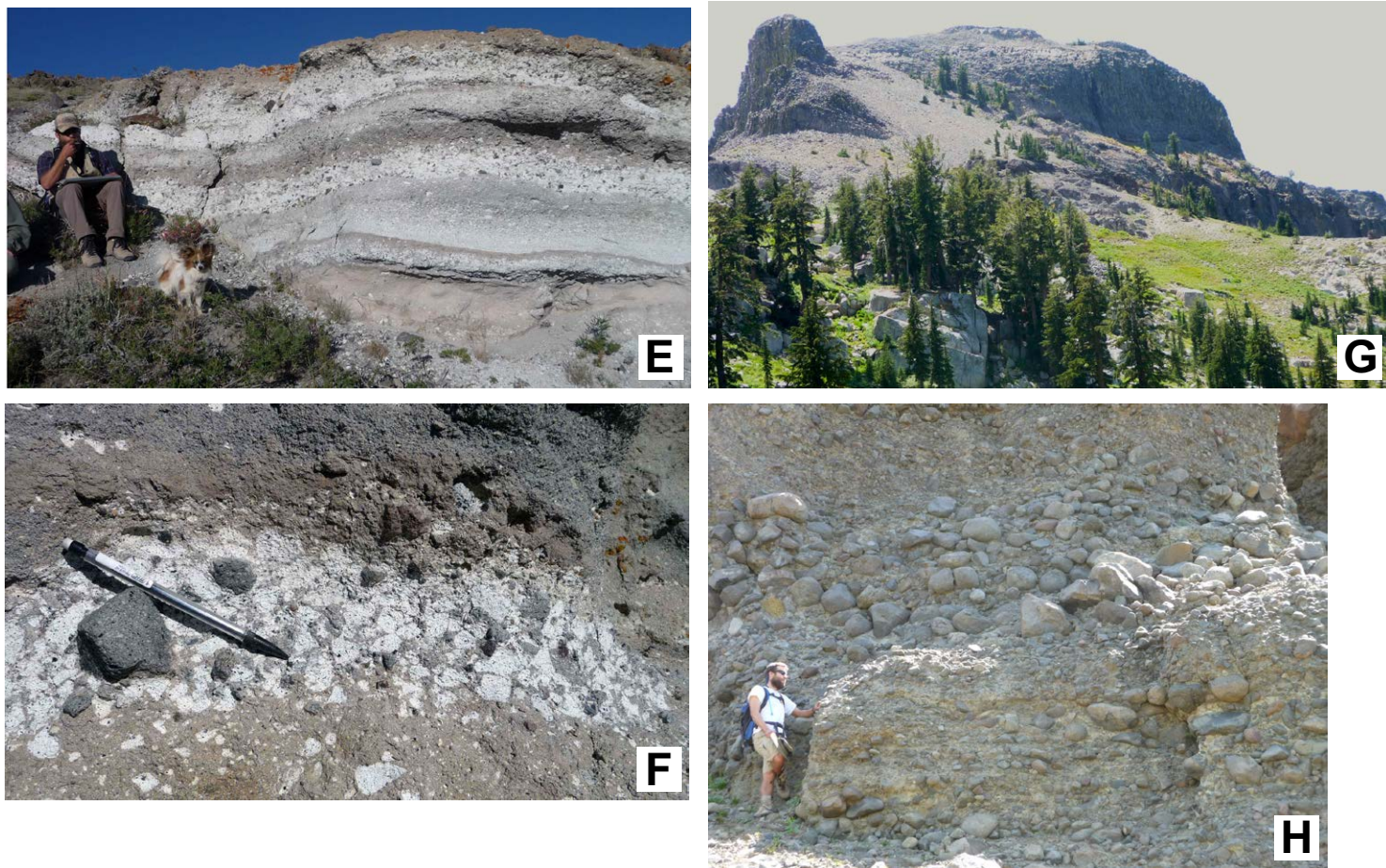


**Figure 11 (continued).** (E) White pumice lapillistone, pumice lapilli tuff and tuff variably mixed with andesitic volcanic rock fragments by streamflow within the NNW-deranged Cataract paleochannel in the Sierra Crest graben. The Disaster Peak Formation has much more abundant silicic pyroclastic debris than the arc rocks that predate the high-K volcanism (Relief Peak Formation), which have an ~1-m-thick silicic pyroclastic deposit at only two localities (at The Dardanelles, described here, and in the Grouse Meadows fault block on the range front, see fig. 9 of Busby et al., 2013b). (F) Closeup of outcrop shown in E, showing sequence 4 Disaster Peak Formation silicic pumice lapilli mixed with andesitic detritus in the fluvial environment. These silicic tuffs and lapilli contain biotite, which is absent from the sequence 2 Relief Peak Formation. (G) Mokelumne paleochannel (Fig. 2B) at Bull Run Peak (Figs. 5A and 12D). View of the north face, showing Mesozoic granitic basement at the base (white, mainly in trees), directly overlain by Sequence 2 Relief Peak Formation andesitic fluvial and debris flow deposits, which are dark gray and ledge-forming. Above that is cliff-forming columnar jointed andesite lava, inferred to be sourced from the 5–4 Ma Ebbetts Pass stratovolcano (Fig. 12D; see Tdpeps, Fig. 5B). (H) Closeup of Relief Peak Formation in Mokelumne paleochannel, showing well-rounded, well-sorted, stratified fluvial boulder to cobble conglomerate.



**Figure 11 (continued). (I)** Closeup of Relief Peak Formation in Mokelumne paleochannel, showing andesitic debris flow deposits that are interstratified with the andesitic fluvial deposits; these debris flow deposits, and the fluvial deposits shown in H, are indistinguishable from the Relief Peak Formation in the Cataract paleochannel (Figs. 8B, 10A, 10B, 10C).

### Sequences 1–3

The Valley Springs Formation (Tvs) is the best indicator of paleochannel positions, and there is no Valley Springs Formation between the Cataract and Mokelumne paleochannels, except in one locality (slide blocks in Fig. 12A). Three very small (~100 × 100 m each) outcrops of white ignimbrite (southwest corner of Fig. 5B) bear quartz, sanidine, and biotite, typical of the Valley Springs Formation. These three small Valley Springs Formation outcrops appear to be slide blocks (see three tiny pink dots along the top of the label "Slide blocks" in Fig. 12A) encased in an andesitic debris flow matrix, deposited in the Sierra Crest graben on the hanging wall of the Arnot Creek fault (Fig. 5B), which ponded the TML to a thickness of ~500 m (Busby et al., 2013a); it is unclear where the Valley Springs Formation slide blocks came from, because the nearest *in situ* Valley Springs Formation is 8 km to the south in the Cataract paleochannel at the Bald Peak–Red Peak area, and 8 km to the north in the Mokelumne paleochannel at the Bull Run ridge area (Fig. 12A). However, slide blocks derived from the Oligocene welded rhyolite ignimbrites are common in the Sierra (e.g., Garrison et al., 2008; Busby et al., 2013a, 2013b), because the welding process instantaneously forms rock that breaks along compaction foliation into slabs, and the welded rhyolite ignimbrite slabs are hard enough to endure transport over relatively long distances.

The Relief Peak Formation, like the Valley Springs Formation, is absent from the Disaster Peak–Arnot Peak segment of the Sierra Crest graben (Fig. 12B), supporting our interpretation that an east-west Nevadaplano paleochannel did not cross the Sierra Nevada at this latitude. This is in striking contrast with the Sonora Pass segment of the Sierra Crest graben (SP, Fig. 12B), where the Relief Peak Formation forms an ~500 m thick, >50 km<sup>3</sup> debris avalanche deposit, composed of slide blocks as much as 2 km long derived from Relief Peak Formation and lesser Valley Springs Formation paleochannel fill in the Cataract and Stanislaus paleochannels (Busby et al., 2013a). There was no preexisting paleochannel fill to resediment into the Disaster Peak–Arnot Peak segment of the Sierra Crest graben as slide blocks. However, the Relief Peak Formation occurs as the basal fill of the northeast-striking transfer zone basins that began to form during sequence 2 (Fig. 12B; see Wolf Creek, Jones Canyon, Murray-Dumont, Mineral Mountain, and Poison Flat faults; Figs. 2B and 5B). This does not represent paleochannel fill, because it consists of massive (wholly unstratified) volcanic debris flow deposits, with no fluvial interbeds, with lesser block-and-ash flow tuff (mapped separately where extensive; Fig. 5B). One of these has a hornblende  $^{40}\text{Ar}/^{39}\text{Ar}$  age of  $11.33 \pm 0.03$  Ma (Busby et al., 2013c; data presented elsewhere). The transfer zone basins formed as part of the ca. 12–9 Ma Sierra Crest graben-vent system of Busby et al. (2013a, 2013b; Figs. 2B, 5B, and 5C).

The Stanislaus Group in the Sierra Crest graben-vent system differs from that in the paleochannels in the following ways: (1) it has no fluvial interbeds, no rounded clasts of Eureka Valley welded ignimbrite, and no reincision surfaces; (2) the lavas do not have kuppaberg joints, perlitic fractures, or peperitic bases; (3) the vent facies deposits consist of scoria cones or scoria fissure ramparts, and do not include phreatomagmatic deposits.

### Sequence 4

We herein divide sequence 4 (Disaster Peak Formation) into two time frames (Fig. 12D): (I) a deranged north-northwest paleochannel (ca. 9–5 Ma), which formed a north-flowing fluvial system preserved on the Arnot Peak–Disaster Peak ridge, and (II) the Ebbetts Pass stratovolcano (5–4 Ma) in the Ebbetts Pass pull-apart basin; this fed lavas into the Mokelumne paleochannel (described in the following). Small subvolcanic intrusions mapped as Disaster Peak Formation (Fig. 12D) are common across the entire map area, but they are identified with crosses in the south half of the map area, in order to indicate that all of the Disaster Peak Formation there consists of intrusions, with no strata, except for queried outcrops in the Stanislaus paleochannel (described in the following).

*I. Deranged North-Northwest Cataract Paleochannel.* The Disaster Peak Formation in the north-northwest-deranged Cataract paleochannel is as much as 540 m thick, similar to paleochannel depths reported from east-west paleochannels of the central Sierra (Wakabayashi and Sawyer, 2001; Busby et al., 2008b; Wakabayashi, 2013). This similarity is not a coincidence; the depth is

**A**

**Sequence 1:**  
**Valley Springs Fm**

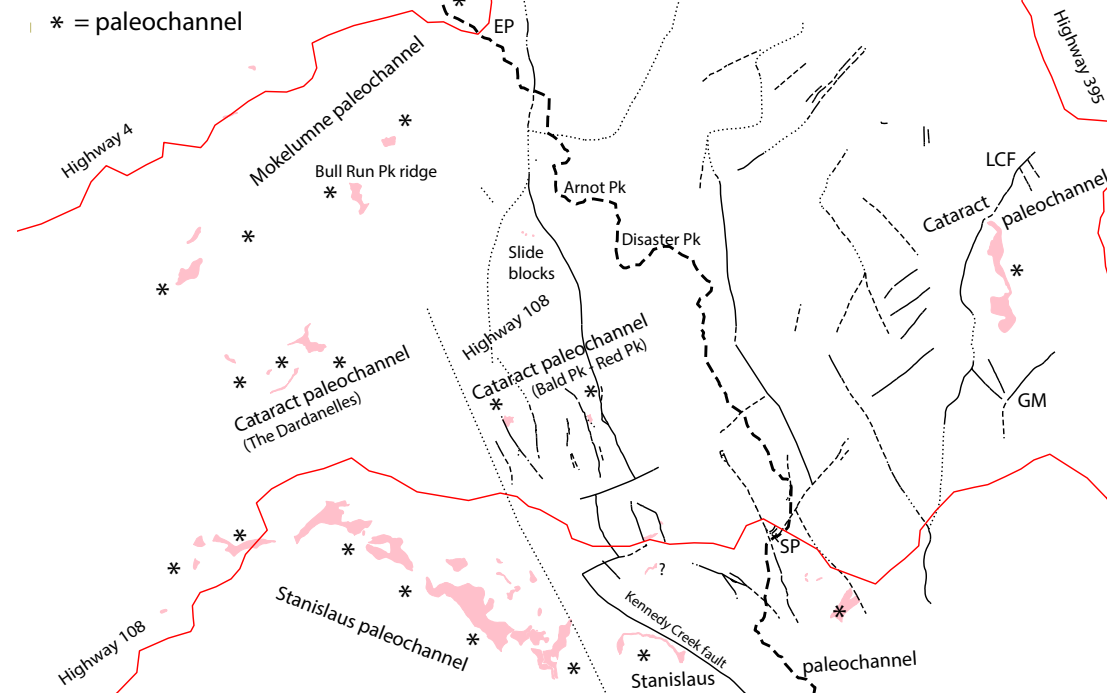


**Figure 12 (on this and following three pages).** Time-slice maps showing outcrops of the four main Tertiary unconformity-bound stratigraphic sequences (Fig. 4), taken directly from Figure 5 to facilitate recognition of paleochannels (shown with stars) and grabens (not starred). No interpretive restorations are shown; for example, we do not conjecture about the original extent of units where they are buried beneath younger units (e.g., compare sequence 3 and sequence 4 in Arnot Peak–Disaster Peak area). Sierra Crest (black dashed line) and highways (red lines) shown for reference. EP—Ebbets Pass, SP—Sonora Pass, LCF—Lost Cannon fault, GM—Grouse Meadows half-graben. Faults are also shown for reference in all four time slices, although none of them were present during time-slice 1 (Valley Springs Formation; for discussion of fault slip histories, see Busby et al., 2013a, 2013b). (A) Sequence 1: Valley Springs Formation. This was deposited entirely within paleochannels, before any faulting occurred, so it is the most reliable indicator of paleochannel courses. However, it is incompletely preserved due to later erosion and faulting. The Stanislaus paleochannel (in the south) preserves the most continuous outcrops in the map area, and contains the 25.4 Ma Nine Hill Tuff (see text). The Cataract paleochannel (center) has the greatest preserved length of Valley Springs outcrops, from a position just west of Highway 395 (see Fig. 5A), to Knight's Ferry on the west (Fig. 3). It appears to be offset in a dextral sense by an unnamed north-northwest-striking fault between Red Peak–Bald Peak and The Dardanelles, and continues off the west of the Figure 5 map area, reappearing ~4 km to the southwest at Whittakers Dardanelles (Fig. 3). The Mokelumne paleochannel in the north contains the ca. 29 Ma Tuff of Campbell Creek (see text). Pk—peak.

consistent with the interpretation that it pirated sediment from the Cataract paleochannel, and funneled it into the Mokelumne paleochannel to the north (I.? in the Mokelumne paleochannel in Fig. 12D). The base of the north-northwest-deranged Cataract paleochannel (unconformity 4) incises through all units of the Eureka Valley Tuff, including the Lava Flow Member, into the TML (cross sections in Busby et al., 2013a, fig. 12 therein).

The Disaster Peak Formation in the north-northwest-deranged Cataract paleochannel forms a north-northwest-dipping fluvial wedge, and paleocurrent indicators, such as cross-stratification, indicate transport toward the north-northwest (Figs. 11C, 11D). The north-northwest-deranged Cataract paleochannel fill consists of debris flow deposits (*Tdpdf*) and interstratified fluvial and debris flow deposits (*Tdpff*) with minor block-and-ash flow tuffs (*Tdpba*) and lavas (*Tdpl*) (Fig. 5B), shown in Figures 11B–11D. The Disaster Peak Formation is distinguished from the Relief Peak Formation by its silicic explosive vol-

canic debris, mixed with andesitic debris (Figs. 11E, 11F). Here and in the larger map area (Fig. 5A) it also differs from the Relief Peak Formation by having lavas, vent facies deposits, and subvolcanic intrusions, indicating that the arc front was along the modern crest, rather than east of it as it was for the Relief Peak Formation. The debris flow deposits are stratified, and have abundant fluvial interbeds consisting of well-rounded boulder conglomerates (which show only weak imbrication due to their rounding; Fig. 11B), and pebbly sandstones and sandstones with planar stratification and cross-stratification (Figs. 11C, 11D). Pumice lapilli tuffs and tuffs with quartz and biotite are variable admixed with andesitic rock fragments (Figs. 11E, 11F), indicating that the region was showered with silicic explosive volcanic products that were reworked within the north-northwest-deranged Cataract paleochannel. In contrast, the north-east-striking transfer zone basins (Fig. 12D) lack fluvial deposits, and are filled with massive debris flow deposits (*Tdpdf*), and lesser block-and-ash flow tuff

**B**Sequence 2:  
Relief Peak Fm

\* = paleochannel

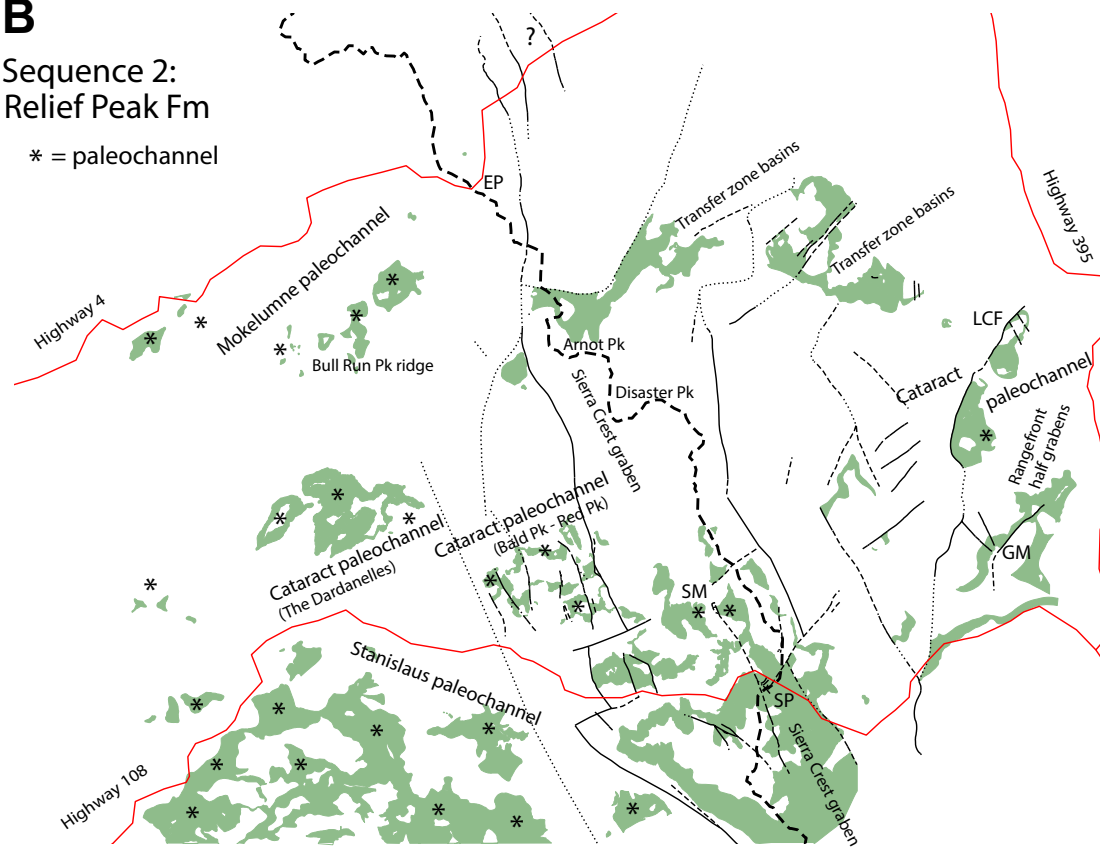


**Figure 12 (continued). (B)** Sequence 2: Relief Peak Formation, with paleochannel fill marked with stars; the rest is graben fill (Sierra Crest full graben, transfer zone grabens, and range-front half-grabens are shown; see Fig. 2B). The grabens preserve remnants of Relief Peak Formation Cataract paleochannel fill in two places: under Sierra Crest graben fill overlying granitic basement on either side of the Saint Mary's Pass faults (SM; right dextral oblique normal fault; see text), and under range front graben fill overlying in situ Valley Springs Formation on the hanging wall of the LCF (see Fig. 12A). Greater preservation of sequence 2 in the southern paleochannel (Stanislaus) relative to the central (Cataract) and northern (Mokelumne) paleochannels indicates that it was beheaded prior to erosion of unconformity 3, as also shown by the absence of sequence 3 lavas there (shown in C).

(Tdpba) and basalt lavas (Tdplb, Fig. 5B), with  $^{40}\text{Ar}/^{39}\text{Ar}$  ages of ca. 7–5 Ma (reported in Busby et al., 2013c; complete age data available elsewhere). We do not consider these part of the north-northwest-deranged paleochannel fill (Fig. 12D).

The age of the base of the north-northwest-deranged Cataract paleochannel fill is younger than 9.34 Ma (age of the Upper Member, Eureka Valley Tuff) and the top (sample JHEP-55, Fig. 5B) is dated as  $4.91 \pm 0.05$  Ma ( $^{40}\text{Ar}/^{39}\text{Ar}$  on hornblende from a block-and-ash flow tuff, reported in Busby et al., 2013c; complete age data available elsewhere).

**II. Ebbetts Pass stratovolcano.** Basal strata of the Ebbetts Pass stratovolcano (Fig. 12D) are dated by  $^{40}\text{Ar}/^{39}\text{Ar}$  as  $4.73 \pm 0.03$  Ma (reported in Busby et al., 2013c; complete age data available elsewhere). Growth of this edifice presumably blocked northward transport in the north-northwest-deranged Cataract paleochannel, the youngest fill of which is dated as  $4.91 \pm 0.05$  Ma. However, the stratovolcano formed within a larger pull-apart basin that proba-

bly began to form by ca. 6 Ma (discussed in the following); therefore, undated strata within the pull-apart basin could include deposits of the north-northwest-deranged paleochannel (shown as I. within the pull-apart basin in Fig. 12D). The Ebbetts Pass area (Fig. 5B) is described further (see following discussion of the Mokelumne paleochannel).

## PART II. TIME-SLICE ANALYSIS OF PALEOCHANNELS, IN ORDER OF DERANGEMENT (SOUTH TO NORTH)

A time-slice analysis of the east-west paleochannels across the region (Fig. 5) uses our new maps that show the present-day erosional remnants of sequences 1–4 (Figs. 12A–12D). We do this in the order we infer they were beheaded, from south to north: the Stanislaus, the Cataract, and the Mokelumne paleochannels.

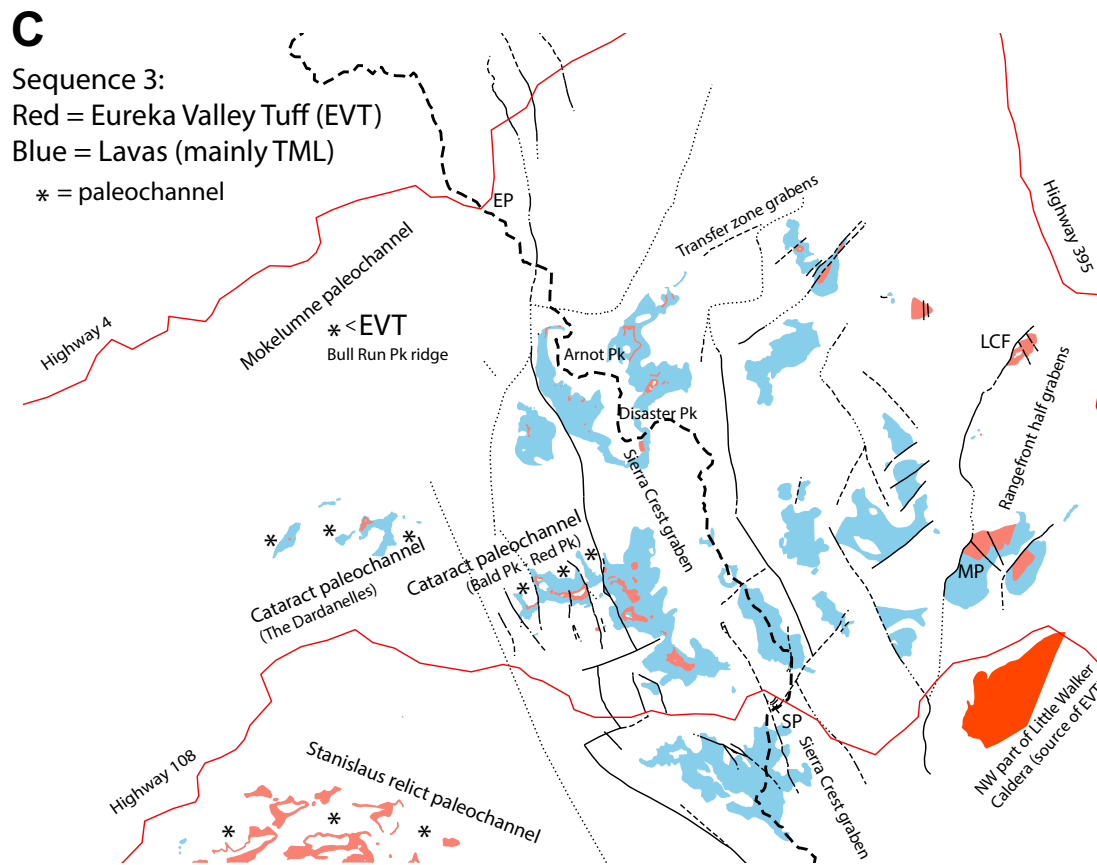
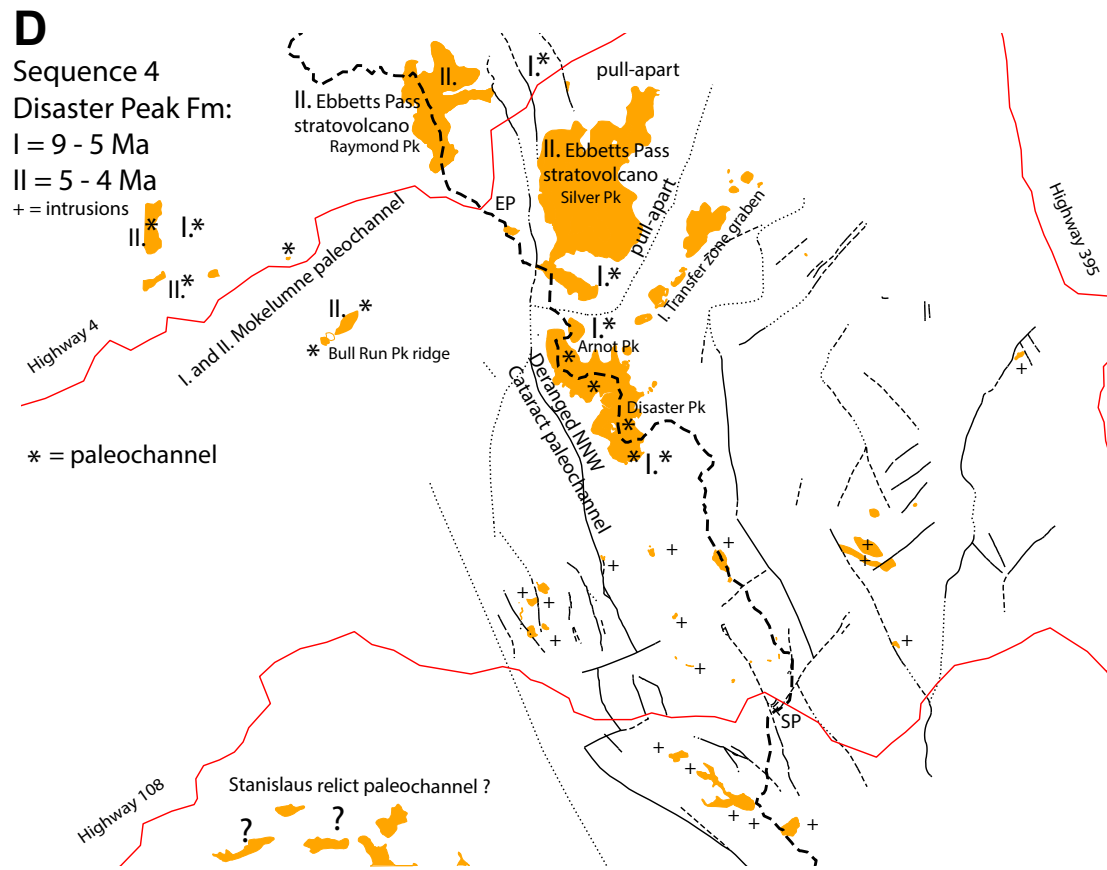


Figure 12 (continued). (C) Sequence 3: Stanislaus Group lavas (mainly Table Mountain Latite) and ignimbrites (Eureka Valley Tuff); paleochannel fill is marked with stars, the rest is graben fill. Lavas are present in the Cataract paleochannel (center), but not in the Stanislaus paleochannel, although the deposits of more mobile pyroclastic flows are present (Eureka Valley Tuff). The Mokelumne paleochannel (north) was beyond the depositional limit for the Stanislaus Group lavas, although one outcrop of Eureka Valley Tuff is present (EVT), attesting to the greater mobility of pyroclastic flows. MP—Mean Peak, where fluvial deposits in the Stanislaus Group follow the approximately north-northwest trend of the half-graben (see text).

### Stanislaus Paleochannel Time-Slice Analysis

The easternmost occurrence of the Valley Springs Formation in the Stanislaus paleochannel is just inside the east margin of the Sierra Crest graben southeast of Sonora Pass (SP, Fig. 12A), where the Valley Springs Formation overlies, *in situ*, granitic basement on the northeast side of Leavitt Lake in Leavitt Creek (Tvs, Fig. 5C; also mapped by Slemmons, 1953). The Valley Springs Formation also occurs as slabs within Relief Peak Formation debris avalanche deposits nearby, for example, at Sardine Falls (Figs. 5C and 8A); this is to be expected, because there is a paleochannel source for the slabs here. The Stanislaus paleochannel has not been found east of the Sierra Crest graben, because the Little Walker caldera (source of the Eureka Valley Tuff) is downdropped there along range-front faults (Fig. 5A); we infer that the Stanislaus paleochannel is deeply buried beneath the caldera.

The absence of *in situ* Valley Springs Formation within most of the Sierra Crest graben is consistent with the interpretation that nearly all of the pre-Stanislaus Group strata within the graben represent debris avalanche deposits shed into the graben immediately before eruption of the Stanislaus Group (Busby et al., 2013a); preexisting paleochannel fill was evidently destroyed during graben subsidence, with the exception of a small paleochannel remnant filled with Relief Peak Formation, offset in a dextral sense along the St. Mary's Pass fault (Fig. 5C; see SM on Fig. 12B). An outcrop of possible *in situ* Valley Springs Formation occurs in the Sierra Crest graben on the north-facing cliffs between the Kennedy Creek fault and Highway 108 (see question mark in Fig. 12A), but we have not been able to access this outcrop to confirm this; it may instead be white fluvial deposits of Relief Peak Formation. *In situ* Valley Springs Formation reappears immediately west of the Sierra Crest graben, on the west side of the Kennedy Creek fault (Figs. 5A and 12A).



**Figure 12 (continued).** (D) Sequence 4: Disaster Peak Formation, subdivided into two time frames. I: 9–5 Ma north-northwest-deranged Cataract paleochannel along the Sierran crest, with fluvial deposits indicating northward flow; transfer zone graben deposits of same age are also shown. Mokelumne paleochannel captured sediments from this. II: 5–4 Ma Ebbets Pass stratovolcano (Tdpeps, Fig. 5B), which formed in a pull-apart basin that probably began to form ca. 6 Ma, and ultimately beheaded the Mokelumne paleochannel, although the stratovolcano fed lava into the paleochannel (see text). Not divided by time frame are the small subvolcanic intrusions mapped as Disaster Peak Formation (Fig. 12D) based on crosscutting relations (i.e., intruding Stanislaus Group or strata of Disaster Peak Formation) or on dates; these are common across the map area, particularly along faults, but they are identified with crosses in the south half of the map area to show that Disaster Peak strata are absent there (except possibly at the southernmost edge, relict Stanislaus paleochannel, marked by question marks; see text).

(Slemmons, 1953; Roelofs, 2004). There the ignimbrite is capped by a section of rhyolitic fluvial sands and gravels, as much as ~100 m thick, and both can be traced for nearly 5 km (Slemmons, 1953). This section ends against a prominent north-northwest shear zone (Fig. 12), referred to herein as the unnamed north-northwest-striking fault; this fault crosses both the Stanislaus paleochannel and the Cataract paleochannel.

The unnamed north-northwest-striking fault is clearly visible on a digital elevation map (DEM) as a linear valley-forming shear zone >25 km long and a few hundred meters wide, the center of which is schematically shown with dashes in Figure 5A. The unnamed north-northwest-striking fault appears to offset the Cataract paleochannel in a dextral sense (Figs. 12A–12C). Paleochannels may meander; for example, the Valley Springs Formation (Tvs) defines an open meander in the Stanislaus paleochannel where it crosses Highway 108 (Fig. 12A). However, all of the units of the Cataract paleochannel are abruptly

offset in what would have been a very sharp northward bend, with no erosional remnants of the intervening missing approximately north-northwest reach preserved (Figs. 12A–12C). Although we have not collected kinematic data along this north-northwest shear zone, all of the other north-northwest shear zones in the region have kinematic indicators of oblique dextral-normal shear (Busby et al., 2013a, 2013b), commonly with volcanic vents exploiting the oblique dextral-normal faults (Fig. 2B). Similarly, we infer that the unnamed north-northwest-striking fault has an extensional component of slip, because is the eruptive site of the ca.  $177 \pm 7$  ka Columns of the Giants basaltic trachy-andesite lava (Farmer et al., 2013), which flowed a short distance down the Middle Fork Stanislaus River on the south side of Highway 108 (Fig. 5A). Along the fault zone at the head of the flow, fresh mafic dikes cut the granitic basement and are in turn cut by faults (J. Tollhurst and Busby, personal observations); these presumably represent feeders to the lava. To the south along the

southwest margin of the fault zone, an undated rhyolite intrusion (mapped as Ti, Fig. 5A; geochemistry presented elsewhere) forms a narrow (~200 m) elongate body (~1 km long) that trends north-northwest and has pervasive flow-banded fabric aligned with the fault, suggesting that its emplacement was fault controlled. Perhaps this undated rhyolite intrusion forms part of a bimodal Quaternary suite that includes the Columns of the Giants. Keith et al. (1982) mapped a swarm of Tertiary intrusions astride a lineament that could represent the northern continuation of the unnamed north-northwest fault, in the headwaters of Highland Creek (Fig. 5A). We have not examined these, but they could be fault controlled; further work is needed to determine if these are intrusions (or lavas) and if they show any crosscutting relations with the unnamed north-northwest fault.

In contrast to the Cataract paleochannel, the Stanislaus paleochannel shows no obvious dextral offset on the unnamed north-northwest fault, suggesting that dextral slip along the fault decreases southward. However, we suggest that the normal component of slip may increase southward, because south of Highway 108 the fault forms a prominent east-facing scarp (visible in the DEM at the south end of the Relief Reservoir; Fig. 5C), with a high relatively flat region to the west that broadly slopes to the west, perhaps due to footwall uplift on the unnamed fault. Further work is needed on the unnamed north-northwest fault and the unmapped region south of Figure 5A, but we suggest that it represents the westernmost strand of the transtensional Walker Lane belt fault zone in the central Sierra, with probable Quaternary slip.

From the unnamed north-northwest-striking fault westward, the Valley Springs Formation forms a relatively continuous deposit (Figs. 5A and 12A); it crosses Highway 108 (Rapp, 1982; Huber, 1983a), where it consists of two ignimbrites described by C. Henry (2013, written commun.). The lower ignimbrite, dated as 26.8 Ma, is probably correlative with upper tuff of Mount Jefferson that erupted from a caldera in the Toquima Range 270 km to the east in Nevada, described by Boden (1992) and Henry and Faulds (2010). The upper ignimbrite is the distinctive 25.4 Ma Nine Hill Tuff, which contains three feldspars (sanidine, plagioclase, and anorthoclase) as well as biotite and quartz, and has high Zr and Nb contents (~400 and 30–40 ppm, respectively; Deino, 1985; Best et al., 1989; Brooks et al., 2008). As shown by Deino (1985, 1989; see also Best et al., 1989), the Nine Hill Tuff is particularly widespread, occurring from the western foothills of the Sierra Nevada to near Ely, Nevada, a present-day distance of ~500 km, and is postulated to have a source beneath the Carson Sink (C. Henry, 2013, written commun.).

The Relief Peak Formation in the Stanislaus paleochannel west of the unnamed north-northwest-striking fault (Fig. 12B) is deeply and complexly incised into the Valley Springs Formation along unconformity 2, showing relief of >500 m across that area. The Relief Peak Formation forms a much broader belt than the Valley Springs Formation there (~5 km versus 1 km; Figs. 5A, 12A, and 12B), suggesting that it filled the paleochannel completely, and was not removed by subsequent reincision events. In this area, the Relief Peak Formation consists of andesitic fluvial and debris flow deposits, with sparse andesite block-and-ash flow tuffs (Busby and J. Tollhurst, personal observations; geo-

chemistry presented elsewhere), and the Jupiter uranium mine is within the paleochannel.

In the Stanislaus paleochannel east of the unnamed north-northwest-striking fault and west of the Kennedy Creek fault (Fig. 5A), Roelofs (2004) mapped Relief Peak Formation andesite lavas interstratified with sandstone and conglomerate; however, his measured section and photos show bodies that are too thin to represent andesite lavas (less than a few meters), with none of the flow-top or flow-bottom breccia that typifies andesite lava. In contrast, we observed many sills and dikes within the sandstone-conglomerate section there, and no lavas (Busby and K. Putirka, personal observation). These undated intrusions are likely to be Disaster Peak Formation age, since those are common in the immediate area (Figs. 5C and 12D) (see supplemental information in Busby et al., 2013a); in contrast, we dated only one intrusion of Relief Peak age across the entire region mapped in Figure 5A, and that is a sill labeled Trp along the easternmost edge (described in detail in Busby et al., 2013b). We found no intrusions truncated by unconformity 3. The lack of intrusions of Relief Peak Formation age is consistent with the lack of andesitic lavas of that age (Fig. 5). Primary volcanic rocks in the Relief Peak Formation mapped in Figure 5 are restricted to (1) the deposits of andesitic block-and-ash flows, which may travel 10 km or more from source domes, particularly if they are funneled down a channel; and (2) basalt lavas in the Cataract paleochannel at The Dardanelles (Fig. 5D) that are more mobile than andesite lavas. This indicates that Relief Peak Formation vents fed material into the paleochannels from a position east of the area mapped in Figure 5.

In the Stanislaus paleochannel west of the unnamed north-northwest fault, the Relief Peak Formation is directly overlain by the Tollhouse Flat Member of the Eureka Valley Tuff; no other members or formations of the Stanislaus Group are present (Figs. 5A and 12C). This is in marked contrast with the Cataract paleochannel to the north (Fig. 5 and 12C) that contains abundant Stanislaus Group lavas (TML, Basal Lava Flow Member, Lava Flow Member, and Dardanelles Formation). This indicates that the Stanislaus paleochannel was beheaded before the Cataract paleochannel was beheaded. In contrast with lavas, pumice-rich pyroclastic density currents are highly mobile, because they are typically fed from Plinian or sub-Plinian eruption columns and drop from great heights (Hayashi and Self, 1992), and can surmount obstacles as much as 1000 m high (Fisher et al., 1993). Therefore, it is not surprising that the Tollhouse Flat Member ignimbrite (by far the most widespread of the three ignimbrites of the Stanislaus Group; Fig. 1C) escaped the Sierra Crest graben to flow westward down the Stanislaus paleochannel. However, we consider it to have been a relict paleochannel by that time (Fig. 12C).

We have not examined the Disaster Peak Formation along the south margin of the Stanislaus paleochannel (west of the unnamed north-northwest-striking unnamed fault, Figs. 5A and 12D); this is shown on an unpublished map made by Slemmons in 1979 and provided to us by David Wagner (California Geological Survey). Therefore we cannot say if the rocks represent paleochannel fill (e.g., fluvial deposits and stratified debris flow deposits), or if they consist of volcanic and/or volcaniclastic rocks or intrusions unrelated to a paleochannel

(question marks in Fig. 12D). However, all other rocks of Disaster Peak Formation age in the southern half of the map area are intrusions (Fig. 12D), so we think it is likely that these rocks are intrusions or lavas related to them.

To summarize, the Valley Springs Formation forms a much more continuous belt in the Stanislaus paleochannel than it does in the Cataract or Mokelumne paleochannels, and the Relief Peak Formation is preserved in a much broader belt (Figs. 12A, 12B). We suggest that this is because the paleochannel was not subjected to the same degree of reincision along unconformities 3 and 4 that the Cataract paleochannel was subjected to, supporting the interpretation that the Stanislaus paleochannel was abandoned prior to regional development of unconformity 3 and the eruption of the TML, which is not present in the Stanislaus paleochannel (Figs. 2B, 5A, and 12C).

### Cataract Paleochannel Time-Slice Analysis

The easternmost occurrence of *in situ* Valley Springs Formation that we have mapped in the Cataract paleochannel (near Highway 395, Fig. 12A) is in the hanging wall of the Lost Cannon fault north of Summit Meadow (Busby et al., 2013b) (LCF in Fig. 12A). There, 245–365 m of Valley Springs Formation overlies, in depositional contact, granitic basement; it is not in fault contact, as mapped by Slemmons (1953), because the welding foliation is conformable with the basal contact, which shows greater relief (due to paleotopography) than would a fault. At this locality the Valley Springs Formation thickens and thins rapidly over a strike length of only 4 km because its upper surface is deeply incised along unconformity 2, in a manner typical of paleochannel fill. Unconformity 2 is overlain by well-rounded, well-sorted fluvial boulder conglomerate of the Relief Peak Formation (sequence 2), with both granitic and andesitic clasts; this is typical of paleochannel fill (not graben fill). However, the overlying Relief Peak Formation debris flow deposits are massive, lack fluvial interbeds, and contain Valley Springs Formation megablocks as much as 40 m long (mapped as Trpdfi, Relief Peak Formation debris flow deposits with large ignimbrite slabs; Busby et al., 2013b); furthermore, most of the andesite clasts are of one type (a dark colored plagioclase two-pyroxene andesite-basaltic andesite), suggesting remobilization from a limited area. This shows that the half-graben on the hanging wall of the Lost Cannon fault (LCF, Fig. 12B) began to form during deposition of the Relief Peak Formation. Furthermore, dips flatten upward within the overlying Stanislaus Group in this half-graben (Fig. 12C; Busby et al., 2013b), demonstrating subsidence during deposition. This indicates progressive disruption of the Cataract paleochannel. (For further information about the faults in the segment, see Busby et al., 2013b.)

In the Grouse Meadows fault block to the south (GM, Figs. 12A, 12B) a 30-m-long outcrop near the base of the Relief Peak Formation was mapped as *in situ* Valley Springs Formation by Priest (1979), but it is clearly surrounded by Relief Peak Formation andesitic debris flow deposits, and therefore does not mark a paleochannel, but rather is a slide block (Busby et al. 2013b). Therefore, *in situ* Valley Springs Formation is not shown there in Figure 12A. The debris flow deposits in the Grouse Meadows half-graben are entirely massive

and lack any fluvial interbeds, although they have slabs of block-and-ash flow tuff (see measured section in fig. 9B of Busby et al., 2013b) in addition to the welded ignimbrite slabs. This is consistent with the interpretation that the Relief Peak Formation here represents graben fill rather than paleochannel fill. We infer that un lithified Relief Peak Formation paleochannel fill was resedimented into the half-graben (GM, Fig. 12B), because slabs of fluvial and debris flow deposits are not present, as they are in the much larger Relief Peak Formation debris avalanche deposit of the southern Sierra Crest graben.

No *in situ* remnants of Valley Springs Formation are preserved in fault blocks between the Lost Cannon half-graben (LC, Fig. 12A) westward to the syndepositionally faulted paleochannel fill (Bald Peak–Red Peak, Fig. 12A) although the Cataract paleochannel must have come through this region. There is only one relict Cataract paleochannel deposit preserved in the floor of the Sierra Crest graben, and that is a narrow (~1 km) V-shaped channel cut into granitic basement and filled with ~200 m of Relief Peak Formation fluvial deposits (Trpf, Fig. 5C), offset in a right-lateral sense by the oblique-normal St. Mary's Pass fault (Fig. 12C; fault labeled SM in Fig. 12B); the rest of the Relief Peak Formation in the Sierra Crest graben consists of debris avalanche deposits (Busby et al., 2013a).

The Stanislaus Group shows evidence for minor north-northwest derangement of the east-west Cataract paleochannel on the footwall of the Lost Cannon fault at Mean Peak (MP, Fig. 12C), where a fluvial section is in the middle of the TML (Tstmlf, Fig. 5A). Synvolcanic faulting there is shown by fanning dips and thickening of the TML toward the Lost Cannon fault. The fluvial pebble conglomerate-sandstone unit within the TML section (Tstmlf, Fig. 5A) thickens dramatically toward the fault, from 10 m to >60 m (Busby et al., 2013b), suggesting that a stream flowed parallel to the approximately north-northwest-striking fault, although due to a combination of erosion (to the north) and burial (by Quaternary sediments to the south), this approximately north-south stream deposit can only be traced for a distance of 4 km (Fig. 5A).

East of the Sierra Crest graben, the Cataract paleochannel was at least partly disrupted during deposition of the Relief Peak Formation (sequence 2) and Stanislaus Group (sequence 3). To the west of the Sierra Crest full graben, however, the Cataract paleochannel continued to receive abundant fluvial sediment of a variety of andesite clast types during deposition of the Relief Peak Formation, showing that the Cataract paleochannel was not fully disrupted during deposition of sequence 2 (Fig. 12B). The Cataract paleochannel west of the Sierra Crest full graben continued to function as a conduit with water in it throughout deposition of sequence 3 Stanislaus Group (Figs. 2B, 12C), funneling lavas and pyroclastic flows to the Sierra foothills (Fig. 3), although fluvial debris was mainly locally sourced from the Stanislaus Group. The Cataract paleochannel west of the Sierra Crest graben was beheaded before Disaster Peak deposition began (sequence 4; Figs. 2B and 12D). We infer that the sequence 4 andesitic sediment load in the north-northwest-deranged Cataract paleochannel (Fig. 12D) was captured from some relict of the Cataract paleochannel east of the Sierra Crest graben (Fig. 2B), but this relict was destroyed by range-front faulting after eruption of the Stanislaus Group, accounting for ~50% of the slip there (described in Busby et al., 2013b).

## Mokelumne Paleochannel Time-Slice Analysis

The Mokelumne paleochannel at Ebbetts Pass is the least well known of the four central Sierra Nevada paleochannels. Unlike the Carson Pass–Kirkwood paleochannel at Carson Pass (Busby et al., 2008b; Hagan et al., 2009) and the Stanislaus and Cataract paleochannels in the Sonora Pass area (Koerner et al., 2009; Busby et al., 2013a, 2013b), no geologic maps have been published on the Ebbetts Pass region for more than 30 yr (Keith et al., 1982; Huber, 1983b; Armin et al., 1984). We present new geologic mapping at Ebbetts Pass (Fig. 5B) (to be described further with geochemical, petrographic, and geochronological data elsewhere). We reinterpret the 1980s published map data to the west of the pass (Fig. 5A), using our own field observations, together with geochemical data (to be presented elsewhere). This represents a first attempt at understanding the evolution of the Mokelumne paleochannel.

Like the other paleochannels, the course of the Mokelumne paleochannel is best defined by the presence of the Valley Springs Formation (Fig. 12A), which predates faulting in the Sierra Nevada. Near Ebbetts Pass, between the Noble Canyon and Grover Hot Springs faults (north end of Fig. 5B), the Valley Springs Formation (Tvs1) consists of a single ignimbrite, as much as 25 m thick, with sanidine, quartz, plagioclase, and biotite, for which Dalrymple (1964) reported a K/Ar age of 20.7 Ma. Henry et al. (2012) correlated this ignimbrite with the tuff of Campbell Creek, a voluminous ( $\sim 3000 \text{ km}^3$ ) ignimbrite that is present in five major paleochannels of the Sierra Nevada. The tuff of Campbell Creek has distinctive vermicular quartz and low Zr and Nb concentrations, and was dated between  $29.04 \pm 0.10 \text{ Ma}$  and  $28.84 \pm 0.09 \text{ Ma}$  by the  $^{40}\text{Ar}/^{39}\text{Ar}$  method on sanidine (Henry et al., 2012). This tuff is one of the most extensive tuffs of western North America, together with the 25.4 Ma Nine Hill Tuff recognized in the Stanislaus paleochannel. Erosional remnants of the Valley Springs Formation extend westward from Ebbetts Pass, on either side of Highway 4 (Tvs1, Fig. 5A), generally preserved beneath andesitic volcaniclastic and volcanic rocks.

Field distinction between the Relief Peak Formation and Disaster Peak Formation is only possible where Stanislaus Group intervenes (Fig. 4); otherwise, radiometric dates are needed to distinguish between older and younger (older than 11–12 Ma, younger than 9 Ma) andesitic volcanic–volcaniclastic rocks. Thus much of the area mapped as the Relief Peak Formation by Armin et al. (1984) along Highway 4 appears on our maps as undifferentiated Miocene or Pliocene volcanic rocks (Tvu, Fig. 5A), and these do not appear on the time-slice maps (Fig. 12). However, we follow Keith et al. (1982) and Huber (1983a) in mapping the Relief Peak Formation south of Highway 4 (Figs. 5A and 2B), because it is overlain at one locality by the Tollhouse Flat Member of the Eureka Valley Tuff (Tset, Fig. 5A; see EVT in Fig. 12C). The Tollhouse Flat Member of the Eureka Valley Tuff is the only Stanislaus Group deposit in the Mokelumne paleochannel (Fig. 12C), consistent with the widespread nature of that ignimbrite (Fig. 3). The Relief Peak Formation in the Mokelumne paleochannel is stratified, with well-rounded well-sorted fluvial boulder to cobble conglomerates (Fig. 11H) intercalated with stratified debris flow deposits (Fig. 11I), consistent with the interpretation that it was deposited in a paleochannel.

Strata that overlie the Valley Springs Formation at Ebbetts Pass are largely too altered to date (Tvu and Tva, Fig. 5B); they could include Relief Peak Formation (question mark in Fig. 12B), or they could consist entirely of the older part (ca. 9–5 Ma) of the Disaster Peak Formation (I in Fig. 12D, and described further in the following); regardless, they are in the substrate of the ca. 5–4 Ma Ebbetts Pass stratovolcano (Tdpeps, Fig. 5B; discussed in the following).

We subdivide the Disaster Peak Formation into frames: (I) deranged north-northwest Cataract paleochannel (ca. 9–5 Ma), and (II) Ebbetts Pass stratovolcano (ca. 5–4 Ma) (see Fig. 12D). Strata of the older time frame appear to be present in the Mokelumne paleochannel north of Highway 4 (I in Fig. 12D), where Armin et al. (1984) reported a hornblende  $7.3 \pm 0.3 \text{ Ma}$  K/Ar age on an andesite lava. This is similar to the  $^{40}\text{Ar}/^{39}\text{Ar}$  hornblende age of  $6.367 \pm 0.017 \text{ Ma}$  on a dacite lava (Tdpld, Fig. 5B) that is south of the ca. 5–4 Ma Ebbetts Pass stratovolcano (Tdpeps, Tdpis, Fig. 5B), in the south end of the Ebbetts Pass pull-apart basin (I in Fig. 12D). It is also similar to a  $^{40}\text{Ar}/^{39}\text{Ar}$  hornblende age of  $6.203 \pm 0.011 \text{ Ma}$  on a slide block of andesite within the Ebbetts Pass stratovolcano section (dates to be presented elsewhere); the slide block was presumably shed from the walls of the pull-apart basin. However, the 7.3 Ma andesite lava Armin et al. (1984) described in the Mokelumne paleochannel is too far from any fault to represent a slide block, and therefore represents a lava that flowed down the paleochannel. The 7.3 Ma lava is also important for providing a maximum age on overlying rocks in the paleochannel that Armin et al. (1984) mapped as Raymond Peak and Silver Peak andesites of Wilshire (1957) and that we map as Ebbetts Pass stratovolcano (Tdpeps; Figs. 5A, 5B, and 12D).

Armin et al. (1984) described the Raymond Peak and Silver Peak andesites of Wilshire (1957) as volcanic debris flow deposits, tuffs, lavas, and volcanic necks, with less alteration than the underlying Tertiary (Paleogene–Neogene) rocks, and distinguished it from the Relief Peak Formation by the presence of lavas and less alteration. We agree that the same formation (Raymond Peak and Silver Peak andesites of Wilshire [1957]) can be correlated along the crest, from the Raymond Peak area to the Silver Peak–Highland Peak area, separated by granitic basement and the Nobel Canyon fault (Figs. 5B and 12D), and that it is less altered than underlying rocks. We interpret this map unit largely as an eroded stratovolcano (Ebbetts Pass stratovolcano, Fig. 12D; Tdpes, Figs. 5A, 5B), with radial dips, composed of lavas, block-and-ash flow tuffs, and volcanic debris flow deposits, with silicic plugs in its core. Armin et al. (1984) also mapped this unit ~10 km west of Ebbetts Pass, north of Highway 4 (Tdpeps, Fig. 5A); we interpret it as lava that was erupted from the Ebbetts Pass stratovolcano and flowed down the Mokelumne paleochannel (II in Fig. 12D). In addition, we propose that the lava on the Bull Run ridge south of Highway 4 (Tdeps, Fig. 5A; see II in Fig. 12D) has the same origin (Fig. 11G). Although Huber (1983a) mapped the lava on Bull Run as the Dardanelles Formation, as noted here and elsewhere (Koerner et al., 2009; Busby et al., 2013a), a variety of lavas were previously erroneously assigned to the Dardanelles Formation; where its stratigraphic context can be demonstrated (overlying the Upper Member of the Eureka Valley Tuff), the Dardanelles Formation consists of a single distinctive jet-black glassy nearly aphyric shoshonite lava. The lava on Bull Run does not

match this description; it is not aphyric or glassy, and its chemical composition is andesite (geochemistry to be presented elsewhere). Thus, although the Mokelumne paleochannel must have been cut off from source areas east of Ebbetts Pass by the time the stratovolcano formed (by ca. 5 Ma), it continued to serve as a conduit for lavas erupted from the Ebbetts Pass stratovolcano (that is, it was a relict paleochannel).

## ■ TIMING OF DERANGEMENT OF SIERRA NEVADA PALEOCHANNELS FROM SONORA PASS TO THE TAHOE BASIN

Here we briefly summarize evidence for the timing of beheading of the next two paleochannels to the north of the three paleochannels described in detail above, then summarize the regional pattern.

The north-south, down-to-the-east fault we refer to as the Grover Hot Springs fault (Fig. 5A) continues northward from Ebbetts Pass ~11 km (Fig. 2B; Armin et al., 1984). We have not mapped this area because the rocks are largely too altered and poorly exposed to be suitable for detailed stratigraphic and structural work. However, <5 km to the west of the northern half of the Grover Hot Springs fault, higher on the range front, are largely unaltered, very well exposed volcanic rocks on either side of and within the north-northwest Hope Valley, a full graben, the western footwall of which forms the modern Sierra Nevada crest (Fig. 3B; see map in Hagan et al., 2009). Like the modern East Fork of the Carson River, the headwaters of which are controlled by faults of the north-northwest Sierra Crest full graben, the headwaters of the modern West Fork of the Carson River are within the north-northwest Hope Valley graben.

The age of the paleochannel fill and the timing for its beheading are very well constrained at Carson Pass (Busby et al., 2008b; Hagan et al., 2009). East of the Hope Valley fault are two paleotributaries that merge within the area of the graben into a single paleochannel mapped from the crest westward to the Kirkwood ski area (Busby et al., 2008b; Hagan et al., 2009). The paleochannel fill includes Valley Springs Formation (including 25.4 Ma Nine Hill Tuff; Henry and John, 2013), and Miocene fluvial and debris flow deposits interstratified with block-and-ash flow tuffs and rare lavas, ranging from  $15.5 \pm 0.6$  Ma to  $6.13 \pm 0.12$  Ma ( $^{40}\text{Ar}/^{39}\text{Ar}$ ; Busby et al., 2008b; Hagan et al., 2009). The Red Lake and Hope Valley faults were active by 6 Ma, as shown by eruption of hornblende andesite lava through the former, and emplacement of the Markleeville intrusive complex along the latter (Hagan et al., 2009). No younger deposits occur in the paleochannel to the west, indicating that it was beheaded when the Hope Valley graben began to form at 6 Ma.

Approximately 40 km to the north of the Carson Pass at the latitude of Lake Tahoe (Fig. 1) is an east-west paleochannel that has been very well studied east of the Sierra Nevada range front (Henry et al., 2012; Henry and John, 2013), but studies of this paleochannel within the Sierra Nevada have focused mainly on the Oligocene ignimbrites (Henry and John, 2013), so relatively little is known about its Miocene to Pliocene history. However, Schweickert (2009) summarized the distribution of andesite lavas in this part of the Sierra, and they ap-

pear to coincide well with the east-west paleochannel defined by the Oligocene ignimbrites on a map (Garside et al., 2005). Cross sections in Schweickert (2009, Fig. 5 therein) show andesitic debris flow and fluvial deposits overlain by andesite lavas, and on these cross sections, the strata appear to be within paleochannels cut into the granitic basement. As summarized by Schweickert (2009), there are 9 whole-rock K/Ar ages on these lavas, ranging from 5.2 to 3.0 Ma (Harwood, in Saucedo and Wagner, 1992); although the K/Ar dating method is not as reliable as  $^{40}\text{Ar}/^{39}\text{Ar}$ , the large number of similar ages suggests to us that the paleochannel continued to function until ca. 3 Ma. Schweickert (2009) showed that the modern west-flowing drainages incise deeply into the dated lavas, and inferred that uplift and westward tilting on the range-front fault began after ca. 3 Ma. Although one could argue that this tilting occurred on faults further east (and therefore does not record beheading of the paleochannel), an age estimate of beheading of ca. 3 Ma is consistent with the age of initiation of tilting of strata directly to the east in the Boca Basin (Mass et al., 2009), discussed by Wakabayashi (2013). We thus estimate the timing of beheading of the paleochannel at Lake Tahoe as 3 Ma.

We demonstrated that the Stanislaus paleochannel was largely abandoned before eruption of the Stanislaus Group (by ca. 11 Ma); the Cataract paleochannel was abandoned by the end of Stanislaus Group eruption (by ca. 9 Ma); and the Mokelumne paleochannel was beheaded between ca. 6 and 5 Ma. The Carson Pass–Kirkwood paleochannel, ~16 km north of that, was beheaded around the same time (ca. 6 Ma), and the next paleochannel, ~40 km to the north of that at Lake Tahoe, was beheaded ca. 3 Ma. The timing of beheading, from the Stanislaus paleochannel to Lake Tahoe, thus corresponds to the northward migration of the Mendocino Triple Junction and northward propagation of the Walker Lane transtensional strain regime (Fig. 2A). This is consistent with the interpretation of Wakabayashi (2013) that initiation of stream incision and inferred rock uplift appear to young northward, from the Kern River in the southern Sierra to the northern limit of the Sierra, consistent with a connection to the northward-migrating triple junction.

## ■ CONCLUSIONS

Although Cenozoic paleochannels in the Sierra Nevada were a major target of the nineteenth century California gold rush, and have been recognized as paleochannels for more than a century (Ransome, 1898; Lindgren, 1911), they have not previously been the subject of detailed geologic mapping. This study, together with our recent studies at Carson Pass (Busby et al., 2008a; Hagan et al., 2009), focused on paleochannels in the central Sierra Nevada, because these are far better exposed than those of the northern Sierra (which is on lower, forested ground), and their fill has not been largely eroded away like those of the southern Sierra (which forms the highest, most deeply dissected ground). Superior exposure has allowed us to make detailed maps of lithofacies, unconformity surfaces, and syndepositional to postdepositional faults. We used these to study the evolution of paleochannels having basal fill that

formed in a tectonically stable environment, and demonstrate how these became progressively disrupted by Walker Lane transtensional grabens (starting ca. 12 Ma), ultimately becoming deranged into north-northwest trends typical of drainages in the Walker Lane belt today.

For the first time, we showed that three distinct ancient east-west paleochannels crossed the Sierra Nevada in the Sonora Pass–Ebbetts Pass region; from south to north these are the Stanislaus, Cataract, and Mokelumne paleochannels (Fig. 12). These formed on the western shoulder of a broad Cretaceous uplift with its drainage divide in eastern Nevada, called the Nevadaplano. Previously it was inferred that a single east-west paleochannel crossed the Sierra at Sonora Pass, variably referred to as the Cataract or Stanislaus paleochannel, but we show here that in part the paleochannel deposits were confused with ca. 12–9 Ma transtensional graben fills of the Sierra Crest graben-vent system (Fig. 2B); the latter was not recognized prior to our recent work (Busby et al., 2013a, 2013b). Using criteria defined herein to distinguish between the paleochannels and the transtensional grabens, we recognize two distinct east-west paleochannels at Sonora Pass, the Stanislaus paleochannel in the south and the Cataract paleochannel in the north (Fig. 12). We also used these criteria to map the course of the east-west Mokelumne paleochannel at Ebbetts Pass (Fig. 12), and distinguish it from the fill of the Ebbetts Pass pull-apart basin (Fig. 2B), which ultimately beheaded it.

We herein define criteria for distinguishing between volcanic-volcaniclastic paleochannel fill versus graben fill; many of these criteria can be applied to other sedimentary settings, although some are particular to volcanically active settings. The most obvious (and most exportable) criteria for distinction of volcanic-clastic paleochannel fill from graben fill are (1) interstratification of abundant fluvial conglomerates and well-stratified (not massive) debris flow deposits with the primary volcanic rocks, (2) deep reincision surfaces (erosional unconformities), as much as hundreds of meters in depth, and (3) widths and depths that are much smaller than the grabens and are consistent with regional data on paleochannel sizes (which deepen southward in the Sierra; Wakabayashi and Sawyer, 2001; Wakabayashi, 2013). Additional paleochannel features specific to the Sierra Nevada include (1) the presence of ignimbrites erupted from calderas that are 200 km to the east; as Henry et al. (2012) pointed out, the pyroclastic density currents could not have traveled so far if they were not funneled through valleys; and (2) the presence of black chert clasts, also derived from Nevada, in the fluvial deposits; these further support the interpretation of long sediment dispersal systems. Other features of nonderanged paleochannels in the Sierra Nevada are west-directed (rather than approximately north or south directed) paleocurrent indicators in sedimentary rocks, and east-west (rather than north-northwest) stretching of vesicles in lavas. Features in volcanic rocks that indicate deposition in the presence of water include kuppaberg jointing on the tops of lavas, peperitic bases on lavas, and well-developed perlitic fracture in ignimbrite vitrophyres. In the Sierra Nevada these only formed in the paleochannels, although in other settings they may form in grabens containing standing water (e.g., lakes), or in association with ice (e.g., kuppaberg jointing in Iceland). Tree molds are also present at the base of lavas in paleochannels but not in the grabens.

Graben-filling volcanic-volcaniclastic sequences contrast with paleochannel fills in several ways. They are dominated by avalanche deposits and massive (nonstratified) debris flow deposits, indicating catastrophic resedimentation. They generally lack fluvial conglomerates (except in graben-controlled deranged paleochannels). They also lack deep erosional unconformities because their fill is highly aggradational. Graben-filling volcanic-volcaniclastic successions are generally 3–10 times thicker than paleochannel fill, and individual formations or members or lavas or ignimbrites are several times thicker, and more sheet like. In contrast, lavas and ignimbrites are preserved as lenticular erosional remnants in the paleochannels; for example, the classic TML flow, with its distinctive paleomagnetic signature, is very thick in at its vent in the Sierra Crest graben on Sonora Peak, and also very thick (>100 m) in the Cataract paleochannel at The Dardanelles and Knight's Ferry in the foothills (locations in Fig. 3; Busby et al., 2008a; Gorny et al., 2009), but it is absent in Red Peak–Bald Peak segment of the Cataract paleochannel (Chris Pluhar, 2012, personal commun.).

Evidence for progressive derangement of paleodrainages by graben-bounding growth faults in volcanic-volcaniclastic successions includes (1) abrupt thickening and thinning of the channelized ignimbrites across faults; ignimbrites are particularly sensitive recorders of growth faulting, because they typically form near flat and horizontal tops; (2) deposition of locally derived slide blocks on the hanging walls of growth faults, and infilling of fault-controlled plunge pools by boulder conglomerates; and (3) siting and preservation of vent deposits along growth faults within paleochannels, including phreatomagmatic deposits indicative of eruption through stream water or associated groundwater. In both the Sierra Crest graben and the Ebbetts Pass pull-apart basin (Fig. 2B), most lavas were trapped within the basins, although some escaped westward into the dying and/or relict paleochannels. However, unlike earlier paleochannel fill, these were not deeply incised and filled with younger deposits, thus indicating loss of stream power due to beheading by faults.

Evidence for derangement of the ancient east-west paleochannels into north-northwest Walker Lane drainage trends, which persist today, is extremely well displayed along the Sierra Crest between Sonora Pass and Ebbetts Pass, in the north-northwest-deranged Cataract paleochannel (Figs. 2B and 12D). This 9–5 Ma paleochannel fill is composed entirely of sequence 4 (Disaster Peak Formation, Fig. 12D), incised into 12–9 Ma Stanislaus Group fill of the Sierra Crest graben (sequence 3, Fig. 12C); the region is between the Cataract and Mokelumne paleochannels and thus lacks sequence 1 and 2 paleochannel strata of the Valley Springs and Relief Peak Formations (Figs. 12A, 12B). The volcaniclastic fill of the north-northwest-deranged Cataract paleochannel closely resembles that of the east-west paleochannels in outcrop features, although the composition of its volcanic-volcaniclastic rocks differs, because it postdates high-K volcanism of the Stanislaus Group (sequence 3), and it has more evolved rocks than the Relief Peak Formation (sequence 2). The depth and width of the north-northwest-deranged Cataract paleochannel is the same as those of the east-west paleochannels of the central Sierra, consistent with the interpretation that it formed part of the same drainage system.

We infer that the north-northwest–deranged Cataract paleochannel pirated sediment from the disrupted east-west Cataract paleochannel, and carried it northward to the east-west Mokelumne paleochannel from 9 to 5 Ma. This drainage system was disrupted by the growth of the Ebbets Pass stratovolcano in the Ebbets Pass pull-apart basin (Figs. 2B and 12D).

The timing of beheading of paleochannels between Sonora Pass and Lake Tahoe, a distance of ~110 km, coincides closely with the south to north passage of the Mendocino Triple Junction (for exact locations through time, see calibration by Putirka et al., 2012, based on initial position at 30 Ma from Atwater, 1970, and positions thereafter proposed by Atwater and Stock, 1998). It is not a new idea that Walker Lane faults have propagated northward in concert with Mendocino Triple Junction migration (Faulds and Henry, 2008); nor is it a new idea that northward propagation of the triple junction, and the opening of the slab window, exerts important controls on tectonic events and volcanic compositions far inboard of the junction (Dickinson and Snyder, 1979; Zandt and Humphreys, 2008; Putirka et al., 2012). However, the northward unzipping along the arc and the siting of the major centers on transtensional stepovers are new concepts (Fig. 2A; Busby et al., 2010; Busby, 2011, 2013). As shown here, the timing of beheading of paleochannels, from the southern part of the central Sierra, to the southern part of the northern Sierra, was controlled by northward migration of the Mendocino Triple Junction.

This paper illustrates in detail the interplay between tectonics and drainage development, exportable to a very broad variety of geologic settings, thus demonstrating the value of detailed geologic mapping.

#### ACKNOWLEDGMENTS

This research was supported by National Science Foundation (NSF) grants EAR-01252 (to Busby, P.B. Gans, and I. Skilling), EAR-0711276 (to K. Putirka and Busby), EAR-0711181 (to Busby), and EAR-1347901 (to Busby and S.M. DeBari), as well as U.S. Geological Survey EDMAP program awards 03HQAG0030, 06HQAO061, and 09HQPA0004 (to Busby) and funds from the University of California, Santa Barbara, Academic Senate (to Busby). Support for geographic information system data and illustrations was also provided by NSF grants EAR-1019559 (to Busby) and HRD-1137774 (to Andrews). Reviews by John Wakabayashi and an anonymous reviewer are gratefully acknowledged.

#### REFERENCES CITED

- Al Rawi, Y.T., 1969, Cenozoic history of the northern part of Mono Basin (Mono county): California and Nevada [PhD Dissertation]: University of California at Berkeley, 188 p.
- Argus, D.F., and Gordon, R.G., 1991, Current Sierra Nevada–North America motion from very long baseline interferometry: Implications for the kinematics of the western United States: *Geology*, v. 19, p. 1085–1088, doi:10.1130/0091-7613(1991)019<1085:CSNAM>2.3.CO;2.
- Andrews, G.D.M., Russell, J.K., Brown, S.R., and Enkin, R.J., 2012, Pleistocene reversal of the Fraser River, British Columbia: *Geology*, v. 40, p. 111–114, doi:10.1130/G32488.1.
- Armin, R.A., John, D.A., and Moore, W.J., 1984, Geologic map of the Markleeville 15-minute quadrangle with Quaternary geology by John C. Dohrenwend: U.S. Geological Survey Miscellaneous Investigations Series Map I-1474, scale 1:62,500.
- Atwater, T., 1970, Implications of plate tectonics for the Cenozoic tectonic evolution of western North America: *Geological Society of America Bulletin*, v. 81, p. 3513–3536, doi:10.1130/0016-7606(1970)81[3513:IOPFT]2.0.CO;2.
- Atwater, T., and Stock, J., 1998, Pacific–North America plate tectonics of the Neogene southwestern United States—An update, in Ernst, W.G., and Nelson, C.A., eds., *Integrated earth and environmental evolution of the southwestern United States: The Clarence A. Hall, Jr. Volume*: Columbia, Maryland, Bellwether Publishing, p. 393–420.
- Axelrod, D.I., 1957, Late Tertiary floras and the Sierra Nevadan uplift: *Geological Society of America Bulletin*, v. 68, p. 19–46, doi:10.1130/0016-7606(1957)68[19:LTFATS]2.0.CO;2.
- Bateman, P.C., and Wahrhaftig, C., 1966, Geology of the Sierra Nevada, in Bailey, E.H., ed., *Geology of northern California: California Division of Mines Bulletin* 190, p. 107–172.
- Best, M.G., Christiansen, E.H., and Blank, H.R., Jr., 1989, Oligocene caldera complex and calc-alkaline tuffs of the Indian Peak volcanic field, Nevada and Utah: *Geological Society of America Bulletin*, v. 101, p. 1076–1090, doi:10.1130/0016-7606(1989)101<1076:OCCACA>2.3.CO;2.
- Boden, D.R., 1992, Geologic map of the Toquima caldera complex, central Nevada: Nevada Bureau of Mines and Geology Map 98, scale 1:48,000.
- Brem, G.F., 1984, Geologic map of the Sweetwater Roadless Area, Mono County, California, and Lyon and Douglas counties, Nevada: U.S. Geological Survey Miscellaneous Field Studies Map 1535-B.
- Brooks, E.R., Henry, C.D., and Faulds, J.E., 2008, Age and character of silicic ash-flow tuffs at Haskell Peak, Sierra County, California: Part of a major Eocene(?)–Oligocene paleovalley spanning the Sierra Nevada–Basin and Range boundary: *California Geological Survey Map Sheet* 55A, 39 p., scale 1:24,000.
- Busby, C.J., 2011, Siting of large volcanic centers at releasing fault stepovers, Walker Lane rift: American Geophysical Union fall meeting, abs. T23F-04.
- Busby, C., 2012, Extensional and transtensional continental arc basins: Case studies from the southwestern U.S. and Mexico, in Busby, C., and Azor, A., eds., *Tectonics of sedimentary basins: Recent advances*: Hoboken, New Jersey, Blackwell Publishing Ltd, p. 382–404.
- Busby, C., 2013, Birth of a plate boundary at ca. 12 Ma in the Ancestral Cascades arc, and implications for transtensional rift propagation, Walker Lane belt: *Geosphere*, v. 9, p. 1147–1160, doi:10.1130/GES00928.1.
- Busby, C.J., and Putirka, K., 2009, Miocene evolution of the western edge of the Nevadaplano in the central and northern Sierra Nevada: Paleocanyons, magmatism and structure, in Ernst, G., ed., *The rise and fall of the Nevadaplano: International Geology Review*, v. 51, p. 671–701, doi:10.1080/00206810902978265.
- Busby, C.J., Hagan, J.C., Putirka, K., Pluhar, C.J., Gans, P.B., Wagner, D.L., Rood, D.H., DeOreo, S.B., and Skilling, I., 2008a, The ancestral Cascades arc: Cenozoic evolution of the central Sierra Nevada (California) and the birth of the new plate boundary, in Wright, J.E., and Shervais, J.W., eds., *Ophiolites, arcs, and batholiths: A tribute to Cliff Hopson*: Geological Society of America Special Paper 438, p. 331–378, doi:10.1130/2008.2438(12).
- Busby, C.J., DeOreo, S.B., Skilling, I., Hagan, J.C., and Gans, P.B., 2008b, Carson Pass–Kirkwood paleocanyon system: Implications for the Tertiary evolution of the Sierra Nevada, California: *Geological Society of America Bulletin*, v. 120, p. 274–299, doi:10.1130/B25849.1.
- Busby, C.J., Hagan, J.C., Koerner, A.A., Putirka, K., Pluhar, C.J., and Melosh, B.L., 2010, Birth of a plate boundary: *Geological Society of America Abstracts with Programs*, v. 42, no. 4, p. 80.
- Busby, C.J., Koerner, A.A., Melosh, B.L., Andrews, G.D.M., and Hagan, J.C., 2013a, The Sierra Crest graben-vent system: A Walker Lane pull-apart in the Ancestral Cascades Arc: *Geosphere*, v. 9, p. 736–780, doi:10.1130/GES00670.1.
- Busby, C.B., Hagan, J.C., and Renne, P., 2013b, Initiation of Sierra Nevada range front–Walker Lane faulting ca. 12 Ma in the ancestral Cascades arc: *Geosphere*, v. 9, p. 1125–1146, doi:10.1130/GES009271.
- Busby, C.J., Putirka, K., Renne, P., Melosh, B., Hagan, J., and Koerner, A., 2013c, A tale of two Walker Lane pull-aparts: *Geological Society of America Abstracts with Programs*, v. 45, no. 6, p. 59.
- Cassel, E.J., and Graham, S.A., 2011, Paleovalley morphology and fluvial system evolution of Eocene–Oligocene sediments (“auriferous gravels”), northern Sierra Nevada, California: Implications for climate, tectonics, and topography: *Geological Society of America Bulletin*, v. 123, p. 1699–1719, doi:10.1130/B30356.1.
- Cassel, E.J., Calvert, A., and Graham, S.A., 2009a, Age, geochemical composition, and distribution of Oligocene ignimbrites in the northern Sierra Nevada, California: Implications for landscape morphology, elevation, and drainage divide geography of the Nevadaplano: *International Geology Review*, v. 51, p. 723–742, doi:10.1080/00206810902880370.
- Cassel, E.J., Graham, S.A., and Chamberlain, C.P., 2009b, Cenozoic tectonic and topographic evolution of the northern Sierra Nevada, California, through stable isotope paleoaltimetry in volcanic glass: *Geology*, v. 37, p. 547–550, doi:10.1130/G25572A.1.

- Cassel, E.J., Graham, S.A., Chamberlain, C.P., and Henry, C.D., 2012a, Early Cenozoic topography, morphology, and tectonics of the northern Sierra Nevada and western Basin and Range: *Geosphere*, v. 8, p. 229–249, doi:10.1130/GES00671.1.
- Cassel, E.J., Grove, M., and Graham, S.A., 2012b, Eocene drainage evolution and erosion of the Sierra Nevada batholith across northern California and Nevada: *American Journal of Science*, v. 312, p. 117–144, doi:10.2475/02.2012.03.
- Cecil, M.R., Ducea, M.N., Reiners, P.W., and Chase, C.G., 2006, Cenozoic exhumation of the northern Sierra Nevada, California, from (U-Th)/He thermochronology: *Geological Society of America Bulletin*, v. 118, p. 1481–1488, doi:10.1130/B25876.1.
- Cecil, M.R., Ducea, M.N., Reiners, P., Gehrels, G., Mulch, A., Allen, C., and Campbell, I., 2010, Provenance of Eocene river sediments from the central northern Sierra Nevada and implications for paleotopography: *Tectonics*, v. 29, TC6010, doi:10.1029/2010TC002717.
- Curtis, G.H., 1954, Mode of origin of pyroclastic debris in the Mehrten Formation of the Sierra Nevada: University of California Publications in Geological Sciences, v. 29, p. 453–502.
- Dalrymple, G.B., 1963, Potassium-argon dates of some Cenozoic volcanic rocks of the Sierra Nevada, California: *Geological Society of America Bulletin*, v. 74, p. 379–390, doi:10.1130/0016-7606(1963)74[379: PDOSCV]2.0.CO;2.
- Dalrymple, G.B., 1964, Cenozoic chronology of the Sierra Nevada: University of California Publications in Geological Sciences, v. 47, 39 p.
- Dalrymple, G.B., Cox, A., Doell, R.R., and Grommé, C.S., 1967, Pliocene geomagnetic polarity epochs: *Earth and Planetary Science Letters*, v. 2, p. 163–173, doi:10.1016/0016-821X(67)90122-7.
- DeCelles, P.G., 2004, Late Jurassic to Eocene evolution of the Cordilleran thrust belt and foreland basin system, western U.S.A.: *American Journal of Science*, v. 304, p. 105–168, doi:10.2475/ajs.304.2.105.
- Deino, A.L., 1985, Stratigraphy, chemistry, K-Ar dating, and paleomagnetism of the Nine Hill Tuff, California-Nevada [Ph.D. thesis]: Berkeley, University of California, 457 p.
- Deino, A.L., 1989, Single crystal  $^{40}\text{Ar}/^{39}\text{Ar}$  dating as an aid in correlation of ash flows: Examples from the Chimney Springs/New Pass Tuffs and the Nine Hill/Bates Mountain Tuffs of California and Nevada: New Mexico Bureau of Mines and Mineral Resources Bulletin 131, *Continental Magmatism Abstracts*, p. 70.
- Dickinson, W.R., and Snyder, W.S., 1979, Geometry of subducted slabs related to the San Andreas transform: *Journal of Geology*, v. 87, p. 609–627, doi:10.1086/628456.
- Dixon, T.H., Miller, M., Farina, F., Wang, H., and Johnson, D., 2000, Present-day motion of the Sierra Nevada block and some tectonic implications for the Basin and Range province, North American Cordillera: *Tectonics*, v. 19, p. 1–24, doi:10.1029/1998TC001088.
- Durrell, C., 1966, Tertiary and Quaternary geology of the northern Sierra Nevada, in Bailey, E.H., ed., *Geology of northern California: California Division of Mines and Geology Bulletin* 190, p. 185–197.
- Fairbridge, R.W., ed., 1968, Encyclopedia of geomorphology: *Encyclopedia of Earth Sciences*, Volume 3: New York, Van Nostrand Reinhold, 1296 p.
- Farmer, G.L., Glazner, A.F., Kortemeier, W.T., Cosca, M.A., Jones, C.H., Moore, J.E., and Schweickert, R.A., 2013, Mantle lithosphere as a source of postsubduction magmatism, northern Sierra Nevada, California: *Geosphere*, v. 9, p. 1102–1124, doi:10.1130/GES00885.1.
- Faulds, J.E., and Henry, C.D., 2008, Tectonic influences and temporal evolution of the Walker Lane: An incipient transform along the evolving Pacific-North American plate boundary, in Spencer, J.E., and Titley, S.R., eds., *Ores and orogenesis: Circum-Pacific tectonics, geologic evolution, and ore deposits*: Arizona Geological Society Digest 22, p. 437–470.
- Fisher, R.V., Orsi, G.M., Ort, M., and Heiken, G., 1993, Mobility of a large-volume pyroclastic flow—Emplacement of the Campanian ignimbrite, Italy: *Journal of Volcanology and Geothermal Research*, v. 56, p. 205–220, doi:10.1016/0377-0273(93)90017-L.
- Garrison, N., Busby, C.J., Gans, P.B., Putirka, K., and Wagner, D.L., 2008, A mantle plume beneath California? The mid-Miocene Lovejoy flood basalt, northern California, in Wright, J., and Shervais, J., eds., *Ophiolites, arcs and batholiths: A tribute to Cliff Hopson*: Geological Society of America Special Paper 438, p. 551–572, doi:10.1130/2008.2438(20).
- Garside, L.J., Henry, C.D., Faulds, J.E., and Hinz, N.H., 2005, The upper reaches of the Sierra Nevada auriferous gold channels, in Rhoden, H.N., et al., eds., *Geological Society of Nevada Symposium 2005: Window to the world: Reno, Nevada*: Geological Society of Nevada, p. 209–235.
- Gibert, C.M., Christiansen, M.N., Al-Rawi, Y., and Lajoie, K.R., 1968, Structural and volcanic history of Mono Basin, California-Nevada, in Coats, R.R., et al., eds., *Studies in volcanology*: *Geological Society of America Memoir* 116, p. 275–329.
- Giusso, J.R., 1981, Preliminary geologic map of the Sonora Pass 15-minute Quadrangle, California: U.S. Geological Survey Open-File Report OF-81-1170, scale 1:62,500.
- Gorni, C., Busby, C.J., Pluhar, C.J., Hagan, J.C., and Putirka, K., 2009, An in-depth look at distal Sierra Nevada paleochannel fill: Drill cores through the Table Mountain Latite near Knights Ferry: *International Geology Review*, v. 51, p. 824–842, doi:10.1080/00206810902944960.
- Hagan, J.C., 2010, Volcanology, structure, and stratigraphy of the central Sierra Nevada range front (California), Carson Pass to Sonora Pass [Ph.D. thesis]: Santa Barbara, University of California, 267 p.
- Hagan, J.C., Busby, C.J., Putirka, K., and Renne, P.R., 2009, Cenozoic palaeocanyon evolution, ancestral Cascades arc volcanism, and structure of the Hope Valley–Carson Pass region, Sierra Nevada, California: *International Geology Review*, v. 51, p. 777–823, doi:10.1080/00206810903028102.
- Halsey, J.H., 1953, *Geology of parts of the Bridgeport (California) and Wellington (Nevada) quadrangles* [PhD thesis]: Berkeley, University of California, 506 p.
- Hayashi, J.N., and Self, S., 1992, A comparison of pyroclastic flow and debris avalanche mobility: *Journal of Geophysical Research*, v. 97, no. B6, p. 9063–9071, doi:10.1029/92JB00173.
- Henry, C.D., 2008, Ash-flow tuffs and paleovalleys in northeastern Nevada: Implications for Eocene paleogeography and extension in the Sevier hinterland, northern Great Basin: *Geosphere*, v. 4, p. 1–35, doi:10.1130/GES00122.1.
- Henry, C.D., and Faulds, J.E., 2010, Ash-flow tuffs in the Nine Hill, Nevada paleovalley and implications for the tectonism and volcanism of the western Great Basin, USA: *Geosphere*, v. 6, p. 339–369, doi:10.1130/GES00548.1.
- Henry, C.D., and John, D., 2013, Magmatism, ash-flow tuffs, and calderas of the ignimbrite flareup in the western Nevada volcanic field, Great Basin, USA: *Geosphere*, v. 9, p. 951–1008, doi:10.1130/GES00867.1.
- Henry, C.D., Hinz, N.H., Faulds, J.E., Colgan, J.P., John, D.A., Brooks, E.R., Cassel, E.J., Garside, L.J., Davis, D.A., and Castor, S.B., 2012, Eocene–early Miocene paleotopography of the Sierra Nevada–Great Basin–Nevadaplano based on widespread ash-flow tuffs and paleovalleys: *Geosphere*, v. 8, p. 1–27, doi:10.1130/GES00727.1.
- Hinz, N.H., Faulds, J.E., and Henry, C.D., 2009, Tertiary volcanic stratigraphy and paleotopography of the Diamond and Fort Sage Mountains, northeastern California and western Nevada—Implications for development of the northern Walker Lane, in Oldow, J.S., and Cashman, P.H., eds., *Late Cenozoic structure and evolution of the Great Basin–Sierra Nevada transition*: Geological Society of America Special Paper 447, p. 101–132, doi:10.1130/2009.2447(07).
- Hren, M.T., Pagani, M., Erwin, D.M., and Brandon, M., 2010, Biomarker reconstruction of early Eocene paleotopography and paleoclimate of the northern Sierra Nevada: *Geology*, v. 38, p. 7–10, doi:10.1130/G30215.1.
- Huber, N.K., 1981, Amount and timing of late Cenozoic uplift and tilt of the central Sierra Nevada, California: Evidence from the upper San Joaquin River basin: U.S. Geological Survey Professional Paper 1197, 28 p.
- Huber, N.K., 1983a, Preliminary geologic map of Dardanelles Cone quadrangle, central Sierra Nevada, California: U.S. Geological Survey Miscellaneous Field Studies Map MF-1436.
- Huber, N.K., 1983b, Preliminary geologic map of the Pinecrest quadrangle, central Sierra Nevada, California: U.S. Geological Survey Miscellaneous Field Studies Map MF-1437, scale 1:62,500, 1 sheet.
- Huber, N.K., 1990, The late Cenozoic evolution of the Tuolumne River, central Sierra Nevada, California: *Geological Society of America Bulletin*, v. 102, p. 102–115, doi:10.1130/0016-7606(1990)102<0102:TLCEOT>2.3. CO;2.
- Huber, N.K., Bateman, P.C., and Wahrhaftig, C., 1989, Geologic map of Yosemite National Park and vicinity, California: US Geological Survey Miscellaneous Investigations Series Map I-1874, scale 1:125,000.
- Hudson, F.S., 1955, Measurement of the deformation of the Sierra Nevada, California, since middle Eocene: *Geological Society of America Bulletin*, v. 66, p. 835–869, doi:10.1130/0016-7606(1955)66[835: MOTDOT]2.0.CO;2.
- Jayko, A.S., and Bursik, M., 2012, Active transtensional intracontinental basins: Walker Lane belt in the western Great Basin, in Busby, C., and Azor, A., eds., *Tectonics of sedimentary basins: Recent advances*: Hoboken, New Jersey, Blackwell Publishing Ltd, p. 226–248.
- Keith, W.J., Dohrnwend, J.C., Guisso, J.R., and John, D.A., 1982, Geologic map of the Carson-Iceberg and Leavitt Lake Roadless Areas, central Sierra Nevada, California: U.S. Geological Survey Report MF-1416-A, scale 1:62,500.
- King, N.K., 2006, Stratigraphy, paleomagnetism, geochemistry, and anisotropy of magnetic susceptibility of the Miocene Stanislaus Group, central Sierra Nevada and Sweetwater Mountains, California and Nevada [M.S. thesis]: Sacramento, California, California State University, 81 p.

- King, N.M., Hillhouse, J.W., Gromme, S., Hausback, B.P., and Pluhar, C.J., 2007, Stratigraphy, paleomagnetism, and anisotropy of magnetic susceptibility of the Miocene Stanislaus Group, central Sierra Nevada and Sweetwater Mountains, California and Nevada: *Geosphere*, v. 3, p. 646–666, doi:10.1130/GES00132.1.
- Kleinhampl, F.J., Davis, W.E., Silberman, M.L., Chesterman, C.W., Chapman, R.H., and Gray, C.H., Jr., 1975, Aeromagnetic and limited gravity studies and generalized geology of the Bodie Hills regions, Nevada and California: Reston, Virginia, U.S. Geological Survey, 8755–531.
- Koerner, A.K., 2010, Cenozoic evolution of the Sonora Pass to Dardanelles region, Sierra Nevada, California: Paleochannels, volcanism and faulting [M.S. thesis]: Santa Barbara, University of California at Santa Barbara, 146 p.
- Koerner, A.K., Busby, C.J., Putirka, K., and Pluhar, C.J., 2009, New evidence for alternating effusive and explosive eruptions from the type section of the Stanislaus Group in the 'Cataract' palaeocanyon, central Sierra Nevada: *International Geology Review*, v. 51, p. 962–985, doi:10.1080/00206810903028185.
- Lindgren, W., 1911, The Tertiary gravels of the Sierra Nevada of California: Washington, D.C., U.S. Geological Survey, 222 p.
- MacGinitie, H.D., 1941, A middle Eocene flora from the central Sierra Nevada: Carnegie Institute of Washington Publication 534, 178 p.
- Mass, K.B., Cashman, P.H., and Trexler, J.H., 2009, Stratigraphy and structure of the Neogene Boca basin, northeastern California: Implication for late Cenozoic tectonic evolution of the northern Sierra Nevada, in Oldow, J.S., and Cashman, P.H., eds., Late Cenozoic structure and evolution of the Great Basin–Sierra Nevada transition: Geological Society of America Special Paper 447, p. 147–170, doi:10.1130/2009.2447(09).
- Mulch, A., Graham, S.A., and Chamberlain, C.P., 2006, Hydrogen isotopes in Eocene river gravels and paleoelevation of the Sierra Nevada: *Science*, v. 313, p. 87–89, doi:10.1126/science.1125986.
- Neuendorf, K.K.E., Mehl, J.P., Jr., and Jackson, J.A., eds., 2005, Glossary of geology (fifth edition): Alexandria, Virginia, American Geological Institute, 800 p.
- Pluhar, C.J., and Cox, R.S., 1996, Paleomagnetism of the Stanislaus Group, Table Mountain Latite Member, Sierra Nevada, California: *Eos (Transactions, American Geophysical Union)*, v. 77, no. 46, p. 158.
- Pluhar, C., Deino, A., King, N., Busby, C., Hausback, B., Wright, T., and Fischer, C., 2009, Lithostratigraphy, magnetostratigraphy, geochronology and radiometric dating of the Stanislaus Group, CA, and age of the Little Walker Caldera, in Ernst, G., ed., The rise and fall of the Nevadaplano: *International Geology Reviews*, v. 51, p. 873–899.
- Priest, G.R., 1979, Geology and geochemistry of the Little Walker volcanic center, Mono County, California [Ph.D. thesis]: Corvallis, Oregon State University, 311 p.
- Putirka, K., and Busby, C.J., 2007, The tectonic significance of high K<sub>2</sub>O volcanism in the Sierra Nevada, California: *Geology*, v. 35, p. 923–926, doi:10.1130/G23914A.1.
- Putirka, K., Jean, M., Cousens, B., Sharma, R., Torres, G., and Carlson, C., 2012, Cenozoic volcanism in the Sierra Nevada and Walker Lane, California, and a new model for lithosphere degradation: *Geosphere*, v. 8, p. 265–291, doi:10.1130/GES00728.1.
- Ransome, F.L., 1898, Some lava flows of the western slope of the Sierra Nevada, California: U.S. Geological Survey Bulletin 89, 74 p.
- Rapp, J.S., 1982, The Valley Springs Formation in the Sonora Pass region: *California Geology*, v. 35, p. 211–219.
- Roelofs, A., 2004, Tertiary magmatism near Sonora Pass: Arc and non-arc magmatism in the central Sierra Nevada, California [M.S. thesis]: Chapel Hill, University of North Carolina, 73 p.
- Saucedo, G.J., and Wagner, D.L., 1992, Geologic map of the Chico quadrangle: California Division of Mines and Geology Regional Geologic Map 7A, scale 1:250,000.
- Schweickert, R.A., 2009, Beheaded west-flowing drainages in the Lake Tahoe region, northern Sierra Nevada: Implications for timing and rates of normal faulting, landscape evolution and mechanism of Sierran uplift: *International Geology Review*, v. 51, p. 994–1033, doi:10.1080/00206810903123481.
- Slemmons, D.B., 1953, Geology of the Sonora Pass region [Ph.D. thesis]: Berkeley, University of California, 444 p.
- Slemmons, D.B., 1966, Cenozoic volcanism of the central Sierra Nevada, California, in Bailey, E.H., ed., *Geology of northern California*: California Division of Mines and Geology Bulletin 170, p. 199–208.
- Smith, K.D., von Seggern, D., Blewitt, G., Preston, L., Anderson, J., Wernicke, B., and Davis, J., 2004, Evidence for deep magma injection Lake Tahoe, Nevada-California: *Science*, v. 305, p. 1277–1280, doi:10.1126/science.1101304.
- Smith, K.D., Kent, G., von Seggern, D.H., Eissis, A., and Driscoll, N.W., 2012, Moho-depth dike swarms and rifting of the Sierra Nevada microplate, northeast California: *American Geophysical Union* fall meeting, abs. T51B–2591.
- Surpless, B.E., Stockli, D.F., Dumitru, T.A., and Miller, E.L., 2002, Two-phase westward encroachment of Basin and Range extension into the northern Sierra Nevada: *Tectonics*, v. 21, p. 2–1–2–10, doi:10.1029/2000TC001257.
- Tolhurst, J., 2012, Sword Lake debris flow, in Hughs, N., and Hayes, G., eds., *Geological excursions in the Sonora Pass region of the Sierra Nevada: Far Western Section, National Association of Geoscience Teachers*, fall meeting, p. 90–102, <http://nagt-fws.org>.
- Unruh, J.R., Humphrey, J., and Barron, A., 2003, Transtensional model for the Sierra Nevada frontal fault system, eastern California: *Geology*, v. 31, p. 327–330, doi:10.1130/0091-7613(2003)031<0327:TMFTSN>2.0.CO;2.
- Wagner, D.L., and Saucedo, G.J., 1990, Age and stratigraphic relationships of Miocene volcanic rocks along the eastern margin of the Sacramento Valley, California, in Ingersoll, R.V., and Nilsen, T.H., eds., *Sacramento Valley Symposium* guidebook, Volume 65: Pacific Section, SEPM (Society for Sedimentary Geology), p. 143–151.
- Wagner, D.L., Jennings, C.W., Bedrossian, T.L., and Bortugno, E.J., 1987, Sacramento quadrangle map no. 1A: California Division of Mines and Geology Regional Geological Map Series, scale 1:250,000.
- Wagner, D.L., Bortugno, E.J., and McJunkin, R.D., 1990, Geologic map of the San Francisco–San Jose quadrangle: California Division of Mines and Geology, Regional Geologic Map Series, scale 1:250,000, 5 sheets.
- Wagner, D.L., Saucedo, G.J., and Grose, T.L.T., 2000, Tertiary volcanic rocks of the Blairsden area, northern Sierra Nevada, California, in Brooks, E.R., and Dida, L.T., eds., *Field guide—Geology and tectonics of the northern Sierra Nevada*: California Division of Mines and Geology Special Publication 122, p. 155–172.
- Wakabayashi, J., 1999, Distribution of displacement on and evolution of a young transform fault system: The northern San Andreas fault system, California: *Tectonics*, v. 18, p. 1245–1274, doi:10.1029/1999TC900049.
- Wakabayashi, J., 2013, Paleochannels, stream incision, erosion, topographic evolution, and alternative explanations of paleoaltimetry, Sierra Nevada, California: *Geosphere*, v. 9, p. 1–25, doi:10.1130/GES00814.1.
- Wakabayashi, J., and Sawyer, T.L., 2001, Stream incision, tectonics, uplift, and evolution of topography of the Sierra Nevada, California: *Journal of Geology*, v. 109, p. 539–562, doi:10.1086/321962.
- Walker, G.P.L., 1993, Basalt–volcano systems, in Prichard, H.M., et al., eds., *Magmatic processes and plate tectonics*: Geological Society, London, Special Publication 76, p. 3–38, doi:10.1144/GSL.SP.1993.076.01.01.
- Whitney, J.D., 1880, The auriferous gravels of the Sierra Nevada of California: Harvard University Museum of Comparative Zoology Memoir 1, 659 p.
- Wilshire, H.G., 1957, Propylitization of Tertiary volcanic rocks near Ebbetts Pass, Alpine County, California: University of California Publications in Geological Sciences v. 32, no. 41, p. 243–271, scale 1:68,500.
- Wing, S.L., and Greenwood, D.R., 1993, Fossils and fossil climate: The case for equable continental interiors in the Eocene: Royal Society of London Philosophical Transactions, ser. B, v. 341, p. 243–252, doi:10.1098/rstb.1993.0109.
- Wolfe, J.A., Schorn, H.E., Forest, C.E., and Molnar, P., 1997, Paleobotanical evidence for high altitudes in Nevada during the Miocene: *Science*, v. 276, p. 1672–1675, doi:10.1126/science.276.5319.1672.
- Zandt, G., and Humphreys, E., 2008, Toroidal mantle flow through the western U.S. slab window: *Geology*, v. 36, p. 295–298, doi:10.1130/G24611A.1.

## Geosphere

### Progressive derangement of ancient (Mesozoic) east-west Nevadaplano paleochannels into modern (Miocene–Holocene) north-northwest trends in the Walker Lane Belt, central Sierra Nevada

C.J. Busby, G.D.M. Andrews, A.K. Koerner, S.R. Brown, B.L. Melosh and J.C. Hagan

*Geosphere* 2016;12:135-175  
doi: 10.1130/GES01182.1

---

**Email alerting services** click [www.gsapubs.org/cgi/alerts](http://www.gsapubs.org/cgi/alerts) to receive free e-mail alerts when new articles cite this article

**Subscribe** click [www.gsapubs.org/subscriptions/](http://www.gsapubs.org/subscriptions/) to subscribe to Geosphere

**Permission request** click <http://www.geosociety.org/pubs/copyrt.htm#gsa> to contact GSA

Copyright not claimed on content prepared wholly by U.S. government employees within scope of their employment. Individual scientists are hereby granted permission, without fees or further requests to GSA, to use a single figure, a single table, and/or a brief paragraph of text in subsequent works and to make unlimited copies of items in GSA's journals for noncommercial use in classrooms to further education and science. This file may not be posted to any Web site, but authors may post the abstracts only of their articles on their own or their organization's Web site providing the posting includes a reference to the article's full citation. GSA provides this and other forums for the presentation of diverse opinions and positions by scientists worldwide, regardless of their race, citizenship, gender, religion, or political viewpoint. Opinions presented in this publication do not reflect official positions of the Society.

---

#### Notes